Year : 2011

Molecular and functional characterization of neuroblastoma-initiating cells

Coulon Aurélie

UNIL | Université de Lausanne
Faculté de biologie
et de médecine

Laboratoire d'Oncologie Pédiatrique

Molecular and Functional Characterization of Neuroblastoma-Initiating Cells

Thèse de doctorat ès sciences de la vie (PhD)

présentée à la

Faculté de biologie et de médecine
de l'Université de Lausanne

par

Aurélie COULON

Biologiste Master de l'Ecole Normale Supérieure de Cachan
et de l'Université Paris XI (France)

Jury

Prof. Michel Duchosal (CHUV, UNIL), Président
Dr Nicole Gross (CHUV, UNIL), Directeur de thèse
Prof. Ivan Stamenkovic (CHUV, UNIL), Co-directeur
Prof. Lukas Sommer (UNIZ), expert
Dr Olivier Delattre (Institut Curie), expert

Lausanne 2011

UNIL | Université de Lausanne
Faculté de biologie
et de médecine

Ecole Doctorale

Doctorat ès sciences de la vie

Imprimatur

Vu le rapport présenté par le jury d'examen, composé de

Président	Monsieur	Prof. Michel	**Duchosal**
Directeur de thèse	Madame	Dr Nicole	**Gross**
Co-directeur de thèse	Monsieur	Prof. Ivan	**Stamenkovic**
Experts	Monsieur	Dr Olivier	**Delattre**
	Monsieur	Prof. Lukas	**Sommer**

le Conseil de Faculté autorise l'impression de la thèse de

Madame Aurélie Coulon

Master Université de Paris XI, France

intitulée

Molecular and Functional Characterization of Neuroblastoma - Initiating Cells

Lausanne, le 18 février 2011

pour Le Doyen
de la Faculté de Biologie et de Médecine

Prof. Michel Duchosal

Mais d'abord je ferai quelques expériences, avant d'avancer plus loin, car mon intention est d'abord d'alléguer l'expérience et ensuite de démontrer par la raison pourquoi cette expérience se produit nécessairement ainsi, et telle est la véritable règle que ceux qui explorent les manifestations de la nature doivent appliquer.

Léonard de Vinci, vers 1513

TABLE OF CONTENTS

RESUME

Le neuroblastome (NB) est la tumeur maligne extra-crânienne la plus fréquente chez le nourrisson et le jeune enfant. Elle se développe tout le long du système nerveux sympathique et dans la partie interne de la glande surrénale, et se caractérise par une grande diversité de phénotypes cliniques et biologiques. Dans les cas les plus sévères, la maladie est d'emblée métastatique et manifeste une résistance multiple aux traitements.
Des études récentes ont proposé un nouveau modèle d'évolution du cancer basé sur l'existence de **cellules souches cancéreuses (CSC)**, qui partagent avec les cellules souches normales des propriétés d'auto-renouvellement et de résistance aux agents cytotoxiques. Ces cellules seraient seules capables d'initier le développement de la tumeur primaire comme celui des métastases. Des CSC ont été identifiées dans les leucémies, les mélanomes ainsi que dans les cancers du sein, du système nerveux central et du colon. La validité d'un tel modèle pour d'autres tumeurs, dont les NBs, reste à démontrer. Nous avons identifié au sein d'échantillons cliniques de NB, des cellules isolées exprimant des marqueurs connus de cellules souches de la crête neurale et de leurs lignages, conduisant à l'hypothèse de l'existence de CSC dans les NB.

Leur capacité à proliférer indépendamment de l'attachement à un substrat sous forme de sphères illustre la fonction d'auto-renouvellement, et représente une des caractéristiques typiques des CSC. Afin de mettre en évidence l'existence de CSC de NB, et de décrire leur phénotype, nous avons exploité cette propriété, et établi à l'aide de puces micro-array un profil d'expression génique associé à la fonction d'auto-renouvellement. Des neuroblastes métastatiques isolés à partir d'échantillons cliniques de NB ont été sélectionnés par cultures en sphères et leur profil d'expression génique comparé à celui de la population initiale. La comparaison des listes de gènes différentiellement exprimés dans les sphères de NB et celles d'autres types de cellules souches apparentées, nous a permis d'établir une liste de gènes communs, qualifiée de **profil d'expression de neurosphères**. Cette liste comprend notamment les gènes de la prominin-1 (CD133), de transporteurs « ATP-binding cassette » (MDR1), des voies WNT et NOTCH. Ces gènes impliqués dans les processus du développement embryonnaire sont surexprimés dans les sphères de la majorité des échantillons de NB analysés.
Le potentiel tumorigène *in vivo* des sphères de NB a été comparé à celui des échantillons originaux par greffes orthotopiques (glande surrénale) dans la souris immunodéprimée (nude), puis analyse de la croissance tumorale. La fréquence de la prise tumorale était significativement plus élevée après greffe des sphères comparée à la greffe de la population cellulaire originale. Une modification de ce caractère hautement tumorigène des sphères de NB métastatiques a été observée après modification du site d'injection ou sélection directe des cellules de NB sur la bases de combinaisons de marqueurs de la SAR.
Notre étude a permis de mettre en évidence un profil d'expression de gènes associé à une fonction caractéristique des CSC. Nos résultats démontrent l'hétérogénéité des populations initiatrices de NB et le caractère complexe de la fonction tumorigène associée aux CSC. Les CSC de NB correspondent vraisemblablement à une population cellulaire dynamique, contrôlée par des signaux provenant du microenvironnement. Les CSC de NB sont décrites dans cette étude comme une fraction de cellules exprimant des combinaisons de marqueurs qui représentent de potentielles cibles thérapeutiques.

SUMMARY

Neuroblastoma (NB) is the most common extracranial malignant tumor in young children and arises at any site of the sympathetic nervous system. The disease exhibits a remarkable phenotypic diversity ranging from spontaneous regression to fatal disease. Poor outcome results from a rapidly progressive, metastatic and drug-resistant disease. Recent studies have suggested that solid tumors may arise from a minor population of **cancer stem cells (CSCs)** with stem cell markers and typical properties such as self-renewal ability, asymmetric division and drug resistance. In this model, CSCs possess the exclusive ability to initiate and maintain the tumor, and to produce distant metastases. Tumor cell subpopulations with stem-like phenotypes have indeed been identified in several cancer including leukemia, breast, brain and colon cancers. CSC hypothesis still needs to be validated in the other cancers including NB.
NB originates from neural crest-derived malignant sympatho-adrenal cells. We have identified rare cells that express markers in conformity with neural crest stem cells and their derived lineages within primary NB tissue and cell lines, leading us to postulate the existence of CSCs in NB tumors.

In the absence of specific markers to isolate CSCs, we adapted to NB tumor cells the sphere functional assay, based on the ability of stem cells to grow as spheres in non-adherent conditions. By serial passages of spheres from bone marrow NB metastases, a subset of cells was gradually selected and its specific gene expression profile identified by micro-array time-course analysis. The differentially expressed genes in spheres are enriched in genes implicated in development including CD133, ABC-transporters, WNT and NOTCH genes, identified in others solid cancers as CSCs markers, and other new markers, all referred by us as the **Neurosphere Expression Profile (NEP)**. We confirmed the presence of a cell subpopulation expressing a combination of the NEP markers within a few primary NB samples.
The tumorigenic potential of NB spheres was assayed by *in vivo* tumor growth analyses using orthotopic (adrenal glands) implantations of tumor cells into immune-compromised mice. Tumors derived from the sphere cells were significantly more frequent and were detected earlier compared to whole tumor cells. However, NB cells expressing the neurosphere-associated genes and isolated from the bulk tumors did not recapitulate the CSC-like phenotype in the orthotopic model. In addition, the NB sphere cells lost their higher tumorigenic potential when implanted in a subcutaneaous heterotopic *in vivo* model.

These results highlighted the complex behavior of CSC functions and led us to consider the stem-like NB cells as a dynamic and heterogeneous cell population influenced by microenvironment signals.
Our approach identified for the first time candidate genes that may be associated with NB self-renewal and tumorigenicity and therefore would establish specific functional targets for more effective therapies in aggressive NB.

ABBREVIATIONS

ABC:	ATP-binding cassette
ALDH:	aldehyde deshydrogenase
Array-CGH:	array-comparative genomic hybridization
APC :	allophycocyanine
ATP :	adenosine-5’-triphosphate
bFGF:	basic fibroblast growth factor
BSA:	bovine serum albumin
CIG:	Center for Integrative Genomics
CNR:	cannabidoid receptor
CSC:	cancer stem cell
CST:	childhood solid tumor
DAFL:	DNA array facility Lausanne
del:	deletion
DMEM:	Dulbecco's Modified Eagle Medium
dNTP:	deoxynucleotide triphosphate
DNA:	deoxyribonucleic acid
EDN:	endothelin
EDNR:	endothelin receptor
EDTA:	ethylene-diamine-tetra-acetic acid
EGF:	epidermal growth factor
EMT:	epithelial to mesenchymal transition
FACS:	fluorescence activated cell sorting
FCS:	fœtal calf serum
FDR:	false detection rate
FGFR:	fibroblast growth factor receptor
FISH:	fluorescence in situ hybridization
GAPDH:	glyceraldehyde 3-phosphate dehydrogenase
GD2:	diganglioside
GO:	Gene Ontology
GPR:	G-protein coupled receptor
H/E:	haematoxylin / eosin
HGF:	hepatocyte growth factor

ABBREVIATIONS

IGF:	insulin growth factor
IL:	interleukine
iPS:	induced pluripotent stem cell
MDR1:	multidrug resistance gene 1
MTS/PMS:	(3-(4,5-dimethylthiazol-2-yl)-5-(3-carboxymethoxyphenyl)-2-(4-sulfophenyl)-2H-tetrazolium)/phenazine methosulfate
NB:	neuroblastoma
NBM:	neural basic medium
NCDC:	neural crest derived progenitor cell
NCS:	neural crest sphere
NCSC:	neural crest stem cell
NEP:	neurosphere expression profile
NGF:	nerve growth factor
p75NTR:	p75 neurotrophin receptor
PBS:	phosphate buffer solution
PDGF:	platelet-derived growth factor
PE:	phycoerythrin
POG:	Pediatric Oncology group
Prom:	prominin (CD133)
RACE:	remote analysis computation for gene expression
RMA:	robust multichip average
RNA:	ribonucleic acid
RT:	room temperature
PCR:	polymerase chain reaction
SIOP:	International Society for Pediatric Oncology
TGF-β:	transforming growth-factor beta
TIC:	tumor initiating cell
UFH:	unfavorable histology
UNIL:	University of Lausanne
VEGF:	vascular endothelial growth factor

INTRODUCTION

The cellular origin of human cancers

The human body: a multicellular organism

The multicellular eukaryotic organisms constitute different levels of organization from the single cell to the functional systems. The 10^{15} cells of the human adult body, distributed among more than a hundred different cell types, are grouped into substructures called tissues that form organs that cooperate inside a systemic function. For instance, the mammary gland, part of the reproductive system, is an organ constituted of several cell tissues fulfilling different functions. Thus the mammary gland is comprised of milk-making alveolar lobes, milk-conducting lactiferous ducts, fat tissue and connective tissue. Each of these tissues functions thanks to differentiated cells that are specialized in one particular task: hormone production and secretion, milk production, duct formation, vascularization, etc.

The epithelial tissue, like the alveoli of mammary lobules, is widely spread in human organs and is characteristic of an exchange surface zone between two compartments. Epithelia are found in the mammary gland but also in the lungs, the liver, the prostate, the skin, the intestine, the bladder, the ovary, and the colon. They are composed of a monolayer of bipolar cells tightly connected to each other by proteins forming a physical barrier between two extracellular spaces. Disruptions of their cell structure due to internal (mammary involution) or external (wound) causes lead to the faithful tissue renewal mobilizing specific multipotent stem cells that are able to regenerate the hierarchy of all the different cell types. The homeostasis of cell tissues is regulated by a number of intrinsic and extrinsic cellular mechanisms such as programmed cell death, telomere reparation, cytokine response, hypoxia, proliferation, and extracellular fluid mechanics.

Carcinogenesis

Research in the 20th century, especially since the disastrous radioactive fallout of the nuclear war in Japan and its affect on human health, has allowed for a significant increase in the understanding of cell homeostasis, revealing cancer to be a dynamic pathology of the genome. The systematic review of gene mutations found in leukemia and solid tumors showed these genes to be distributed into four classes: proto-oncogenes, tumor suppressor genes, “caretaker” genes which code DNA repair proteins, and “gatekeeper” genes. These mutations can result from the mutagenic action of endogenous chemical products generated during physiological processes such as cell death, or exogenous factors including chemicals, radiation, and viruses. In rare familial cancer syndromes, these mutations are inherited through the germinal cell lines.

The genetic mutations that occurred in cancerous cells lead to altered gene products and therefore are responsible for defects in regulatory circuits that govern normal cell proliferation and homeostasis. The malignant growth of a transformed cell has been described by the acquisition of six essential alterations affecting the cell physiology (1):

- Self-sufficiency in growth signals
- Insensitivity to antigrowth signals
- Evasion of programmed cell death (apoptosis)
- Limitless replicative potential
- Sustained angiogenesis
- Tissue invasion and metastasis

These six capabilities are proposed to be shared by most if not all types of human tumors.

Tumor microenvironment

Tumors are no longer considered as a simple bulk of cancer cells proliferating independently from the surrounding tissue cells of the host organ. Indeed, past studies have shown that most solid tumors are composed not only of neoplastic cells but also of a variety of extracellular matrix components and cell types, notably fibroblasts, myofibroblasts, adipocytes, endothelial cells, pericytes, and immune cells which collectively form the tumor stroma (2-4).

The most obvious evidence of a tumor-stroma interaction was supported by studies of tumor neovascularization resulting from the release of proangiogenic factors by the tumor cells (5-7). In addition, first assumed to attenuate tumor development, inflammatory cells such as lymphocytes, were shown to play a critical role in the malignant progression of many types of solid tumors (8-10).

In carcinomas such as those found in breast cancer, the most abundant mesenchymal cells correspond to fibroblasts and myofibroblasts which promote tumor progression and are used as markers of invasiveness and poor progression by the pathologists (11-13). Finally, the extracellular matrix formed by mesenchymal cells is thought to regulate tumor cell growth and mobility. For instance, in the mammary gland, the composition and density of the extracellular matrix is a determinant of breast cancer risk (14). In neuroectodermal tumors, including neuroblastoma and melanoma, tumor cells cross-talk with stromal cells via chemokine secretion and thereby regulate angiogenesis, tumor growth, immune response, and metastasis (15). A large roster of cytokines, chemokines and growth factors have been found to promote tumor progression and thus highlight the critical role of paracrine signaling between tumor and host cells in the local microenvironment (16). Although normal stroma has been shown to delay or prevent tumorigenesis (17), abnormal stromal components can even promote tumor growth when mutations occured in the stromal cell genome but not in the tumor cells (18, 19).

Heterogeneity in tumor cells

Since the 19th century, the studies of Müller, Virchow and many others up to the present, have confirmed and extended the earlier observations that heterogeneity among cancer cells was a common and prominent feature of most human solid tumors. In particular, the phenotypic and genetic heterogeneity of all types of cancers have been repeatedly demonstrated since the late 1970s (20, 21). The different parameters of cellular heterogeneity have been catalogued and correspond to numerous phenotypic characteristics including cellular morphology or tumor histopathology, the expression of cell markers and the production of differentiated cell products, growth properties *in vitro*, the ability to be affected by a host immune response, the ability to invade and metastasize, sensitivity to chemotherapeutic agents and tumorigenicity *in vivo* (22, 23).

Cancer paradigms

Stochastic model

Until recently, cancer has been considered as a genetic disease where inherited or somatic alterations in the genome of any cell of the body are selected for providing an uncontrolled cell growth, a sustained angiogenesis, a limitless replicative potential, and an evading from apoptosis to the transformed cells (1, 24). This clonal evolution model of tumorigenesis, referred as the "stochastic" model, was well accepted and explains not only the clinical observations but also the great intra- and inter-tumoral heterogeneity in term of proliferation, differentiation and tumorigenic potential (25). Cancer cells were assumed to be genetically unstable and it was proposed that as a population expands, the probability of mutations increases (26).

However, although it was clear that such genetic mutations drive tumor formation, several observations were difficult to reconcile with the idea that transformation events can occur in differentiated cells. Indeed, the terminally differentiated cells within an epithelial tissue are unlikely to accumulate mutations as they rarely divide. Moreover, it was difficult to imagine how a well differentiated cell, even transformed could give rise to a heterogeneous tumor showing a large panel of cell differentiation degrees. Finally, it has been experimentally observed that the overall efficiency of obtaining cancer cell lines and even tumor xenograft from patient tumors was very low. In experimental models, the implantation of a large number of cells from most cancer cell lines was often required to induce tumor growth (27). These observations suggest that among the tumor bulk cells, only a cell subset has the ability to proliferate extensively and form new tumors.

Cancer stem cell model

The historical emergence of the stem cell origin of cancer

The stem cell origin of cancers is not a recent notion. In 1855, Rudolph Virchow, a German pathologist, proposed the "embryonal-rest hypothesis" of tumor formation, based on histological similarities between tumors and embryonic tissues (28). This theory, later expanded by other pathologists such as Julius Cohnheim who proposed in 1875 the hypothesis that stem cells "misplaced" during embryonic development were the source of tumors that formed later in life (29, 30). In the early 1960s, human autotransplantation assays demonstrated a low frequency of tumor-initiating cells in various solid-organ malignancies (31). Fortunately, such human *in vivo* studies have been completely forbidden today by ethical committees.

Leukemia stem cell research first led the way in cancer stem cell research. The use of mice models allowed the demonstration in 1963 of the low *in vivo* clonogenic efficiency of mouse lymphoma cells (32). Between 1967 and 1981, Philip Fialkow and his coworkers showed the clonal origin of leukemic cells and indicated the involvement of en early stem or progenitor cell in myelogenous leukemia and acute myelogenous leukemia (33, 34). The development between 1968 and 1973 of the fluorescent-activated cell sorting (FACS) by Leonard Herzenberg and coworkers (35) ratified the new era of *in vivo* single cell implantation in the SCID mice model which was refined in the early 1990s and allowed the isolation in 1994 of a leukemic cell capable of initiating human acute myeloid leukemia after transplantation into SCID mice (36). Finally, between 1985 and 1995, research has seen the arrival of the immunocompromised animal model with the characterization in 1992 of the NOD/SCID mouse.

Together, the results obtained in leukemia studies led to the postulate that the leukemic cells can be considered as an aberrant hematopoietic system which would have arisen from the accumulation of mutations in the corresponding normal stem or progenitor cell. In this paradigm, the principles of normal stem cell biology can therefore be applied to understand better how tumors develop.

CSC definition

As described above, research on leukemia models first suggested that analogies between normal stem cells and tumorigenic cells may be appropriate (36-40). These observations led to the definition of the cancer stem cell (41) as a minor tumor cell subset which is critical for the tumor initiation and propagation, and fulfills functional criteria of normal stem cells such as:

- Self-renewal: CSC can divide asymmetrically and produce another CSC and a more differentiated cancer cell thus driving tumorigenesis.
- Indefinite proliferation potential: CSC can reactivate telomerase activity.

- Pluripotency: the presence of cells with various degree of differentiation within a tumor corresponds to the generation of different progeny by CSC and hence cellular heterogeneity.
- Drug resistance: CSC, as normal stem cell, shows high resistance to drug-mediated toxicity.
- Dependence on a specific micro-environment or "niche". Tumor cells are interwoven with a heterogeneous stroma which could be the equivalent of the stem cell niche.

CSCs are distinct from the cell of origin. The cell of origin specifically refers to the cell type that receives the first oncogenic hit(s). Moreover, CSCs do not necessarily originate from the transformation of normal stem cells. CSCs may arise from restricted progenitors or more differentiated cells that have acquired the capacity to self-renew (42-44). In studies in the field, the semantic has not been clarified. Thus some researchers would use the term "cancer stem cell" (CSC) as others would prefer "tumor-initiating cell" (TIC). "TIC" preferentially refers to the experimental observation of isolated tumor cells to propagate tumors in an *in vivo* model whereas "CSC" encompasses the theoretical properties of tumor cell populations to self-renew and to sustain a cancer for producing differentiated progeny that form the bulk of the cancer. However, the two terms will be considered equivalent in this study.

CSC in solid tumors

Solid tumors account for the major cancer burden; epithelial cancers arising in tissues that include breast, lung, colon, prostate and ovary constitute approximately 80% of all cancers. Thus, the CSCs hypothesis provided an attractive cellular mechanism to explain the chemotherapeutic resistance and the long-term relapses exhibited by many of these tumors.

A decade following the pioneering work of leukemia stem cells studies (45), Al-Hajj and his colleagues showed that human breast cancers also adhere to the hierarchical or CSC model; as few as 200 $ESA^{+}CD44^{+}CD24^{-/low}Lin^{-}$ cells were able to generate tumors recapitulating the heterogeneity of the initial tumor in immunosuppressed nonobese diabetic/severe combined immunodeficient (NOD/SCID) mice, whereas 100-fold more cells without these markers isolated from the same tumors were nontumorigenic (46). Since then, many studies tried to characterize the breast CSC and identified alternative markers including the aldehyde dehydrogenase (ALDH) that could be use to enrich for tumor-initiating breast CSC populations (47). Interestingly, these sets of markers identified overlapping but nonidentical cell populations.

Likewise, CSC populations were identified in brain tumors including glioblastoma and medulloblastoma (48-51). Brain CSC were reported on the basis of cell sorting for the neural stem cell marker CD133 on acutely dissociated brain tumor cell populations and were isolated from low-grade and high-grade tumors from both children and adults (52, 53). However, in a recent study,

tumor-propagating cells were shown to express CD15 and not CD133 in a mouse model for medulloblastoma (54).

In addition, the CSC concept was also investigated in colon cancer and melanoma which are two severe and frequent cancers and many markers were proposed as specific tools to identify functional CSC populations. Thus, CD133 have been first proposed as a colon CSC marker (55, 56) but its relevance has been challenged by further studies (57). In the same way, many different markers including ABCB5, CD133, ABCG2, CD271 (LNGFR/p75) were shown to be associated with putative melanoma CSC populations harboring self-renewing and tumorigenic properties (58-61).

Finally, since the report of the breast CSC identification in 2003, the CSC hypothesis has been addressed in a very large panel of solid tumors. However, no consensus on its reliability has yet been found as experimental methods and specific markers have not been decided on. In the last four years, an important number of reviews addressed the numerous unresolved questions and nurtured the debate (62-71).

CSC identification and clinical relevance

Self-renewal

Proliferation and self-renewal constitute two distinct cell processes. Self-renewal corresponds to a unique cell division in which the capacity of one or both progeny to proliferate and differentiate is similar to those of the parental cells. Although a committed progenitor cell might have an extensive ability to proliferate, it is destined to eventually become terminally differentiated and stop dividing. Self-renewal is a hallmark of any human stem cell such as hematopoietic stem cell. Indeed it has been shown that a single hematopoietic stem cell or a progeny that arose from a self-renewing cell division could be serially transplanted several times and restored blood production in lethally irradiated animals (72).

The sphere assay, originally developed for neural cells (73), has formed an important basis for the development of an *in vitro* assay to study both normal stem and progenitor cells and CSCs in a variety of solid tumors including brain (51) and breast (74) cancers. In the context of sphere assays for tumor cells, a number of groups have found that glioblastomas efficiently form tumor spheres in a clonogenic manner (49, 51). $CD133^+$ cells in the brain tumors have a greater potential to form neurospheres than $CD133^-$ cells (75). In addition, the most aggressive clinical samples of medulloblastoma demonstrated the highest secondary sphere-forming capacity (48). Moreover, this assay provides a useful and predictive model to test the therapeutic response of CSC-containing tumors to a specific drug or compound before testing *in vivo*.

Tumorigenicity

CSCs refer to a subset of tumor cells that has the ability to continually sustain tumorigenesis. Experimentally, the putative CSC populations need to be evaluated for their potential to show tumor propagation. The gold standard assay that fulfills this criterion is serial orthotopic transplantation in animal models, which, although imperfect, is regarded as the best functional assay (41, 76).

Metastasis

Metastasis is the predominant cause of lethality in cancer patients. However, not every cell in a tumor has the ability to metastasize to other organs. Metastatic potential depends on multiple factors that determine overall tumor cell growth, survival, angiogenesis, and invasion. For epithelial malignancies, the epithelial-mesenchymal transition (EMT) is considered to be a crucial event during embryogenesis which may be misappropriated by cancer cells in the metastatic process, which involves disruption of epithelial cell homeostasis and the acquisition of a migratory mesenchymal phenotype (77, 78). Cells undergoing EMT could conceivably be the precursors to metastatic cells and correspond to metastatic CSCs (79). Recent data have supported the concept of a metastatic CSC in pancreas and liver cancers in particular and suggested that the SDF-1/CXCR4 axis could be involved in both the trafficking of normal stem cells and the metastasis of CSC (80-82).

Drug resistance

Normal stem cells have many properties that separate them from mature, differentiated cells. Thus, their drug resistance provides for a long lifespan through the expression of high levels of specific ABC transporters including ABCB1 (MDR1) and ABCG2 (83-85), the resistance to apoptosis, and the active DNA-repair capacity. It has been assumed that CSC could share many properties of the normal stem cells and therefore might also possess these resistance mechanisms. Evidence has emerged that CSCs represent a subpopulation of cells within cancers that is characterized by increased resistance to chemo- and radiotherapy, indicating that conventional anticancer approaches might frequently fail to eradicate the cell subset that perpetuates tumorigenesis. For example, CSC chemoresistance has been reported in human leukemias (86-89), in malignant melanoma (59, 61), and in brain (90), breast (91), pancreatic (80), and colorectal (92) cancers. Furthermore, CSC radioresistance has been identified in brain (93) and breast (94, 95) cancers.

Angiogenesis and vascular mimicry

It is now broadly accepted that cancer cells can induce angiogenesis (i.e. the formation of new vessels) from preexisting vessels via the secretion of paracrine factors or direct cell-cell contacts. A recent study in human brain cancers has shown that $CD133^{+}Nestin^{+}$ CSCs in medulloblastomas,

ependymas, oligodendrogliomas, and glioblastomas were preferentially located within a perivascular niche, where they interact closely with the endothelial cells. Moreover, cografting endothelial cells with human medulloblastoma tumor xenografts induced the expansion of the self-renewing CSC fraction and accelerated cancer initiation and growth (96). In addition, glioma stem cells have also been shown to promote angiogenesis through the vascular endothelial growth factor (VEGF) (97).

With regard to vascular mimicry, this phenomenon was first described in 1999 and corresponds to an important mechanism in cancer cells which organize themselves as perfusable channels and express few endothelial markers (98). Vascular mimicry could explain the failure of currently available inhibitors of angiogenesis to fully effect tumor eradication. It has been shown that bone morphogenic proteins (BMPs) such as BMP4 are involved in the vascular mimicry of melanoma cells (99) and that BMP4 could regulate the size of the CSCs population in human glioblastoma (100). Moreover, $ABCB5^+$ melanoma CSC were shown to preferentially express the vasculogenic markers TIE-1 and CD144 as well as BMPR1A (BMP receptor) (61). All together, these results suggest that it could be relevant to address the role of CSCs in vascular mimicry.

Immune evasion and modulation

Immunomodulatory functions are established properties of the physiologic stem cells in particular mesenchymal stem cells (101-104). Therefore, it has been hypothesized that CSC may foster tumor initiation and growth at least in part via attenuation of the antitumor immune response.

The CD200 transmembrane glycoprotein has been shown to be an important player in immunoregulation, tolerance and cancer prognosis. In the putative $CD44^+$ prostate CSCs derived from prostate cancer cell lines, the genomic expression of CD200 was increased (105). Moreover, the majority of CD200 expressing cells were found on the putative $CD44^+CD24^-$ breast CSCs derived from the MDA-MB231 cell line (105). In more recent studies, the CD133 expressing and tumorigenic neurosphere cells derived from primary glioblastoma multiforme specimens were assessed for the expression of immunologic molecules and were found to lack proteins necessary for the antigen presentation, whereas the inhibitory costimulatory molecule B7-H1 was present. The glioma-associated CSCs also produce immuno-suppressive cytokines including TGF-β1, the Treg chemokine attractant CCL-2, VEGF and prostaglandin E2 and thus inhibit T-cell activation and proliferation via STAT3 signaling pathway (106, 107). Finally, T-cell activation has also been shown to be modulated by the $ABCB5^+$ malignant melanoma CSCs derived from established melanoma xenografts and clinical tumor specimens showed a low expression levels of immunogenic molecules and inhibited the proliferation of human peripheral blood mononuclear cell (PBMC) (108). These findings suggest specific roles of CSCs in the evasion of antitumor immunity and in cancer immunotherapeutic resistance.

Niche

Normal stem cells of various tissues exist within protective "niches". The niche corresponds to the immediate cell micro-environment comprising extra-cellular components and a variety of differentiated cell types such as immune, endothelial and mesenchymal cells (109, 110). These mature cells provide direct cell contacts and secreted factors that maintain stem cells primarily in a quiescent state or induce their symmetric or asymmetric self-renewal. For instance, mouse tissue studies suggested that neural stem cells were present within a vascular niche together with endothelial cells which regulate stem cell self-renewal (111-114). It has been reported that CSC might arise from normal stem cells that have acquired mutations that enable them to escape from niche control (115). Alternatively, one could imagine that deregulation of extrinsic factors within the niche might lead to uncontrolled proliferation of stem cells and tumorigenesis as shown by Clarke and Fuller (44). Recently, an increasing number of endothelial cells or blood vessels in orthotopic brain tumor xenografts has been shown to expand the fraction of self-renewing $CD133^+$ brain CSCs and accelerated the initiation and growth of brain tumors (96). A molecular and cellular portrait of a CSC niche will be required in the future to identify components in the tumor microenvironment that are necessary for maintaining the functions of CSCs to use these components as therapeutic targets.

Clinical Relevance

CSC populations in many types of cancer are thought to be responsible for drug resistance, immune evasion, and dormancy, criteria that have severe consequences on the prognosis and the treatment of patients. Indeed, their relative abundance in clinical cancer specimens has been correlated with malignant disease progression in human patients. Conventional anticancer approaches are directed predominantly at bulk tumor populations and might frequently fail to eradicate the cancer stem cell subset that perpetuates tumorigenesis.

Putative CSCs are prospectively isolated using methods based on either surface markers or intracellular enzyme activity that are also detected in normal stem cells. The challenge will be to characterize molecules and signaling pathways that are specifically associated with CSC biology to spare physiologic stem cells by targeted therapeutic treatment. Recent studies have carried out drug and RNAi screening to identify factors that could be targeted to specifically kill CSC. For example, a kinome-wide RNA interference screen in glioblastoma multiforme has been performed and showed that the knockdown of the adaptor protein TRRAP significantly increased differentiation of cultured brain CSCs, sensitized cells to apoptotic stimuli, and negatively affected cell cycle progression (116). In a chemical screen, compounds have be shown to be selectively toxic for breast CSCs, including salinomycin that reduced the proportion of CSC in mammosphere cell population 100-fold more than paclitaxel, a commonly used chemotherapy in breast cancer treatment (117). These screens

constitute promising strategies to discover complementary treatment to efficiently eliminate cancer cells.

Neuroblastoma: biological and clinical data

Neuroblastoma (NB) is the second most frequent and deadly solid tumor in children. It accounts for 7-10% of all childhood malignancies, but for far more deaths (118). The prevalence is about one case in 7,000 live births and there are about 700 new cases per year in the United States alone. This incidence is fairly uniform throughout the industrialized nations. For instance, about 10 new cases are diagnosed every year in Switzerland. Even though much progress has been achieved in understanding the biology of this cancer, its complex clinical and biological behavior remains enigmatic.

Neuroblastoma, a pediatric neuroectodermal tumor

In many forms of adult cancer, the original cell type is well defined based on the location of the tumor, the molecular markers expressed by tumor cells, and the histological and clinical features of the disease. For childhood solid tumors (CST), the cell of origin and the environment in which tumorigenesis occurs are much more difficult to define (119). In contrast to adult tumors, many CST are embryonal tumors as they originate from immature tissue. CST cells not only morphologically resemble embryonal cells, but they functionally mimic their behavior.

Among CST, neuroectodermal tumors originate from the multipotent neural crest cells generated in the early embryo that give rise to the central and peripheral nervous systems. These malignancies include several pediatric examples such as NB, PNETS (Ewing sarcomas) and medulloblastomas, as well as melanomas and small cell lung carcinomas (120).

NB is derived from pluripotent neural crest-derived precursor cells of the sympathoadrenal cell lineage. These cells develop a highly dynamic and growth factors-rich environment.

In vivo and *in vitro* observations have shown that neuroblastic tumors strikingly recapitulate the development of differentiating sympathetic neurons and the chromaffin (neuroendocrine) cells of the sympathetic neural system. Thus, NB displays several typical characteristics and features of its originating cells, such as heterogeneity and pluripotential differentiation, and it also has a high potential for migration and distant metastasis formation (121-124). This indicates that in contrast to adult tumors, NB as well as other CST results from defects in mechanisms that control normal development, arresting the normal process of differentiation, and thus can be seen as a developmental disorder (122, 123).

International NB Staging System

The origin and migration pattern of neuroblasts during fetal development explains the multiple anatomic sites where these tumors occur and the location of these tumors appears to vary with age. The median age at diagnosis for NB patients is about 18 months; so approximately 40% are diagnosed by one year of age, 75% by four years of age and 98% by ten years of age (125). Tumors can occur in the abdominal cavity (40% adrenal, 25% paraspinal ganglia) or involve other sites (15% thoracic, 5% pelvic, 3% cervical tumors, 12% miscellaneous). Infants are more likely to have thoracic and cervical tumors, whereas older children more frequently have abdominal tumors (126). According to the International Neuroblastoma Staging System, the tumors are divided into 4 different stages (Figure 0-1).

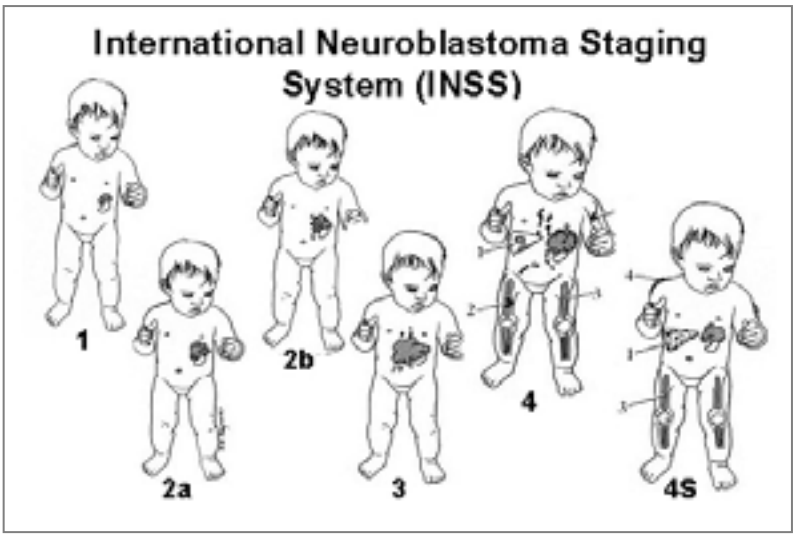

<u>Figure 0-1:</u> International Neuroblastoma Staging System (INSS)

Stage 1

- Localized tumor with complete gross excision and/or microscopic residual disease
- Ipsilateral lymph nodes negative for tumor (nodes attached to the primary tumor may be positive for tumor.)

Stage 2A

- Localized tumor with incomplete gross resection
- Representative ipsilateral nonadherent lymph nodes negative for tumor microscopically

Stage 2B

- Localized tumor and/or complete gross excision, with ipsilateral nonadherent lymph nodes positive for tumor
- Enlarged contralateral lymph nodes, which are negative for tumor microscopically

Stage 3

- Unresectable unilateral tumor infiltrating across the midline and/or regional lymph node involvement
- Alternately, localized unilateral tumor with contralateral regional lymph node involvement

Stage 4

- Any primary tumor with dissemination to distant lymph nodes, bone, bone marrow, liver, skin, and/or other organs (except as defined for stage 4S)

Stage 4S

- Localized primary tumor (as defined for stages 1, 2A, or 2B) with dissemination limited to skin, liver, and/or bone marrow (<10% involvement)
- Limited to infants

The disease exhibits a remarkable clinical phenotype diversity reflected in the outcome, ranging from spontaneous regression to fatal disease. Whereas a favorable outcome, essentially due to spontaneous maturations and regressions is generally associated to low stages and localized tumors (stage1-2 and stage 4s), stage 3 (large, progressing tumors) and stage 4 (metastatic) NB are extremely difficult to treat and are thereby responsible for most deaths, due to a rapidly progressive, metastatic and drug-resistant disease. Interestingly, the spontaneous regression of NB is often observed in patients under one year of age (stage 4s) and mimics a developmentally regulated programmed cell death of sympathetic neurons during the perinatal period. Thus, stage 4s NB is associated with a good prognosis even if the patients present a unique and unexplained pattern of metastatic spread limited to bone marrow, liver, and skin.

Patients older than one year with metastatic disease have very severe prognosis; fewer than half of these patients are cured, even with the use of high-dose therapy followed by autologous bone marrow or stem cell rescue (127). Metastatic dissemination of advanced stage tumors mainly occurs in the bone marrow, bone, liver and skin. Bone marrow involvement and clearing are key prognostic factors for NB (128).

This classification has recently been redefined by the new International Neuroblastoma Risk Group (INRG) classification composed of four NB categories: L1/L2 for localized tumors, M for metastatic disease (stage 4), and MS for stage 4s (from the SIOPEN annual general meeting, 2007).

Consequently, molecular and functional characterization of the cell populations that control NB tumor progression and metastasis is crucial to design effective therapies and improve the prognosis of these patients.

Histology of NB tumors

Histologically, neural crest tumors can be classified as NB, ganglioneuroblastoma (GGNB), and ganglioneuroma (GGN), depending on the degree of maturation/differentiation of the tumor (129).

Most NB are undifferentiated tumors consisting of small, round, blue cells called neuroblasts and have little, if any evidence of neural differentiation. The typical tumor shows small uniform cells with scant cytoplasm and hyperchromatic nuclei. Neuron specific enolase (NSE), chromogranin, synaptophysin, and S-100 immunohistochemical stains usually are positive.

In contrast, the most differentiated form consists in the completely benign GGN which is typically composed of clusters of mature neurons surrounded by a dense stroma of Schwann cells, whereas GGNB include the whole spectrum of differentiation between pure GGN and NB. Because of the presence of different histological components, the pathologist must evaluate the tumor thoroughly; the regions with different gross appearance may demonstrate a different histology.

Genomic and biologic markers in NB

Chromosome alterations

During the last 2 decades, the genetic alterations of NB tumors have been explored through a panel of techniques including array-CGH. Many chromosomal and molecular identified abnormalities have been evaluated to determine their value in assigning prognosis (130-133). NB can be classified into subtypes that are predictive of clinical behavior based on these patterns of genetic changes. Some of them have been incorporated into the strategies used for risk-assignment. Thus, the oncogene MYCN amplification, the first genetic alteration described in NB, is observed in 25-30% of cases and is strongly related to disease progression and poor outcome. Deletion of the short arm of chromosome 1 is one of the most common chromosomal abnormalities present in NB, and is associated with a high risk of relapse and poor prognosis. The 1p chromosome region likely harbors tumor suppressor genes or genes that control neuroblast differentiation. Deletion of 1p is more common in near-diploid tumors and is associated with a more advanced stage of the disease. Most of the deletions of 1p are located in the 1p36 area of the chromosome (134-136). The other segmental copy number alterations mainly include deletions of chromome 3p, 4p, 9p, 11q, 18q and gain of 1q, 2p and 17q (137-139). Partial 17q gain is frequently observed in primary tumors in association with segmental alterations, whatever MYCN status. The recurrent segmental alterations are thought to lead to the loss of putative tumor suppressor genes and/or to the gain of oncogenes (140, 141). The expression profiles of these regions, where genetic alterations occur, suggest some candidate genes involved in NB progression (142, 143).

Tumors from the youngest patients with lower stages of the disease are often hyperdiploid or near-triploid and numerical chromosomal alterations without structural rearrangements are associated with a favorable outcome (144-146).

Molecular markers for NB clinical features

Abnormal patterns of expression for some markers can also distinguish different NB clinical groups.

The three neurotrophin receptor gene products, NTRK1, NTRK2, and NTRK3, are tyrosine kinases that code for a receptor principally binding nerve growth factor (NGF), brain-derived neurotrophic factor (BDNF), and neurotrophin-3 (NT3), respectively. Interestingly, NTRK1 expression is correlated with lower age, lower stage and absence of MYCN amplification (147, 148), while the expression of the NTRK2 gene is strongly associated with MYCN-amplified tumors. As NTRK1/NGF signaling might have an important role in the differentiation of neuroblasts, the NTRK2/BDNF autocrine pathway seems to contribute to both enhanced angiogenesis and to drug resistance (149-152).

Other biological markers associated with poor prognosis include the increase of the multidrug resistance 1 transporter (MDR1), the multidrug resistance-related protein (MRP), and the telomerase, as well as the lack of expression of glycoprotein CD44 on the tumor cell surface (153-157).

Sporadic activating mutations in NB

Recently, somatic and activating mutations in the ALK sequence have been identified and represent an important new insight into the NB pathogenesis. To date, 54 ALK mutations in 680 sporadic NB cases (8% of cases) have been analyzed and shown in some cases to be responsible for an *in vitro* cytokine-independent growth of cell lines (158-162).

Normal biology of the neural crest cells

The neural crest lineages

The neural crest (NC) is a transient structure of the vertebrate embryo formed by the lateral borders of the neural tube and divided into four main functional (but overlapping) domains: cranial, trunk, vagal, and sacral NC. The constitutive NC stem cells, after losing their epithelial arrangement, migrate away through embryonic tissues to stop at elected sites where they generate a prodigious number of differentiated cell types [Table 0, adapted from (163)]. For instance, the trunk NC cells generate glia, neurons and melanocytes.

Derivative	Cell type or structure derived
I-Peripheral nervous system	Neurons, including sensory ganglia, sympathetic and parasympathetic ganglia Neuroglial cells Schwann cells
II-Endocrine and paraendocrine derivatives	Adrenal medulla Calcitonin-secreting cells Carotid body type I cells
III-Pigment cells	Melanocytes
III-Facial cartilage and bone	Facial and anterior ventral skull cartilage and bones
IV-Connective tissues	Corneal endothelium and strom Tooth papillae Dermis, smooth muscle and adipose tissue of skin of head and neck Connective tisue of salivary, lachrymal, thymus, thyroid and pituitary glands Connective tissue and smooth muscle in arteries of aortic arch origin

Table 0: Cell types and structures that are derived from human neural crest stem cells derivatives.

The gene regulatory network of neural crest cells

A complex gene regulatory network mediated the process of NC formation, which involves the early induction and maintenance of the precursor pool, emigration of the NC progenitors from the neural tube via an epithelial to mesenchymal transition (EMT), migration of progenitor cells along distinct pathways, and differentiation into diverse cell types. Several signaling pathways and transcription factors are involved in this succession of events (164).

Thus, WNT, bone morphogenetic proteins (BMP), and fibroblast growth factor (FGF) are responsible for NC induction, while products of genes such as SNAIL1, SNAIL2, SOX8, SOX9, SOX10, FOXD3, AP-2, TWIST, c-MYC, and the ID family members are involved in the NC specification.

The growth and survival factors present at the sites where NC cells migrate, are critical in choosing among the variety of differentiation potentialities of NC derivatives in each part of the body. Such factors include BMP2/4, which drive NC cells to an autonomic sympathetic-like neuronal fate (165-167); neuroregulin-1 and Notch ligands, which favor gliogenesis (168-170); and endothelin 3 (EDN3), which promotes survival and proliferation of glial-melanocytic bipotent precursors as well as committed melanocytic and glial cells (171-173) (Figure 0-2).

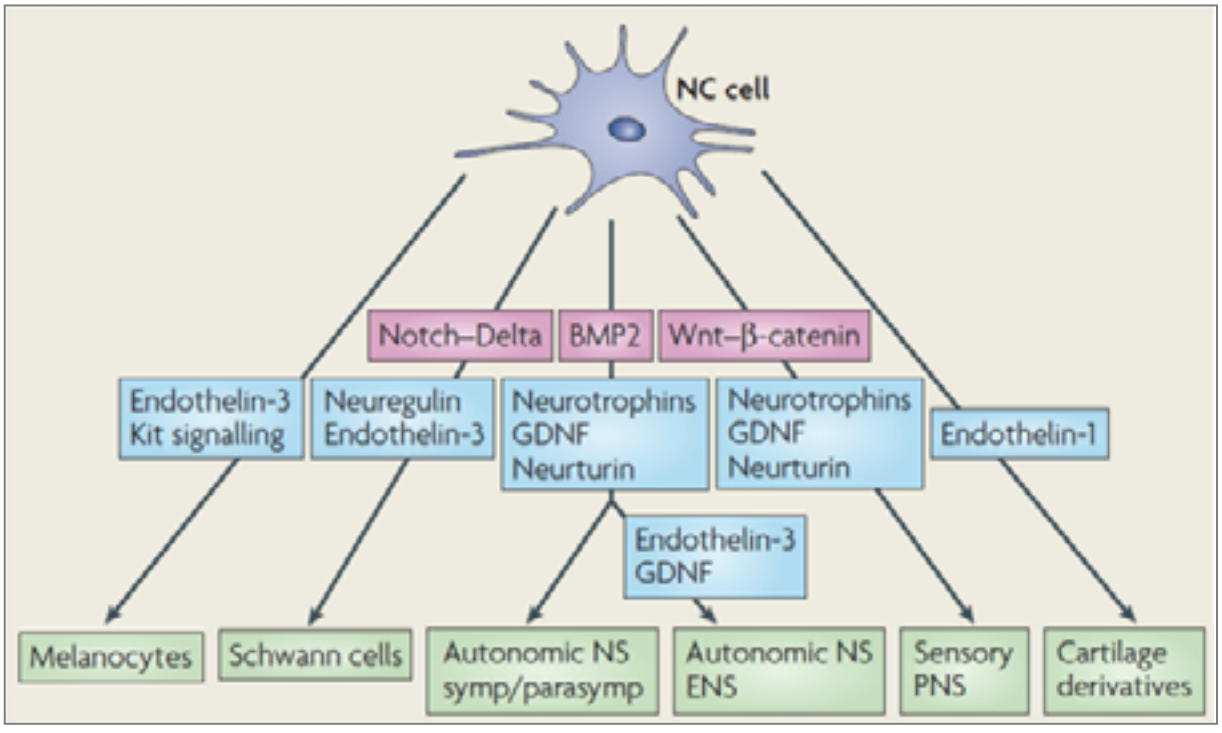

Figure 0-2: Molecular signals involved in fate determination and differentiation of the neural crest cells in human [from T. Sauka-Spengler and M. Bronner-Fraser (164)].

During NC cell migration, the cells, that have acquired a signaling receptor toolkit, receive many external cues allowing them to interact with other cells and the environment through which they migrate (174-176). These cues sensors include the Eph receptor and their ligands that may have a role in guiding and restricting the fate of the cell (177-179). Other signaling pathways have been shown to be essential in NC migration regulation such as the neuropilin-1 (NPL1) receptor and the semaphorin-III (SEMA3) ligand (180, 181), SLIT, and ROBO1-2 signaling molecules (182), and the glial-cell-derived neurotrophic factor (GDNF) (183).
NC cells can be isolated *in vitro*; they therefore exhibit a striking heterogeneity in their development potentials and have the capacity to self-renew (184-187).

CSC hypothesis suggests that CSC usurp the normal stem cell compartment pathways. These NC essential molecular signaling pathways may also be critical in the NB-CSC population gene networks.

Neuroblastoma and CSC

Stem-like NB cell subpopulations in NB cell lines

More than thirty years ago, observation of the cell phenotype diversity among NB cell lines identified morphologically and biochemically distinct cell types: N (neuroblastic) cells with noradrenergic neuron phenotype, S (substrate-adherent) cells resembling epithelial or fibroblast cells with melanocytic, Schwannian and/or meningeal properties, and morphologically intermediate I-type cells (121, 188-190). The three NB cell-types have been shown to express distinct neural crest lineages. In particular, I-type cells including the SK-N-Be(2)c cloned cell line have biochemical features of both N and S cells, could generate multipotent I-type progeny indicating their capacity of self-renewal, initiated tumors *in vivo,* and were clonogenic in anchorage-independent growth in soft agar assay. Thus I-type cells were proposed to represent a malignant neural crest stem cell (121, 191-194). The clonogenic self-renewal capacity of I-type cells have been shown to require the Polycomb group family transcription repressor Bmi-1 in a concentration-dependent manner (195).
These cells could represent a tool for *in vitro* assays alternative to primary NB samples to address the stem-like cell features in NB.

NB CSCs in primary NB tumors

Based on the hypothesis that stem-like cells harbor drug resistance phenotype, a dye-exclusion assay has been performed on NB cell lines to address the existence of a "side population" (SP) corresponding to a tumor cell fraction which is able to efflux the Hoechst33342 fluorescent dye. A distinct SP was found in NB cells from 15 of 23 analyzed patients and in 5 NB cell lines ranging from 4% to 37% of the total viable cells. Cells of the SP showed a higher expression level of the ABCG2 transporter gene than the non-SP fraction (196). However, this study did not address the tumorigenic and self-renewing potentials of the SP cells in primary NB samples by relevant methodologies.

More recently, Hansford and her colleagues were able to isolate sphere-forming cell populations by *in vitro* culture in a serum-free medium of dissociated tumors and bone marrow aspirates obtained from NB patients at diagnosis, remission or relapse (197). Primary sphere formation was observed within 2 to 8 weeks and all sphere cells expressed the NB84 marker, tyrosine hydroxylase (TH), fibronectin, nestin, and CD271 (p75 neurotrophin receptor) but were negative for CD133. No side population was observed in these cells. However, they were not able to confirm the presence of cytogenetic alterations typical of NB in all the primary cell lines. High-risk NB derived cell lines were shown to self-renew to a greater extent than tumor spheres from low-risk NB and to exhibit much less differentiation potential. In addition, 10 of the sphere cells were orthotopically grafted in the adrenal fat pad of immunocompromised mice and were able to develop a tumor that metastasized and could be serially transplanted. $CD34^{+}/CD24^{+}$ NB sphere cells were shown to be tumorigenic and to be responsible for a significantly higher morbidity in implanted animals compared to the non-sorted sphere cell population. However, the expression of these markers was not addressed in NB primary samples and their relevance to identify NB CSCs was not discussed.

The NB sphere lines established in this study were further used to identify selective NB-CSCs targets by small-molecule screens (198). In order to find chemical drugs that would also spare the normal pediatric stem cells, they included dermal stem cells, termed skin-derived progenitors (SKPs) in the screen. SKPs that have been isolated and cultured as spheres in serum-free media from neonatal skin, are non tumorigenic and exhibit properties similar to neural crest stem cells (199-201). Sixteen compounds were identified to specifically kill NB CSCs. In particular, DECA14 were shown to induce 100-fold more cell death in the NB CSC population than in the SKP cells. However, NB cell lines such as SK-N-AS and SH-SY5Y had a very low sensitivity to DECA14. Smith et al. also addressed the cytotoxic effect of rapamycin, an m-Tor inhibitor that was previously shown to be a leukemic stem cell specific drug but was not found in their screen (202). Rapamycin decreased the NB CSC derived tumor growth *in vivo*.

Finally, a large-scale transcriptome analysis of the NB CSCs vs. SKPs was performed to determine enriched RNAs in NB CSCs (203). 321 genes were found to be over-expressed in NB CSCs compared to SKP cells. In particular, BRCA1 showed an elevated expression level in NB CSCs. In addition, the list of NB CSC associated genes was used to identify new potential specific treatments. Thus, the inhibition of AURKB, overexpressed in NB CSCs, by shRNA induced an 80% reduction of cell growth.

These findings supported the hypothesis of NB CSCs existence. However, all results were obtained from the same samples in particular the NB12 sphere line described by Hansford et al. (197), and used SKP cells as a control. Moreover, the NB12 cell line has been shown to express CD20, a marker for hematopoietic stem cells, casting doubt on the phenotype of this putative NB CSC line. The truthfulness of the CSC model in NB tumors needs to be further investigated by increasing the number of patients and defining more reliable methodological strategies and controls.

AIM OF THE PROJECT

Neuroblastoma (NB) remains one of the deadliest tumors in early childhood, for which new therapies are urgently needed. This neural crest-derived tumor displays a surprising heterogeneity at clinical and biological levels, which origin remains an enigma. There is increasing evidence that a fraction of cells called “cancer stem cells” (CSCs) present within the tumor is responsible for initiation and maintenance of many tumor types and represents a powerful potential therapeutic target.

However, for several cancers, including NB and other childhood solid tumors, this population has not yet been identified nor characterized. Actually the identification and targeting of CSCs to definitively eradicate the disease represent an essential challenge for oncologists and researchers.

In preliminary results, we identified cells within NB primary tumors which harbored markers of neural crest stem cells and neural crest lineages leading us to hypothesize that CSCs concept could explain the NB tumor cell heterogeneity and thus be relevant in NB tumors.

In this project we proposed to address the existence of CSCs in NB by prospectively characterizing their self-renewal and *in vivo* tumorigenic properties by using novel and original combinations of sphere-forming assays, gene expression profiling and *in vivo* orthotopic implantations for tumorigenic assays.

Stage 4 patients frequently show resistance to treatment and relapse. Thus they were elected as relevant material to address the presence of CSC fraction. Clinically, the identification of cells within this group of NB that could be responsible for tumor initiation and propagation, resistance to cytotoxic agents and metastases may offer new trails for therapeutic treatment targeting specifically the CSC population. Moreover, the results of this study may bring supplementary insights into the origin and development of NB that could also lead to new data for the comprehension of other related aggressive tumors.

MATERIALS AND METHODS

Patients and genomic profiling by array-Comparative Genomic Hybridization (CGH)

For this study, a cohort of 10 patients (referred to the CHUV hemato-oncology Unit for diagnosis and/or tumor biology assessment) with NB diagnosed between 2004 and 2009 were analyzed. The cohort includes five stage 4 patients (NB1-5), one stage 3 patient (NB6), three stage 4s patients (NB7-9) and one patient with a post-chemotherapy differentiated ganglioneuroma (NB10). The biopsies and the bone aspirations were collected at diagnosis except for NB6 and NB10 whose primary tumors were removed after at least one course of chemotherapy, and NB4 which corresponds to the infiltrated bone marrow at relapse. For the two samples obtained after the chemotherapy, the patients were treated according to local and international protocols (SIOP, POG). The material was collected after informed consent and in agreement with local institutional ethical regulations.

To determine the genetic type of the NB samples, array-CGH were performed either at the array-CGH platform of the Curie Institute in Paris (NB1 and NB9) or at the cytogenetic department of the hospital of Lausanne (Agilent) (NB2, NB3, NB6-8 and NB10) as described previously (204) with a resolution of approximately 1 Mb. Genomic pattern has been determined for NB4 and NB5 by Fluorescence In Situ Hybridization (FISH) on 1p, 2p, 17p and 17q chromosomal segments (Children's Cancer Research Institute, Vienna and Inselspital, Bern respectively). Tumor cell content was greater than 60% in all analyzed samples and DNAs were extracted from the primary sample according to consensual DNA extraction protocol.

Histopathological and immunohistochemical analyses

Standard haematoxylin/eosin (H/E) staining procedures and immunostaining of p75 (CD271), CD44, CD31 and Ki67 were performed on paraffin-embedded tissues. 4 µm sections were deparaffinated in a xylol bath for 15 min and 5 times rinsed with xylol. Sections were rehydrated by transfers in alcohol baths for 5 min with descending concentration (100%, 95%, 70%, and 40%) and finally in H_20. Then, they were washed for 5 min in 3% H_2O_2 to inhibit endogenous peroxydase. Slides were incubated in citrate buffered 10mM Tris at pH6 for 5 min and heated in a microwave oven for 15 min at 500W. Mouse monoclonal anti-human p75 [clone ME20.4, (205)], rabbit polyclonal anti-human CD31 (Thermo Fisher Scientific, USA), and mouse monoclonal anti-human Ki67 (clone MIB-1, DAKO) primary antibodies were added in 1/5, 1/200, and 1/50 dilutions respectively, in citrate buffered 10mM Tris at pH6 and incubated overnight. Incubation with secondary antibody was performed

using HRP EnVision anti-mouse antibodies (Dako, Glostrup, Denmark) for 30 min. Treatment with 100µl DAB (Dako, Glostrup, Denmark) at 1/50 dilution for 8min, was then performed and slides were mounted using Eukitt (EMS, Hatfield, PA). Washings between each step were done in TBS pH 7.6.

Preparation of single cell suspensions of tumor cells

Primary solid tumor samples were stored sterile in Dulbecco's Modified Eagle's Medium (DMEM)/F12 (Gibco, Paisley, UK) and processed within 10h after resection. Primary human tumors or xenograft tumors were washed, cut into fragments and further mechanically minced using sterile scissors. To obtain a single cell suspension, the minced tissues were incubated in PBS containing 0.01 mg/ml collagenaseII (Invitrogen, Grand Island, NY, USA) and 0.1 mg/ml DNaseI (Roche, Switzerland) for 30 minutes at 37°C with frequent pipetting, followed by filtration through CellTricks® (50µm, Partek, Germany). Erythrocytes were lysed by incubating the cells in 0.88% NH_4Cl for 15 min at 37°C and washing in PBS. Viable cells were counted after trypan blue staining.

Cells and culture media

Neuroblastoma cell lines, including LAN-1 (189) and SK-N-BE(2)C (121), were grown in DMEM containing 10% fetal calf serum (FCS) (Sigma, Taufkirchen, Germany), 100 U/ml penicillin and 100ug/ml streptomycin (Invitrogen) and referred as FCS-medium.

The NB1-FCS and NB1-NBM cell lines were established by plating the cell suspension of dissociated NB1-xenograft tumor in FCS-medium and Neural Basic Medium (NBM) respectively. NBM is a stem-cell permissive medium, consisting in DMEM/F12 supplemented with penicillin/streptomycin, 2% B27 (Gibco), human recombinant FGF-basic (20 ng/mL; Peprotech, USA) and EGF (20 ng/mL; Peprotech). Cells grown adherent were passed every 3-4 days using 0.05% trypsin-EDTA (Gibco). Enzymatic digestion was stopped using FCS-medium for all cell lines except NB1-NBM. For this cell line, we used trypsin inhibitor (from Glycin max, Sigma) at 1:1 with trypsin and washed cells once with PBS.

For sphere culture, a neural crest sphere (NCS)-medium which was specifically defined to support the selected growth of neural-crest cell stem cells and progenitors was used. NCS-medium was adapted from (206) and contained DMEM-F12, 20 ng/ml FGF2, 20 ng/ml IGF1, 20 ng/ml EGF (all Peprotech), 1% N2 supplement, 2% B27, 1% Penicillin/Streptomycin (all Invitrogen), 50 µM 2-mercaptoethanol, 35 ng/mL retinoic acid (Sigma) and 15% chicken embryonic extract (CEE). CEE was prepared as described in (186). Briefly, for CEE preparation, fertilized eggs were incubated for 11 days. Embryo bodies were then passed through sterile syringes and enzymatically dissociated by a 10mg/ml

hyaluronidase solution for one hour at 4°C. Tissues were therefore centrifuged at 30'000g for 6 hours at 4°C, the supernatant was filtrated and kept at -80°C as aliquots.

Sphere cultures

For sphere culture, human NB tumor cells were transferred at the concentration of 30 to 80.10^5 cells/ml into NCS-medium and cultured in poly(2-hydroxyethyl methylacrylate) (16 mg/mL in EtOH; Sigma) coated 6-well culture plates to eliminate adhesion of cells to the plastic surface, in 37°C/5% CO_2 conditions. Spheres were passed every 7-10 days by dissociation in 0.05% trypsin-EDTA (Gibco). The enzymatic digestion was stopped by trypsin inhibitor (Sigma) and the cells were filtered in CellTricks® (50-µm, Partec) to obtain a single cell suspension.

To assess self-renewal, sphere assays were performed by plating 5.10^3-10^4 tumor cells in NCS-medium in coated 24-well culture plates in quadruplicates. Spheres were passaged every 7-10 days. Secondary spheres with a diameter>400 µm were counted in each well. To determine the ratio of sphere cell survival after each passage, the number of live cells obtained after passage of the spheres in one well was reported to the total number of cells from the previous passage that were plated in this well.

Endothelin axis inhibition

Bosentan, a specific antagonist of endothelin receptors (207), has been supplied by L. Juillerat-Jeanneret, Pathology Institute of the University Hospital (Lausanne, Switzerland). An 8mM aqueous stock solution has been used for the self-renewal assay and was added in the sphere culture at the final concentration of 80 µM. 10^4 cells were seeded as previously described and secondary spheres were counted 7 days after plating.

Cell viability assay

To induce cell death, NB cells (1 to 2×10^4/well in 96-well-plates; 100 µl) were plated in FCS-medium or NBM (NB1-NBM) 24 hours before a 72h-treatment with 0-120 µM Bosentan. Cell viability was measured in quadruplicate using the MTS/PMS® cell proliferation kit from Promega (Madison, WI, USA) according to manufacturer's instructions. The percentage of viable cells in treated groups was compared to that in the untreated controls.

Total RNA extraction

Dissociated tumor cells and trypsinized cell lines were collected and pelleted. The non-adherent spheres were collected by decantation for each passage. Cells were lysed by TRIZOL® Reagent (Invitrogen) and total RNAs were obtained by two extractions with UltraPure™ Phenol:Chloroform:Isoamyl Alcohol (25:24:1) (Invitrogen) and by purification using RNeasy MicroKit columns (Qiagen, Hilden, Germany). The quality of each RNA sample was verified by a Bioanalyser 2100 of Agilent Technologies.

Gene expression profiling

Genechip™ hybridization

Micro-array experiments were carried out at the DNA Array Facility Lausanne (DAFL), of the Center for Integrative Genomics (CIG), University of Lausanne, in collaboration with Dr. O. Hagenbüchle and Dr. K. Harshman. The DAFL provided support for the bioinformatics and data analysis. Expression profiling experiments were performed using the Human Genome U133Plus 2.0 Affymetrix GeneChip oligonucleotide array containing 47'000 probe sets.

Each GeneChip™ was hybridized using targets synthesized from 100-250 ng starting material (total RNA). Target synthesis, hybridization, staining and washing were performed using standard protocols as recommended by the manufacturer (Affymetrix Santa Clara, CA, USA).

Data analyses and statistical methods

The Remote Analysis Computation for gene Expression data (RACE) system has been used (208). This suite of programs was developed by the DAFL bioinformatics group (UNIL) and allows for automated and batch-wise analysis of micro-array data. The system provides an interface that allows easily configuration of multi GeneChip data quality visualizations, multi GeneChip data normalizations and calculation of expression ratios. Expression values are measured using RMA algorihm, from the BioConductor "affy" package, comprising background correction, quantile normalization and probe set summary by robust regression (from DAFL data). The resulting expression values are on the log2 scale and range from 0 to 16.

The statistical analyses of differentially expressed genes were performed using the "R" statistical version 2.0.1. The statistical value for the "step" gene analysis has been calculated by the formula:

with X="step" statistics and mean(P1:P4)-P0 = "step" change. A cut-off has been defined as the absolute value of X=3.

The p-values associated to the fold change (fold-change ≥ 2) were corrected for multiple testing using the false discovery rate (FDR) method and the FDR cut-off level was set at 5%.
The enrichment analysis in the neurosphere expression profile of genes for canonical pathway genes or GO annotations has been performed using the software MetaCore from GeneGo Inc. (http://www.genego.com).

cDNA synthesis and semi-quantitative real-time PCR

Reverse transcription of total RNAs was performed using random primers and SuperScript II reverse transcriptase, according to manufacturer's instruction (Invitrogen). The relative expressions of sphere-associated genes were assessed by real-time semi-quantitative PCR using the ABI PRISM 7900 HT real-time PCR system of Applied Biosystem with SYBR Green© detection (Qiagen). The expression levels of two or three independent experiments evaluating the expression levels of the CD133, EDNRB, GPR177, NOTCH3, MDR1, NOTCH2, ROBO1, ABCA1 and IGFBP5 transcripts for each sample were calculated relatively to the level of the housekeeping gene HPRTI. The $\Delta\Delta C_t$ method was used to evaluate the relative gene expression. Amplification reactions were performed with pairs of primers specific for human HPRT1 (5'-TGACACTGGCAAAACAATGCA-3' and 5'-GGTCCTTTTCACCAGCAAGCT-3'), CD133 (5'-CATGGCAACAGCGATCAAG-3' and 5'-AGCACAGAGGGTCATTGAG-3'), MDR1 (5'-TTCTGGGAAGAT-3' AND 5'-TATGGTACCTGCAAACTCTG-3'), EDNRB (5'-CGAAACGGTCCCAATATC-3' and 5'-CCAGCTTACACATCTCAG-3'), NOTCH3 (5'-AGTGGCGACCTCACTTACGACT GTGCCTGTC-3' and 5'-GGGCACTGGCAGTTATAG-3'), SNAI2 (5'-CTACAGCGAACTGGACACACA-3' and 5'-TTGTGGTATGACAGGCATGG-3'), GPR177 (5'-CTGGATGCTGCTGTTTGG-3' and 5'-TACCCTGCGATGTGGTTC-3'), ROBO1 (5'-TTGCTTTGGGACGGACTG-3' and 5'-ATCGGCTGGATGACTGTG-3'), ABCA1 (5'-GACATCCTGAAGCCAATC-3' and 5'-AGAGTCCCAAGACTATGC-3'). PCR program corresponded to: 2 min at 50°C for stabilization, 5 min at 95°C for SYBR activation, 40 cycles of three repeated steps of amplification (10 sec at 95°C, 30 sec at 60°C, 15 sec at 95°C) and 15 sec at 65°C.

Endothelin axis PCR analysis of NB samples

cDNA from NB samples were obtained as described above. Standard PCR amplifications of endothelin (EDNs) and endothelin receptor (EDNRA/B) sequences were performed using pairs of primers specific for EDN1 (5'-CTTCTGCCACCTGGACATCATTTGG-3' and 5'-CAGTCTTTCTCCATAATGTCTTCAGC-3'), EDN2 (5'-CTTCTGCCACTTGGACATCATCTGG-3' and 5'-GGCCTCCTGTTGTCGCTTGGCAA-3'), EDN3 (5'-CTATTGCCACCTGGACATCATTTGG-3' and 5'-GAGGCAGCGGGGGCAGGTAGAT-3'), EDNRA (5'-TTGCCCTCAGTGAACATC-3' and 5'-CATCGGTTCTTGTCCATC-3') and GAPDH (5'-

AGATCATCAGCAATGCCTCC-3' and 5'-GTGGCAGTGATGGCATGGAC-3') as a control (EDNRB primers described above). The amplification reaction was performed in 20µl volume containing Hotstart Buffer 10X, 0.25mM of each dNTP, 1 µM of forward and reverse primers and 0.5U Hotstart-Taq DNA polymerase (Quiagen). All primers were used under standard PCR conditions (95°C 15 min; [94°C 30 sec; 55°C 45 sec; 72°C 1 min]x35 cycles; 72°C 7 min). To visualize the amplification products, PCR reactions were loaded on 2% agarose gels.

Cell staining for Fluorescent-Activated Cell Sorter (FACS) analysis

Adherent cells were detached by 0.05% trypsin-EDTA (Gibco). Cells were counted and then transferred to a 5-ml tube, washed twice in PBS containing 0.5% bovine serum albumin (BSA) and 2mmol/L-EDTA and stained with CD133/1-APC (Clone AC133, Miltenyi Biotech, Germany) and MDR1-PE (P-glycoprotein, clone UIC2, Beckman Coulter, USA) conjugated monoclonal antibodies. Antibodies (appropriate dilution per antibody according to manufacturer's instructions) were incubated for 20 min at 6°C and then washed twice with PBS/BSA-EDTA. For disialoganglioside staining, primary antibody used was anti-GD2 (Clone 14.G2a, BD Pharmingen, USA) and staining was visualized using anti-mouse AlexaFluor-488 (Molecular Probes) antibody conjugate. A total of 10 millions cells were analyzed and sorted at 4°C in sterile conditions according to the appropriate cell marker by FACSAriaII^{TM} cellsorter (BD Biosciences, USA) and then transferred in DMEM/F12 medium. Side scatter and forward scatter profiles were used to eliminate dead cells and cell doublets during the sorting.

In vivo studies

All animal experiments were carried out with athymic Swiss nude mice (Balb/C nu/nu), in accordance to the European Community guidelines (directive no. 86/609/CEE). For surgical and ultrasonic procedures, mice were anaesthetized using isoflurane and received paracetamol as analgesia the day before the surgery.

Fresh NB specimens, either NB cells obtained from involved bone marrow aspirations after dead cells removal and Ficoll gradient separation or biopsies fragments were subcutaneously implanted in the mice left flanks.

Tumorigenic assays

For heterotopic assays, groups of 6 mice were subcutaneously injected in the flank with 10^4 cells suspended in 200 µl 1:1 mix of DMEM/F12 and BD Matrigel^{TM}. Matrigel, used to enable cell grouping

and attachment in *in vivo* engraftments, contains extra-cellular matrix components (56% laminin, 31% collagen IV and 8% entactin) and growth factors (0-0.1 pg/ml bFGF, 0.5-1.3 ng/ml EGF, 15.6 ng/ml IGF-1, 12 pg/ml PDGF, <0.2 ng/ml and 2.3 ng/ml TGF-β). The grafted animals were then weekly monitored with calipers for tumor growth. The tumor volume was calculated using the formula: volume = (length×width^2)/2.

For orthotopic assays, cells were implanted in the adrenal gland of athymic Swiss nude mice as previously described (209). Briefly, the implantation was performed through a midline incision practiced under the microscope. A total of 10^4 NB cells in 15 µl PBS were injected in the left adrenal gland using a 22G needle connected to a Hamilton syringe. The abdominal wall and skin were closed with a continuous suture of 4.0 Safil Quick® (B/Braun). Tumor development and growth were assessed by ultrasound imaging every 15 days in the Lausanne animal imaging platform for a period of up to 100 days. Macroscopic metastases to the liver and other organs have been evaluated by gross examination.

Statistical analysis

Statistical analyses were carried out using GraphPad Prism 4.0 (La Jolla, CA, USA). *p<0.05 was consider to represent significance, **p<0.01 and ***p<0.001 were interpreted to be highly significant.

RESULTS

Neuroblastoma patient samples

Neuroblastoma (NB) is characterized by an important heterogeneity. In this study, we postulated that cells with stem-like characteristics (CSC) would be more likely detectable in high stage and progressing NBs, capable to generate serial spheres in particular culture conditions (197). We took advantage of this property to characterize a CSC-associated phenotype in clinically and biologically well characterized material.

NB cell lines, although in majority established from stage 4 metastatic cells, may not always faithfully represent the aggressive features of clinical material. A surprisingly important population of tumorigenic and sphere-forming cells can be isolated with some cell lines, suggesting that a likely selection of self-renewable, tumorigenic functions over the time in culture has occurred (Morrison and personal observation). In contrast, some cell lines with a more differentiated phenotype produced very few spheres in identical conditions, and thus illustrated the heterogeneity observed with clinical material. Moreover, *in vitro* culture in serum-containing medium has been shown to induce additional chromosomic alteration in the cell genome and modification in the gene expression pattern (210). These observations suggested that NB cells derived from primary NB may be a more reliable model than many commonly used cancer cell lines to address the existence of CSCs population. Moreover, as metastatic population were also more likely to show CSC phenotype, we have in priority worked with metastatic cells isolated from involved bone-marrows at diagnosis. In isolated cases we also worked with cells dissociated from primary tissue.

As shown in Table 1, 10 patient tumor samples and 4 cell lines were included in the study. Clinical characteristics such as age, stage, sample type, histology follow-up and genetic properties, MYCN and pan-genomic status are shown.

Sample	Sex	Age at diagnosis	Stage (INSS)	Specimen type	Histology	BM infiltration	NMYC	Genetic type	Follow-Up	Xenograft tumor	Spheres	NBM cell-line	Risk Group
NB1	M	10 months	4	bm	FH	yes	NA	B	DOD	yes (P16)	P5	yes (P>>10)	HR
NB2	F	44 months	4	bm	UH	yes	NA	B	CR	yes (P8)	P2	no	HR
NB3	M	40 months	4	pt	UH	yes	NA	B	DOD	yes (P1)	P1	yes*/P2	HR
NB4	M	12 years	4	bm-rel	UH	yes	NA	B	DOD	yes (P3)	P3	yes*/P2	HR
NB5	M	24 months	4	bm	UH	yes	A	C/E	CR	yes (P2)	P2	no	HR
NB6	F	58 months	3	pt-pc	UH	no	NA	D	AD	no	P2	*nd*	HR
NB7	F	1day	4s	bm	FH	yes	NA	D	CR	no	no	yes*/P2	LR/IR
NB8	F	8 months	4s	cut	FH	no	NA	nd	VGPR	*nd*	no	no	LR/IR
NB9	F	5 day	4s	pt	FH	nd	NA	D	VGPR	no	no	no	LR/IR
NB10	F	22 months	3/GGN	pt-pc	GGNB-GGN	no	NA	flat	CR	no	no	no	LR
NB1-NBM			4	bm			NA			yes	P5		
NB1-FCS			4	bm			NA			no	no		
LAN-1			4	bm			A			yes	>>P5		
SK-N-BE(2)C			4	bm			A			yes	>>P5		

Table 1: Patients and cell lines characteristics.

The tumor growth capacity of NB samples was assessed by subcutaneous engraftment in nude mice. The NB specimens were also tested for their sphere-forming capacity and *in vitro* growth in a serum-free medium. The genetic type has been determined using the published classification of NB according to overall genomic pattern (211).

* indicates that the cells were non adherent and spontaneously grew as spheres.

Abbreviations: GGN=ganglioneuroma, nd=not determined, bm=bone marrow, pt=primary tumor, pc=post-chemotherapy, cut=cutaneous metastasis, rel=relapse, FH/UFH= favorable/unfavorable histology, NA=no amplification of NMYC locus, A=amplified NMYC locus, DOD = dead of disease, CR=complete remission, AD= alive with disease, VGPR=very good partial response, P=No. passage, HR=High risk group, LR: low risk group, IR=Intermediate risk group.

Clinical/genetic features

Five stage 4, two stage 3 (NB6 and NB10) and three stages 4s clinical samples were included. Tumor samples were isolated from the bone marrow in 5 cases (at relapse for NB4), from the primary tumor in 4 other cases (after chemotherapy for NB6 and NB10) and from a cutaneous nodule in NB8. Histology as defined by Shimada et al. was determined for all cases (129). Histology at diagnosis was found favorable for NB7-9, while it was unfavorable for NB1-6. MYCN amplification was observed in 1 out of the 6 stage 4 samples. Array-CGH was performed for most patient samples, allowing us to determine the genetic type, as proposed (211). All stage 4 samples showed segmental and /or numerical chromosomic alterations, and were types B to E. One stage 3 showed numerical and segmental alterations. The stage 3 NB10 sample, obtained after chemotherapy, had fully differentiated into a ganglioneuroma and presented a compatible flat profile. The 4s tumors, NB7 and NB9, were type D (Table1).

Four cell lines were also included. Two cell lines originated from the bone marrow of the single MYCN copy patient NB1. The NB1-NBM cell line was established in serum-free, EGF-, bFGF- and B27-supplemented medium (NBM), while NB1-FCS cell line was established in 10% FCS-containing DMEM medium. The I-type SK-N-BE(2)C, and the N-type LAN-1 cell lines were propagated in classical medium in presence of serum.

Analysis of neural crest stem cell markers in NB samples: on the way to NB-CSCs hypothesis

NB tumors are composed of a heterogeneous population of tumor cells with respect to their ability to proliferate and differentiate and may contain cancer stem cells that are responsible for this diversity. Immortalized I-type NB cell lines such as SK-N-Be(2)c were shown to have neural crest stem cells (NCSC) features (191, 212) and *in vitro* studies in immortalized NB cell lines have shown that activation of distinct signal transduction pathways could generate cells with neuronal (213), chromaffin (214) or Schwannian (215) phenotypes, further supporting the evidence of a cell with stem cell properties in NB.

Expression of NCSC and neural crest lineage progenitor markers in NB tumors and cell lines

NB1-10, primary and xenograft tumors were analyzed by immunohistochemistry (IHC). They showed an inter-cellular heterogeneity regarding the expression of specific genes associated to neural crest stem cells and their derivatives, including the low affinity nerve growth factor receptor (p75), the smooth muscle actine (ACTA2), the glial fibrillary acidic protein (GFAP) and the neurofilament 160 (NFEM) .

Cells showing a positive staining for p75 in IHC, a recognized neural crest stem cell marker, were observed in the NB1, NB3 and NB4 tumors but not in NB5 (Figure 1). No primary sample for NB2 was available for the analysis.

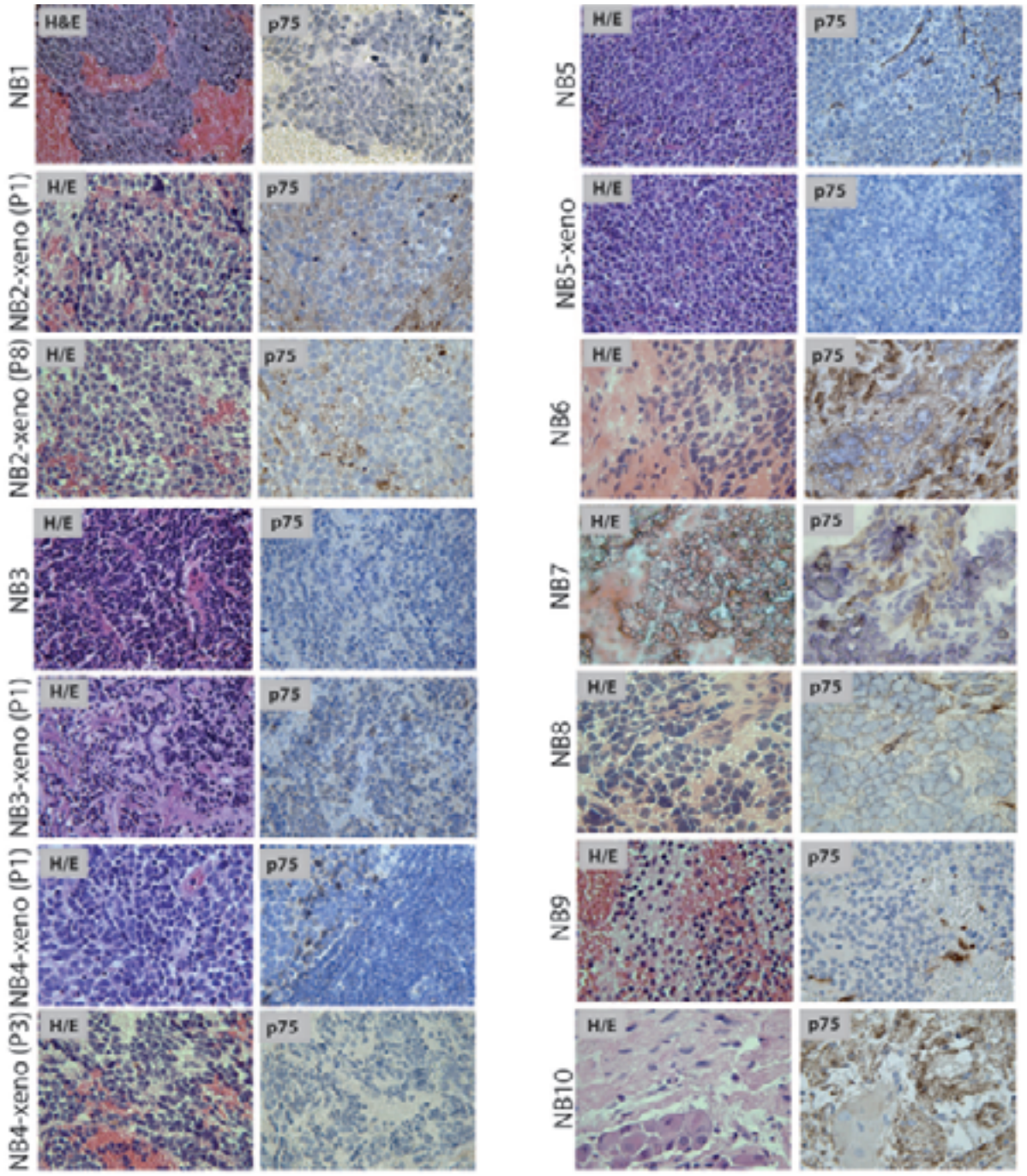

Figure 1: Histology of neuroblastoma primary and xenograft tumors, and p75 tissue expression.
To analyze the histology of the five stage 4 NB1-5, the stage 3 NB6 sample, the three stage 4s NB7-9 and the ganglioneuroma NB10 primary and xenograft tumor samples (*cf.* Table 1), tumor sections were stained by Hematoxylin/Eosin (H/E) reaction and observed with a microscope with a 40x magnification. The samples were also tested by immunohistochemistry (IHC) for their expression of the low-affinity NGF receptor p75. The derived xenograft tumors were established in nude mice (NB1-5-xeno). The passage number (P) of the xenograft tumor is indicated.

To indirectly address the existence within these NB samples of cells with glial, neuronal and connective features, GFAP, NEFM and ACTA2 expressions were analyzed (Figure 2). All tumor samples showed the expression of at least one or two markers for neural crest progenitor cells, highlighting the hierarchical organization of the tumors that mimics the physiological organization of the neural crest derived-tissues.

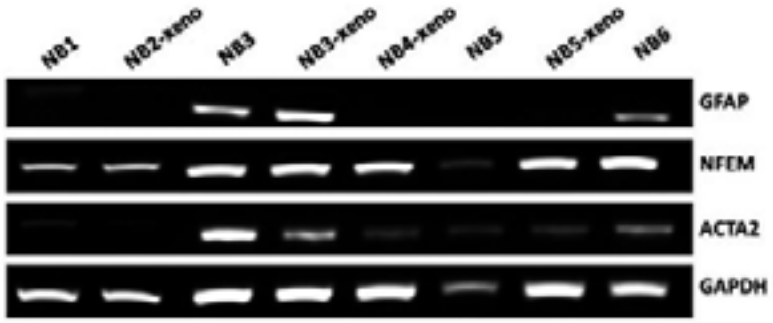

Figure 2: Neuroblastoma primary and xenograft tumors express various markers of neural crest lineages.
Analysis by RT-PCR for the presence of the GFAP, NFEM, ACTA2 and GAPDH gene transcripts in total RNAs extracted from the primary tumors NB1, NB3, NB5 and NB6, and the corresponding NB2, NB3, NB4 and NB5 xenograft tumors.

Finally, the cellular heterogeneity of NB tumors, their differential disease course related to patient age at diagnosis, the treatment response and their origin from the embryonic neural crest led us to consider the existence of NB-CSCs.

The validation of the NB-CSCs hypothesis was therefore required and addressed by functional assays based on CSCs-properties, such as self-renewal and *in vivo* tumorigenicity, in NB tumor samples.

High stage NB1 tumor as study model

NB1 tumor, a model to study NB-CSCs

The patient sample NB1 presented the highest capacities to form NS, and to induce serial tumor formation in the animal (Table 1). We hypothesized that NB1 tumor was the most likely to contain identifiable CSCs and was therefore selected for further thorough investigations.

Two other high stage NB tumors, NB2 and NB4 (Table 1), have been analyzed to validate the results observed in the NB1 study model.

In vivo maintenance of the NB1 sample and NB1 derived cell lines

In order to have available live tumor tissue throughout months, NB1 sample was maintained by serial *in vivo* tissue engraftments; the NB1 patient bone-marrow cells were initially used to establish a NB1-xenograft tumor by s.c. nude mouse engraftment (Figure 3A). The same procedure was applied on NB2 and NB4 samples to generate NB2-xenograft and NB4-xenograft tumors respectively (Figure 3B). These tumors were maintained alive by serial implantations of tissue fragments in nude mice.

As shown in figure 3A, we also established NB1-NBM and NB1-FCS cell lines (Table 1) from dissociated NB1-xenograft tumor, by culture in a defined medium to support the growth of neural crest cells (NBM medium) and in classical FCS-supplemented medium respectively.

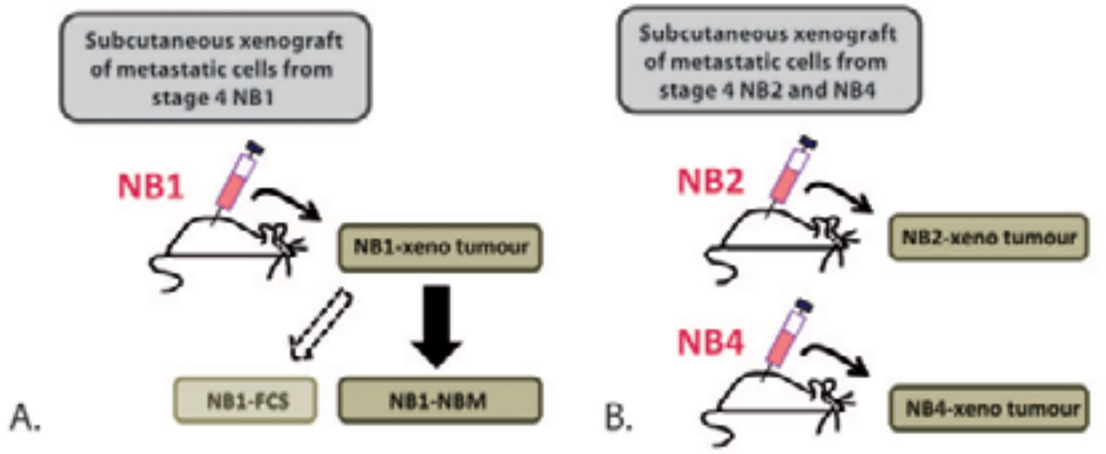

Figure 3: Model for *in vivo* propagation of NB xenografts derived from stage4 NB1, NB2 and NB4 bone marrow cells

Subcutaneous implantation of infiltrated bone marrow cells from NB1, NB2 and NB4 patients generated the heterotopic tumors NB1-xeno (**A**), NB2-xeno and NB4-xeno (**B**) in Swiss nude mice, respectively.

NB1-NBM and NB1-FCS correspond to established cell lines from NB1-xeno in serum-free and 10%-FCS medium respectively.

Stability of the NB phenotype in the xenograft tumors and derived cell lines

NB specific marker expression

To confirm the NB origin of the xenograft tumors derived from NB1 sample, the expression of NB-specific markers was measured. NB cells can be easily identified by the expression of the disialoganglioside GD2, a specific and sensitive marker of tumors of neuroectodermal origin, or p75, the low affinity receptor for NGF associated with neural crest lineages. FACS analysis showed that 95.1% cells from the dissociated NB xenografts were positive for GD2 (Figure 4A). NB1-NBM and NB1-FCS derived from this sample were also made up of a majority of GD2 positive cells (Figure 4A). Likewise, NB2-xenograft and NB4-xenograft tumors were also checked by FACS for GD2 positivity (Figure 4A).

To rule out a possible subcutaneous growth of either transformed or fused hematopoietic progenitors from the NB1 bone marrow, we measured by FACS the surface expression of CD20, a typical B-cell marker, in NB1-NBM (Figure 4B). CD20 surface expression was detected neither in the NB1-xeno cells nor in the NB1 derived cell line, confirming the NB phenotype of the NB1-xenograft cells.

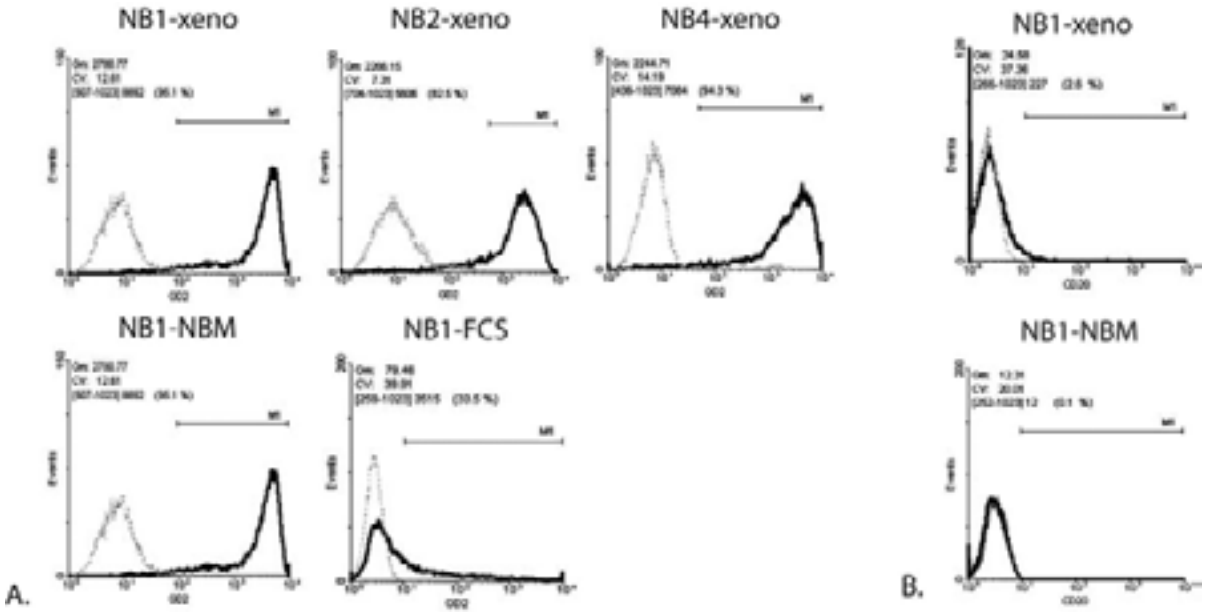

Figure 4: NB origin of the NB xenograft tumors by FACS analysis.

A. Cell surface expression of GD2 specific marker for NB cells in the NB1, NB2 and NB4 dissociated tumor xenografts and the NB1-NBM and NB1-FCS cell lines. **B.** Cell surface expression of CD20 marker in the NB1-xenograft cells and its NB1-NBM derived cell line. Black lines represent the fluorescent signals for GD2 (A) and CD20 (B) specific antibodies and the grey line corresponds to control with secondary antibody alone (A) or isotype antibody (B).

Histology features

To address the retention of original NB1 histology features in different passages of NB1-xenograft tumors, paraffin sections of these samples have been stained with Hematoxylin/Eosine (H/E) and checked for Ki67 proliferation marker and CD31 endothelial cell marker expression (Figure 5). As shown on H/E prints (left panel), the histology of NB1 tumor evaluated at diagnosis, revealed NB1 as a typical proliferative and stroma poor tumor, showing a high degree of vascularization, and was thus classified in the Unfavorable Histology (UFH) group (Table 1) (129). The NB1-xenograft tumor deriving from bone-marrow metastatic cells, showed typical poorly differentiated NB histology, with undifferentiated and highly proliferating small round blue cells, and an important vascularization (CD31 expressing cells) with infiltration of erythrocyte (H/E).

The expression of p75 marker, as measured by IHC on NB1 and NB1-xenograft paraffin sections, remained stable over several *in vivo* passages (Figure 5). These results demonstrated the stability of patient tissue morphology and cellular phenotypes in the derived-xenografts.

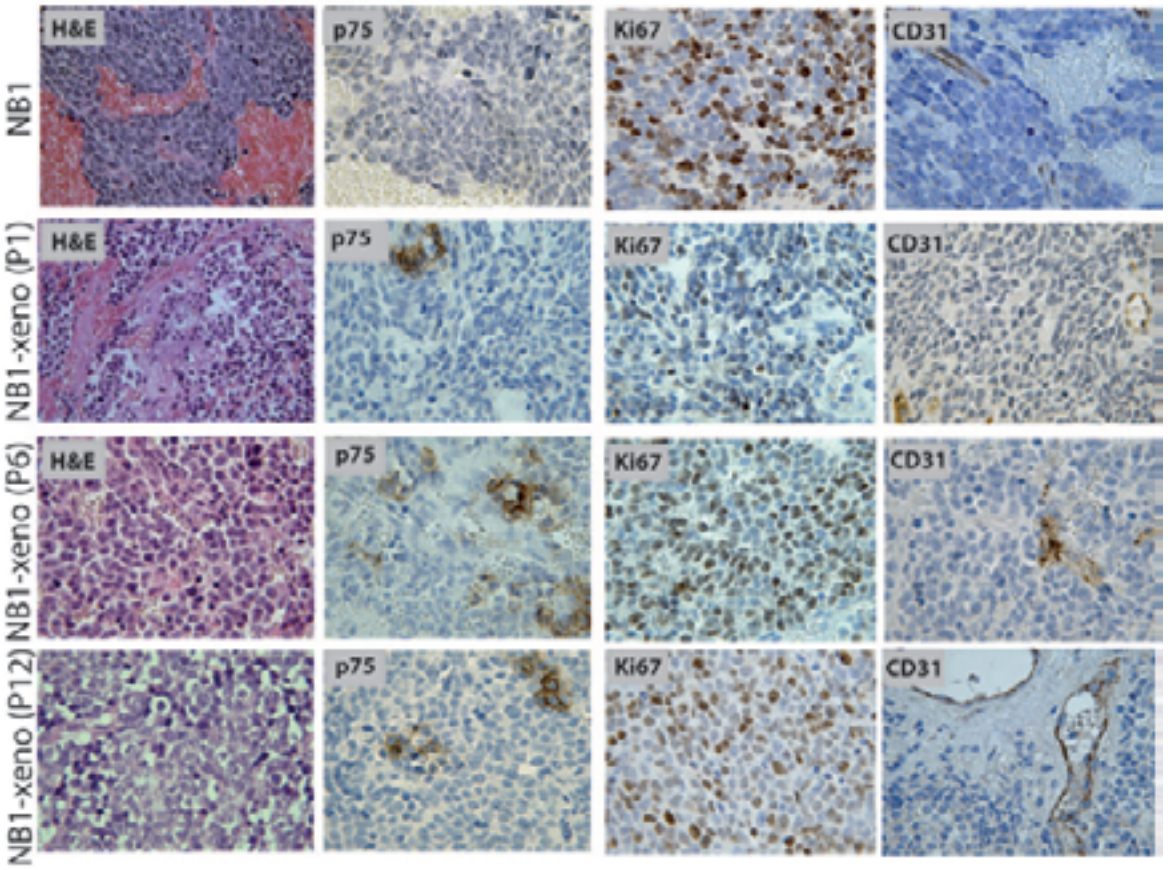

Figure 5 : The histology of the NB1 primary tumor is stable in its derived xenografts in nude mice

NB1 primary tumor and 3 passages (P1, P6 and P12) of the derived NB1-xenograft were analyzed by H/E and IHC staining of p75, Ki67 and CD31 markers.

Genomic profiles

NB tumors are characterized by several genetic alterations, recently shown to be strongly related to their clinical aggressive behavior. The pan-genomic analysis of the original NB1 tumor, and its derivatives, NB1-xenograft, NB1-xeno secondary spheres (NB1-T2), NB1-NBM and NB1-FCS cell lines, were analyzed by array-CGH. These derivatives (Figure 6B) possessed the same genomic alterations as the NB1 patient primary tumor (Figure 6A). Indeed, all NB1 samples showed identical array-CGH profiles with typical NB-associated segmental chromosomic alterations such as 1pdel, 1qgain, 17qgain, 8qgain, 4qgain. No MYCN amplification or MYCN gain on 2p24 was detected in the NB1 tumor, but a chromosomic gain in 8q, which was identified as a *c-myc* gain. Loci found on the 4q and 8q amplicons in NB1 genome are shown in the Appendix 1. Interestingly, 4q amplicon carried the VEGFC coding sequence, this protein playing a key role in the regulation of angiogenesis.

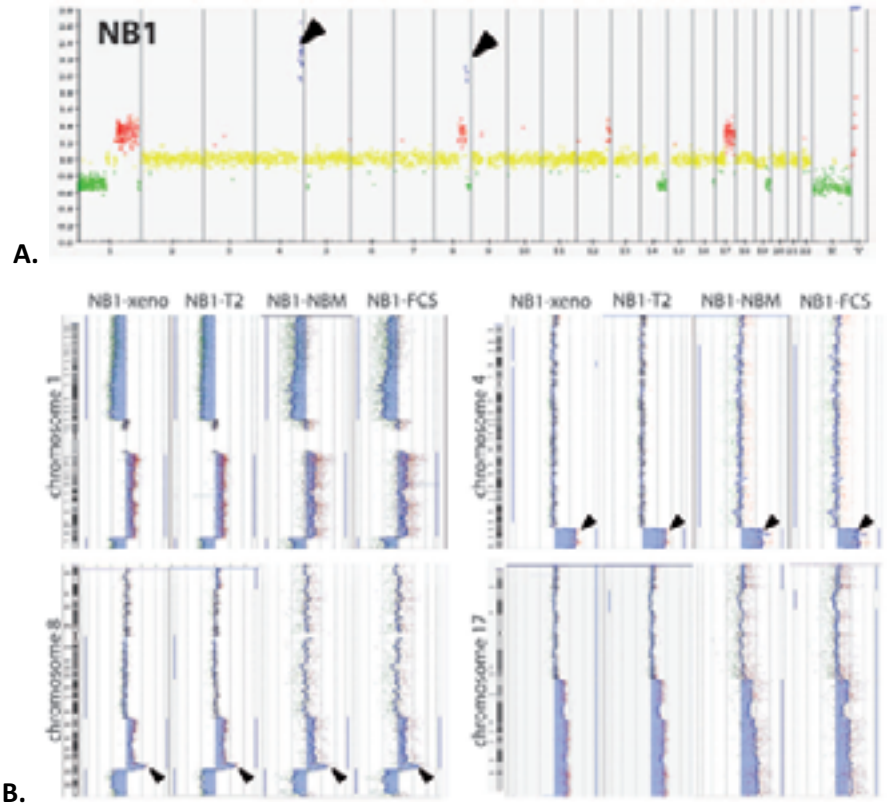

Figure 6: The genomic alterations of the NB1 primary tumor are conserved in the derived xenograft and cell lines.

A. Array-based Comparative Genomic Hybridization (array-CGH) was carried out on the genome of the derivatives of the NB1 tumor cells and highlighted chromosomic alterations as a gain of the c-MYC locus on chromosome 8 and an amplification on the 4q (black arrow heads) in addition to specific stage4-associated translocations on chromosomes 1 and 17. **B.** Detailed array-CGH for the chromosome 1, 4, 8 and 17 in the genome of NB1-xenograft cells and the secondary derived spheres (NB1-T2). The same alterations than in NB1 primary tumor are found in the xenograft, and the derived spheres and cell lines (black arrow heads).

Long-term in vivo maintenance of NB1-xeno tumor

The tumorigenic potential of cells obtained from dissociated NB1-xenografts of early and late passages in mice was assessed by subcutaneous injections in nude mice (Figure 7). Cells from passage 15 (15th xeno-transplantation in mice) of NB1-xenograft showed a decreased tumorigenicity compared to the passage 7 cells (7th xeno-transplantation in mice). Thus, early passages of NB1, NB2 and NB4 xenograft tumors were preferentially used in this study.

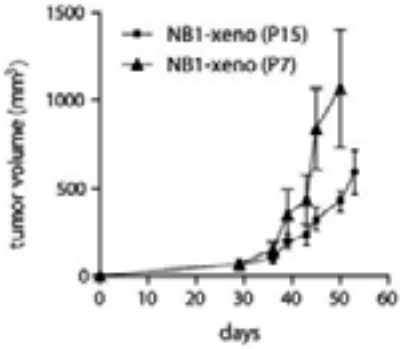

Figure 7: Late passage NB1-xenograft tumor cells showed decreased tumorigenic potential
10^4 NB1-xeno cells at passages 7 (7th grafted mouse, P7) and 15 (15th grafted mouse, P15) were subcutaneously grafted in Matrigel in the back of 6 nude mice and the mean tumor volumes measured twice a week for at least 50 days.

All together, the above results confirmed that such *vivo/vivo* serial transplantation procedure allows maintaining NB tissue over months with fully stable histology, genetic and biological features. The particular properties of the NB1-xenograft tumor also support the suitability of such tumor model for the investigation of CSC in NB. Likewise, NB2 and NB4 xenografts were thus considered as faithful representative of the original NB2 and NB4 primary tumors.

The terms NB1, NB2 and NB4 will therefore hereafter refer to the original patient tumors, while NB1-T, NB2-T, NB4-T will refer to any early passage (between 5 and 10) of the corresponding xenograft.

Self renewal and *in vivo* tumorigenicity of the NB tumors and cell lines

The ability of tumor cells to grow as spheres, to generate and propagate tumors *in vivo* (nude mice) are recognized as typical hallmarks of self-renewal and tumorigenicity, two essential properties of CSCs (41, 68). We thus assessed all the listed NB primary samples for *in vitro* sphere-forming capacity and *in vivo* tumor growth in nude mice.

Self-renewal

NB clinical samples and cell lines listed in Table 1 were analyzed for their ability to form serial spheres, when cultured in NCS-medium and non-adherent suspension, conditions that specifically support the growth of neural crest stem cells and assess self-renewal ability (Figure 8 and Table 1). NB1-T, NB2-T, NB3, NB4-T, NB5 and NB6 samples were able to grow as spheres up to passage 5 (NB1-T), while in the group of stage 3 or stages 4s samples, only NB6 sample could form spheres up to passage 2. NB8 formed primary spheres which could not be passed. NB7-10 and NB1-FCS were not able to grow as sphere in serum-free medium.

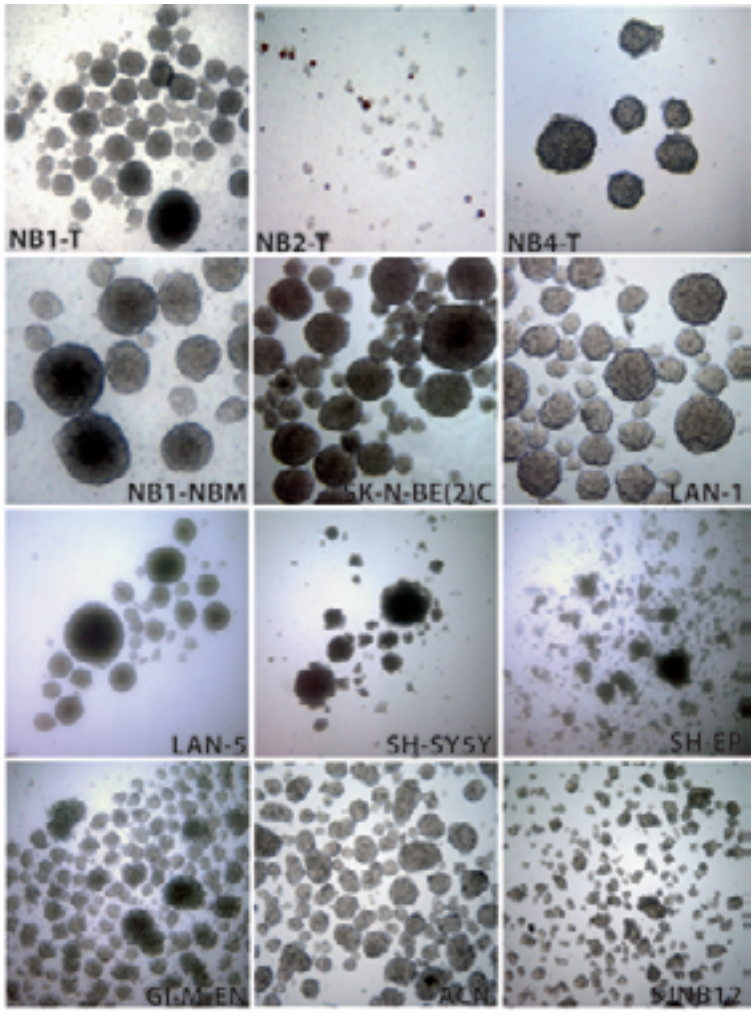

Figure 8: Sphere-forming capacity of NB tumors and cell lines.
Microscopic observation (40x magnification) of the secondary spheres (tertiary for ACN and SJNB12) derived from three stage 4 NB samples (NB1, NB2 and NB4), NB1-NBM cell line established in the lab and eight well-characterized NB cell lines.

Cell viability in sphere conditions was measured and found to be variable (Figure 9A). The highest viability was measured for NB1-T, NB5 and NB6 samples at first passage, and for NB1-T and NB3 at second passage. As it is generally accepted that long-term passages assessment is more relevant to study self-renewal capacity, NB1-T was postulated to have the highest proportion of self-renewal cells.

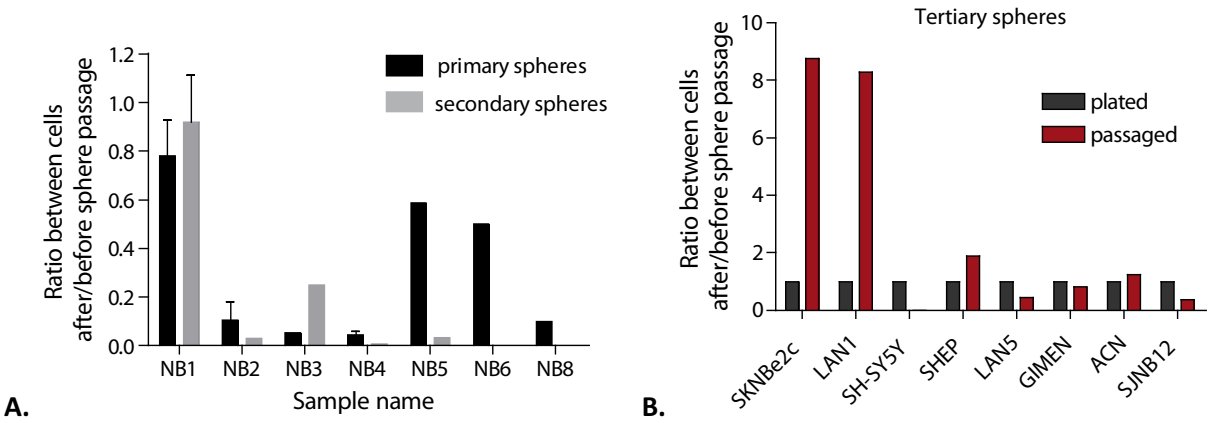

Figure 9: Cell survival at primary and secondary sphere passages for NB primary samples and cell lines
A. Cell survival at the first and second passages of NB tumor-derived spheres. **B.** Cell survival at the third passage of cell line-derived spheres. The reported ratio of cell survival has been calculated by using the number of living cells counted after dissociation divided by the number of initially plated cells.

We tested a panel of well-characterized NB cell lines for their sphere-forming capacity and survival in NCS-medium.

To measure the cell survival in sphere conditions, live cells were counted after each sphere passaging (Figure 9B). All cell lines were able to grow in NCS-medium at least until tertiary spheres, except SH-SY5Y (N-type) and SHEP (S-type) which showed a limited survival in sphere conditions. LAN-1 and SK-N-BE(2)C showed the highest survival after three passages in sphere conditions compared to other cell lines . Moreover, the number of secondary spheres derived from 10'000 plated cells in sphere culture was counted to determine the self-renewal potential of these cell lines (Figures 8 and 10). LAN-1 and SK-N-Be(2)c showed the highest sphere-forming capacity. We therefore selected these two NB cell lines for further investigations. We included in the study NB1-NBM and NB1-FCS cell lines, both derived from NB1-T and harboring different self-renewal capacity *in vitro*. Interestingly, NB1-FCS did not survive in NCS-medium.

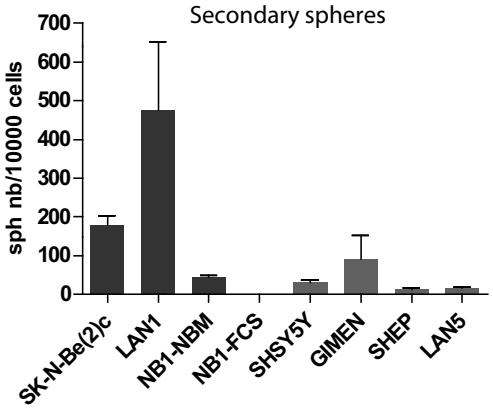

Figure 10: LAN-1 and SK-N-Be(2)c cell lines are *in vitro* models for NB cells with a high sphere-forming capacity

Self-renewal assay for 8 different NB cell lines was performed. The number of secondary spheres was counted for 10^4 plated cells in sphere culture conditions.

In vivo tumorigenicity

The *in vivo* tumorigenic properties of the NB samples were evaluated. The ability to initiate serial tumors was measured *in vivo*, in a xenograft model (sub-cutaneous engrafting in immuno-compromised Swiss nu/nu mice). Although NB1-NB5 samples were all able to initiate tumors in mice, the time required to initiate a detectable tumor varied from 40 (NB1) to 140 days (NB4), and the number of serial passages obtained was also variable, from 1 (NB3) to 16 (NB1). Sample NB1 showed the highest long-term *in vivo* serial passage capacity. No tumor growth in mice was obtained with samples NB6-NB10, even after 180 days observation (Table 1).

Correlation with clinical aggressiveness

The low-risk, intermediate-risk, and high-risk group assignments for the 10 patients were determined according to the criteria currently used by the Children's Oncology Group (COG). The capacity of the different NB samples to form serial xenograft tumors and serial passage sphere was compared (Figure 11). The data clearly showed that long-term serial xenograft passaging and expanded sphere passages were realizable with the NB samples of the high-risk group but not with the less aggressive NBs. This indicated that tumorigenicity and self-renewal are associated to aggressive and metastatic tumors but not low/intermediate grade NB.

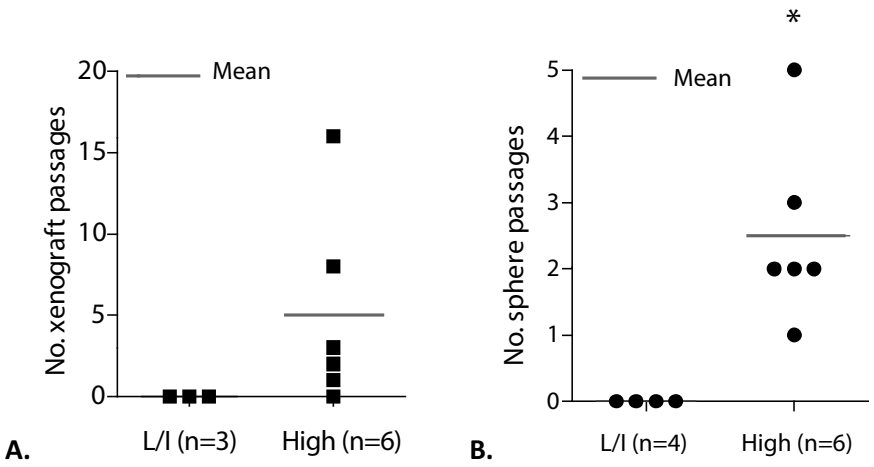

Figure 11: *In vivo* tumorigenicity of the NB cells is associated with the clinical stage.
In vivo tumor propagation (**A**) and *in vitro* sphere formation (**B**) capacities for the high-risk group (High) of NB samples were compared to the low- and intermediate-risk group (L/I). * indicates $p<0.05$ (Student's t-test).

Gene expression profiles of NB spheres: characterization of a NB neurosphere expression profile

As a starting hypothesis, we postulated that NB spheres, generated by tumor cell culture in a defined serum-free medium, could be **progressively** enriched in self-renewing cells, one of few essential CSC features.

To characterize this cell population, gene expression profiles of NB1-T, NB2-T and NB4-T, and their serially derived spheres were generated by micro-arrays. Differentially expressed genes were identified by two statistical analyses selecting genes with either a "linear" or a "step" evolution through the sphere passages.

Time-course micro-array analyses of NB1-T sphere gene expression profile

The detailed experimental protocol designed for identification by microarray of NB1-CSC associated genes is described in Figure 12: a **time-course** micro-array expression analysis was performed on NB1-T (T0) and NB1-NBM (C0) samples and on their serial sphere passages T1-T4 and C1-C4 samples using Affymetrix© Human Genome U133 Plus 2.0 array.

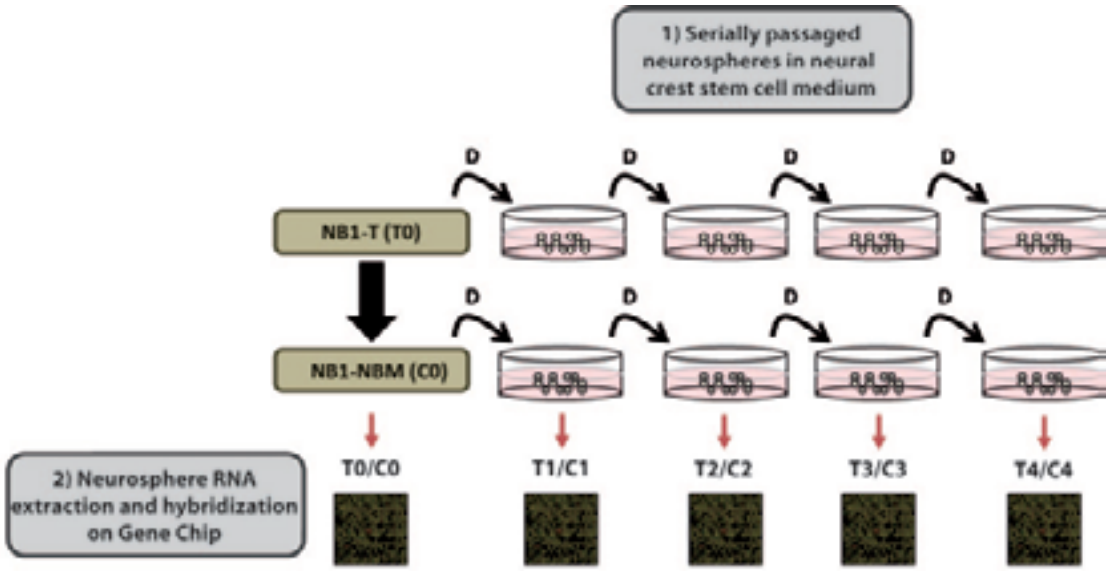

Figure 12: Gene expression profilings of four passages of spheres derived from NB1-T and NB1-NBM.
Dissociated NB1-T cells (T0) and NB1-NBM cell line (C0) were grown as spheres in NCS-medium and serially passaged until quaternary spheres were obtained. Total RNAs were extracted from T1/C1 to T4/C4 with the parental sample T0/C0 and then hybridized on gene chips for time-course micro-array analysis.

In our analysis, we envisaged two scenarios of cell selection in sphere cultures: either an increased number of self-renewing cells would appear as increased sphere passages were obtained ("linear" evolution model) or a drastic selection of self-renewing cells would occur at first passage in sphere conditions ("step" evolution model) (Figure 13).

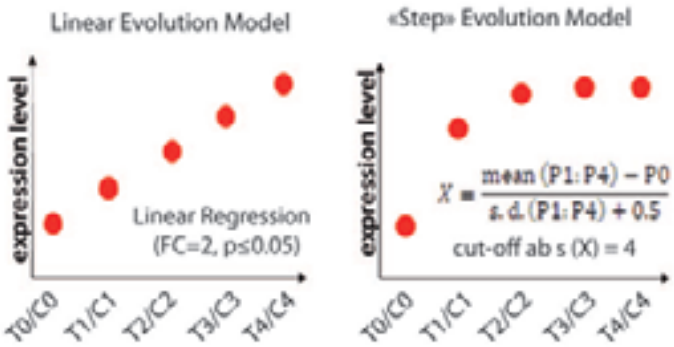

Figure 13: Linear regression and «step-genes» analysis of the spheres gene expression profiles.
Directed analyses were carried out in R to statistically determine which group of genes are gradually over-expressed ("linear") or mostly enriched in the first passage ("step") in cells through the sphere passages.
Statistic values p (regression linear-associated p-value) and X ("step gene" statistic value) were obtained and threshold p-value was set at $p \leq 0.05$ and $abs(X) \geq 4$. P0, P1, P2, P3, and P4 stand either for T0, T1, T2, T3, and T4 or for C0, C1, C2, C3, and C4.

The “linear” hypothesis designed in R program corresponded to a selection of the over- or under-expressed genes which significantly followed a linear regression (p-value≤0.05) through the five expression points T0 to T4 or C0 to C4, with a fold-change higher than 2 (Sylvain Pradervand, University of Lausanne).
The “step” hypothesis designed in R program was based on the following formula to describe genes that were significantly over- or under-expressed at T1/C1:

with *X* =”step” statistics, and *mean (P1:P4)-P0* = “step” change, with P0 corresponding to the initial sample (T0/C0) and (P1: P4) to the first four passages of spheres (Thierry Sengstag, Swiss Institute of Bioinformatics in Lausanne).

To *in silico* select differentially expressed genes with expression profile changes occurring with successive sphere passages, a cut-off has been defined at either *p≤0.05* or *abs(X) =4* in the “linear” and the “step” analyses respectively.
The “linear” evolution analysis performed with NB1-T provided a list of 728 over-expressed and 545 under-expressed probe sets. On the other hand, the “step” evolution analysis showed 232 over- and 176 under-expressed probe sets in the NB1 spheres. By overlapping those two results, a global list of **1601 deregulated genes** in the spheres derived from NB1 was obtained, 700 down-regulated and **901 up-regulated genes**.
We applied the same reasoning to NB1-NBM microarray analysis, which indicated **426 differentially expressed genes**: 137 down-regulated genes vs. 289 up-regulated with either a “linear” or a “step” selection through C0 to C4.

Gene expression profiles of NB2/NB4 secondary spheres

NB1, NB2 and NB4 samples were all metastatic samples of *NMYC* non-amplified stage 4 NBs.
Although we were not able to grow the NB2 and NB4 spheres until their quaternary passages, we nevertheless used these NB samples to validate the differentially expressed genes characterized in NB1-T and NB1-NBM experiments. A second microarray analysis was therefore performed on primary (T1) and secondary (T2) spheres derived from NB2-T and NB4-T tumors (T0) with the same gene-chip device (Figure 14A). Triplicates of T0 and T1 samples were statistically compared and a first set of differentially expressed genes were selected if their fold change absolute value in T1 vs.T0 was higher than 2. Then, only the genes that showed a persistent deregulation in T2 vs. T1 were definitely selected, as shown in Figure 14B. Thus, in NB2 secondary spheres, **545 differentially expressed**

genes, 335 up- and 210 down-regulated, were identified. Likewise, **961 genes were deregulated** in NB4 secondary spheres, 475 over- and 486 under-expressed.

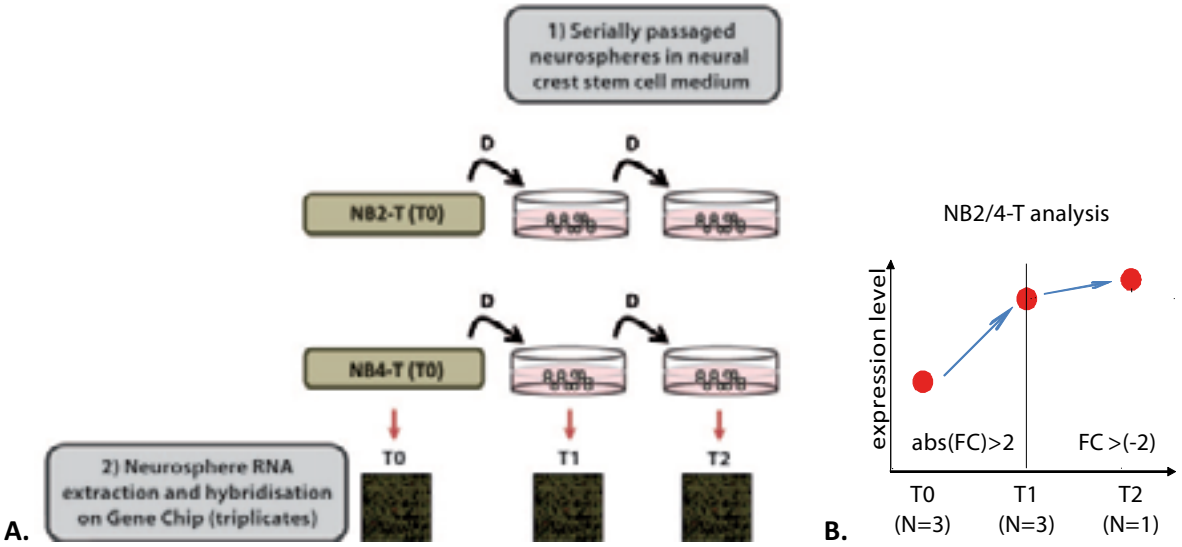

Figure 14: Gene expression profiling of NB2-T and NB4-T tumors and the derived spheres.
A. Total RNAs from the dissociated parental tumors as well as triplicates of the primary spheres (NB2-T1 and NB4-T1), and monoplicates of the secondary spheres (NB2-T2 and NB4-T2) were hybridized on genechips for gene expression profiles. **B.** NB2 and NB4 sphere profiles were determined by selecting over-expressed genes with a fold-change (FC) between T0 and T1 superior to 2 and superior to -2 in T2 vs. T1 (under-expressed genes: FC inferior to -2 and inferior to 2 respectively).

Gene expression profiles of high stage NB derived spheres

Gene lists overlapping

In order to identify genes that were deregulated in two or more samples of NB spheres, we crossed the lists of deregulated genes found in NB1-T, NB2-T, NB4-T and NB1-NBM analyses. The number of overlapping genes is indicated in the Venn diagram (Figure 15).

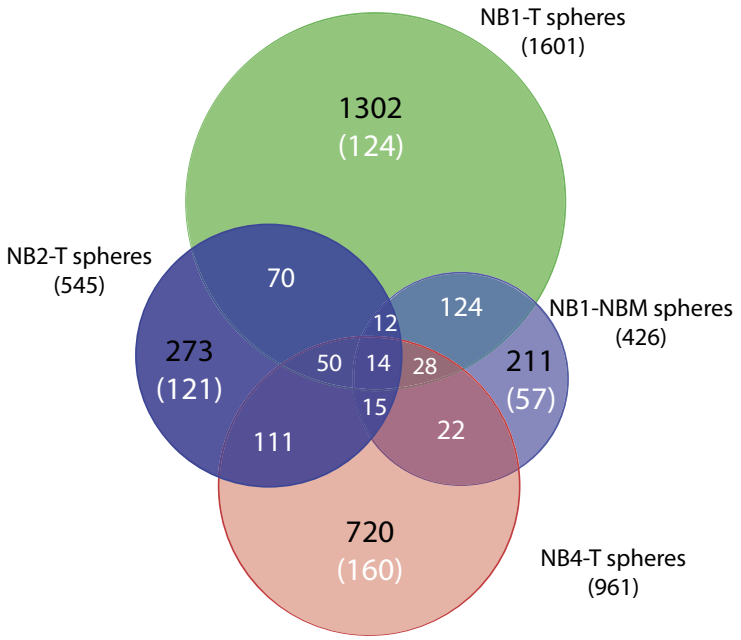

Figure 15: Venn diagrams summarized the overlap of up- and down-regulated transcripts obtained in the NB1-T, NB2-T, NB4-T and NB1-NBM profiling experiments.
The deregulated genes in white are detailed in the supplementary data (*cf.* Appendix 3).

446 genes were found commonly deregulated in the various combinations of experiments. In particular, only 14 genes were commonly deregulated in NB1-T/ NB1-NBM quaternary spheres and NB2/NB4 secondary spheres (Table 2). When excluding the NB1-NBM list, and overlapping the lists of deregulated genes in NB1-T, NB2-T and NB4-T spheres, 64 common genes were identified, corresponding to 50 new common genes that were added to the 14 genes describes above (Table 3), including the *cannabidoid receptor 1* (***CNR1***), 14-fold over-expressed in NB1-T spheres and interacting with the IL6 receptor in neuronal development (216), and *IGFBP3* gene, a modulator of the cell growth effects of IGFs and detected with a 11-fold increase in NB1-T spheres.

Interestingly, among the 12 genes in NB1-T, NB1-NBM and NB2-T (Table 4), the ATP-binding cassette ***ABCB1*** (***MDR1***), already described in the lab as involved in multidrug resistance in NB (217), was observed with 7-fold and 3-fold over-expression in NB1-T, NB1-NBM quaternary spheres respectively and 4-fold in NB2-T spheres.

The highest up-regulated gene shown in NB1-T, NB1-NBM and NB2-T spheres corresponded to the aldehyde deshydrogenase ***ALDH1A2*** gene previously described as a malignant human mammary stem cell marker (47). However the results in NB samples were not consistent as this gene was 181-fold and 3-fold upregulated in NB1-T and NB1-NBM respectively, while it decreased 7-fold in NB2 spheres.

[illegible]	[illegible]	[illegible]	[illegible]	[illegible]	[illegible]	[illegible]	[illegible]	[illegible]
[illegible]	[illegible]	[illegible]	[illegible]	[illegible]	[illegible]		[illegible]	[illegible]
[illegible]	[illegible]	[illegible]	[illegible]	[illegible]	[illegible]	[illegible]	[illegible]	[illegible]
[illegible]	[illegible]	[illegible]	[illegible]	[illegible]	[illegible]		[illegible]	[illegible]
[illegible]	[illegible]	[illegible]	[illegible]	[illegible]	[illegible]		[illegible]	[illegible]
[illegible]	[illegible]	[illegible]	[illegible]	[illegible]	[illegible]	[illegible]	[illegible]	[illegible]
[illegible]	[illegible]	[illegible]	[illegible]	[illegible]	[illegible]		[illegible]	[illegible]
[illegible]	[illegible]	[illegible]	[illegible]	[illegible]	[illegible]		[illegible]	[illegible]
[illegible]	[illegible]	[illegible]	[illegible]	[illegible]	[illegible]		[illegible]	[illegible]
[illegible]	[illegible]	[illegible]	[illegible]	[illegible]	[illegible]	[illegible]	[illegible]	[illegible]
[illegible]	[illegible]	[illegible]	[illegible]	[illegible]	[illegible]	[illegible]	[illegible]	[illegible]
[illegible]	[illegible]	[illegible]	[illegible]	[illegible]	[illegible]	[illegible]	[illegible]	[illegible]
[illegible]	[illegible]	[illegible]	[illegible]	[illegible]	[illegible]	[illegible]		[illegible]
[illegible]	[illegible]	[illegible]	[illegible]	[illegible]	[illegible]		[illegible]	[illegible]
[illegible]	[illegible]	[illegible]	[illegible]	[illegible]	[illegible]	[illegible]	[illegible]	[illegible]

<u>Table 2</u>: 14 genes were commonly deregulated in NB1-T/ NB1-NBM quaternary spheres and NB2/NB4 secondary spheres.

Foldchange of up-regulated (red) or down-regulated (blue) genes as measured by the microarray analyses are shown for the NB1, NB2 and NB4-T experiments. The overlapping results with published lists of NCSC and NDCD (218), neural stem cells (219), iPS (220) and NB-TICs (203) expressed genes are mentioned in the "Other list" column.

Table 3 (Part 1): 29 common upregulated genes were identified in NB1-T, NB2-T and NB4-T spheres.

Foldchange of up-regulated (red) or down-regulated (blue) genes as measured by the microarray analyses are shown for the NB1, NB2 and NB4-T experiments. The overlapping results with published lists of NCSC and NDCD (218), neural stem cells (219), iPS (220), and NB-TICs (203) expressed genes are mentioned in the "Other list" column.

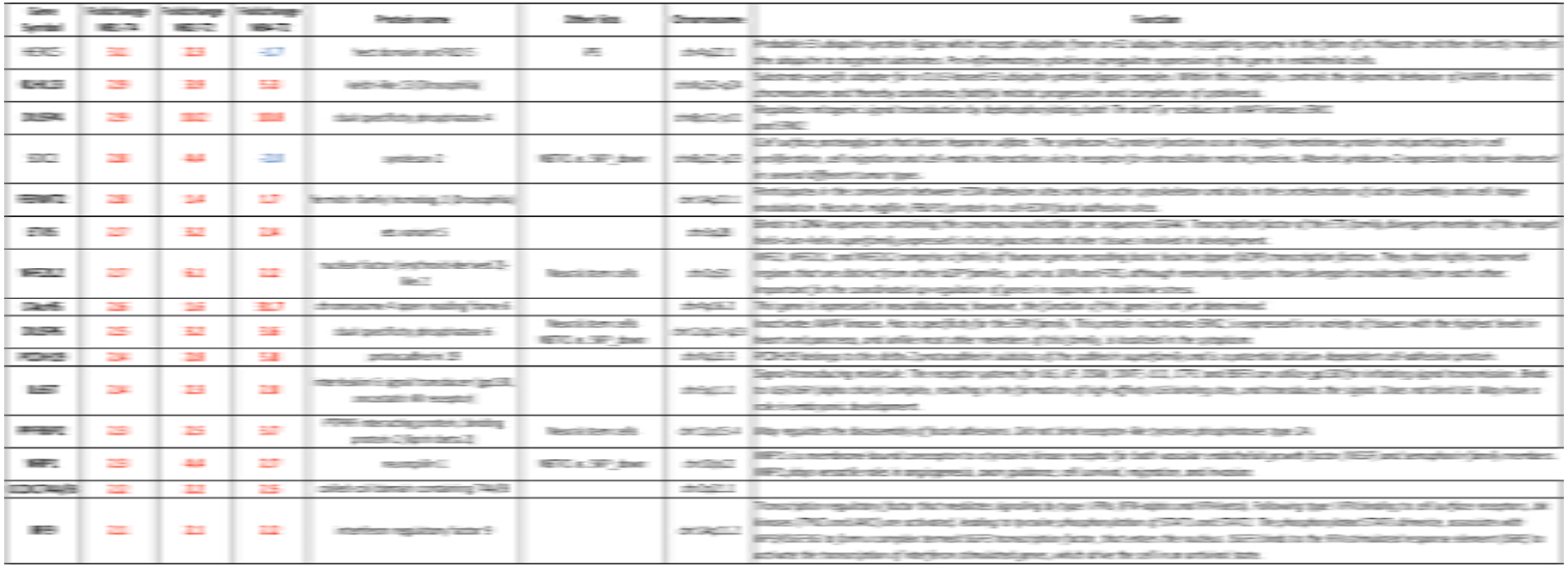

Table 3 (Part 2): 29 common upregulated genes were identified in NB1-T, NB2-T and NB4-T spheres.

Foldchange of up-regulated (red) or down-regulated (blue) genes as measured by the microarray analyses are shown for the NB1, NB2 and NB4-T experiments. The overlapping results with published lists of NCSC and NDCD (218), neural stem cells (219), iPS (220), and NB-TICs (203) expressed genes are mentioned in the "Other list" column.

Gene Symbol	Foldchange NB1-T4	Foldchange NB2-T2	Foldchange NB4-T2	Protein name	Other lists	Chromosome	Function
SIK1	-2.0	-3.5	-8.9	salt-inducible kinase 1		chr21q22.3	*Transient role during the earliest stages of myocardial cell differentiation and/or primitive chamber formation and may also be important for the earliest stages of skeletal muscle growth and/or differentiation. Potential role in G2/M cell cycle regulation. Inhibits CREB activity by phosphorylating and repressing the CREB-specific coactivators, CRTC1-3.*
IPO11 /// LRRC70	-2.1	-3.7	-4.4	importin 11 /// leucine rich repeat containing 70		chr5q12.1	*Functions in nuclear protein import as nuclear transport receptor. Serves as receptor for nuclear localization signals (NLS) in cargo substrates. Is thought to mediate docking of the importin/substrate complex to the nuclear pore complex (NPC) through binding to nucleoporin and the complex is subsequently translocated through the pore by an energy requiring, Ipo11-dependent mechanism. At the nucleoplasmic side of the NPC, Ipo11 binds to the importin, the importin/substrate complex dissociates and importin is re-exported from the nucleus to the cytoplasm where GTP hydrolysis releases Ipo11. The directionality of nuclear import is thought to be conferred by an asymmetric distribution of the GTP- and GDP-bound forms of Ipo11 between the cytoplasm and nucleus*
APCDD1	-2.1	-2.5	-5.2	adenomatosis polyposis coli down-regulated 1		chr18p11.22	*Probably plays a role in colorectal tumorigenesis. May be a developmental target gene of the Wnt/Beta-catenin pathway.*
CCDC91	-2.2	-2.9	-2.4	Coiled-coil domain containing 91		chr12p11.22	*Involved in the regulation of membrane traffic through the trans-Golgi network.*
AHI1	-2.5	-3.6	-13.1	Abelson helper integration site 1		chr6q23.3	*This gene is apparently required for both cerebellar and cortical development in humans. This gene mutations cause specific forms of Joubert syndrome-related disorders. Joubert syndrome (JS) is a recessively inherited developmental brain disorder with several identified causative chromosomal loci. Alternatively spliced transcript variants encoding different isoforms have been identified.*
JUNB	-2.6	-3.9	-9.3	jun B proto-oncogene		chr19p13.2	*Transcription factor involved in regulating gene activity following the primary growth factor response. Binds to the DNA sequence 5'-TGA[CG]TCA-3'.*
CDK6	-2.7	-2.7	-6.3	cyclin-dependent kinase 6		chr7q21	*Probably involved in the control of the cell cycle. Interacts with D-type G1 cyclins.*
FUS	-2.8	-2.6	-2.1	fused in sarcoma		chr16p11.2	*Binds both single-stranded and double-stranded DNA and promotes ATP-independent annealing of complementary single-stranded DNAs and D-loop formation in superhelical double-stranded DNA. May play a role in maintenance of genomic integrity*
RHOU	-2.9	2.0	-2.3	ras homolog gene family, member U		chr1q42.11-q42.3	*Stimulates quiescent cells to reenter the cell cycle. Has no detectable GTPase activity but its high intrinsic guanine nucleotide exchange activity suggests it is constitutively GTP-bound. This protein can activate PAK1 and JNK1, can induce filopodium formation and stress fiber dissolution and regulates the actin cytoskeleton, adhesion turnover and increase cell migration. It may also mediate the effects of WNT1 signaling in the regulation of cell morphology, cytoskeletal organization, and cell proliferation.*
FAM131A	-3.2	-2.8	-1.6	family with sequence similarity 131, member A		chr3q27.1	
TESC	-3.3	-5.6	-12.3	tescalcin		chr12q24.22	*Essential for the coupling of ERK cascade activation with the expression of ETS family genes in megakaryocytic differentiation.*
NPAS4	-3.5	-11.5	-13.6	neuronal PAS domain protein 4		chr11q13	*NPAS4 is a member of the basic helix-loop-helix-PER, -ARNT, -SIM (bHLH-PAS) class of transcriptional regulators, which are involved in a wide range of physiologic and developmental events.*
LOC284454	-3.7	-2.7	-3.8	hypothetical protein LOC284454		chr19p13.13	*Hypothetical protein.*
GABRB1	-4.1	-2.7	-10.2	gamma-aminobutyric acid (GABA) A receptor, beta 1		chr4p12	*GABA, the major inhibitory neurotransmitter in the vertebrate brain, mediates neuronal inhibition by binding to the GABA/benzodiazepine receptor and opening an integral chloride channel.*
DUSP1	-4.5	-3.4	-5.2	dual specificity phosphatase 1	NBTIC vs. SKP_down	chr5q34	*Dual specificity phosphatase that dephosphorylates MAP kinase ERK2 on both 'Thr-183' and 'Tyr-185'. DUSP1 may play an important role in the human cellular response to environmental stress as well as in the negative regulation of cellular proliferation.*
ARC	-5.0	-3.2	-3.9	activity-regulated cytoskeleton-associated protein	iPS	chr8q24.3	*Required for consolidation of synaptic plasticity as well as formation of long-term memory. Regulates endocytosis of AMPA receptors in response to synaptic activity. Required for homeostatic synaptic scaling of AMPA receptors.*
DSCR6	-5.4	-2.1	-4.9	Down syndrome critical region gene 6		chr21q22.2	*Expressed at a low level in fetal kidney and fetal brain.*
FOSB	-7.7	-31.9	-54.2	FBJ murine osteosarcoma viral oncogene homolog B		chr19q13.32	*The Fos gene family consists of 4 members: FOS, FOSB, FOSL1, and FOSL2. These genes encode leucine zipper proteins that can dimerize with proteins of the JUN family, thereby forming the transcription factor complex AP-1. As such, the FOS proteins have been implicated as regulators of cell proliferation, differentiation, and transformation.*
EGR3	-8.1	-3.7	-103.6	early growth response 3		chr8p23-p21	*The gene encodes a transcriptional regulator that belongs to the EGR family of C2H2-type zinc-finger proteins. It is an immediate-early growth response gene which is induced by mitogenic stimulation. The protein encoded by this gene participates in the transcriptional regulation of genes in controling biological rhythm. It may also plays a role in muscle development.*
KLF4	-8.9	-22.4	-6.3	Kruppel-like factor 4 (gut)	NBTIC vs. SKP_down	chr9q31	*Transcription factor which acts as both an activator and repressor. Binds the CACCC core sequence. Binds to multiple sites in the 5'-flanking region of its own gene and can activate its own transcription. Required for establishing the barrier function of the skin and for postnatal maturation and maintenance of the ocular surface. Involved in the differentiation of epithelial cells and may also function in skeletal and kidney development.*
HBE1	-11.8	-145.3	-650.0	Hemoglobin, epsilon 1		chr11p15.5	*The epsilon chain is a beta-type chain of early mammalian embryonic hemoglobin.*

Table 3 (Part 3): 21 common down-regulated genes were identified in NB1-T, NB2-T and NB4-T spheres.

Foldchange of up-regulated (red) or down-regulated (blue) genes as measured by the microarray analyses are shown for the NB1, NB2 and NB4-T experiments. The overlapping results with published lists of NCSC and NDCD (218), neural stem cells (219), iPS (220), and NB-TICs (203) expressed genes are mentioned in the "Other list" column.

Gene Symbol	Foldchange NB1-T	Foldchange NB2-T	Foldchange NB1-NBM	Protein name	Other lists	Chromosome	Function
[illegible]	[illegible]	[illegible]	[illegible]	[illegible]		[illegible]	[illegible]
[illegible]	[illegible]	[illegible]	[illegible]	[illegible]		[illegible]	[illegible]
[illegible]	[illegible]	[illegible]	[illegible]	[illegible]		[illegible]	[illegible]
[illegible]	[illegible]	[illegible]	[illegible]	[illegible]	[illegible]	[illegible]	[illegible]
[illegible]	[illegible]	[illegible]	[illegible]	[illegible]	[illegible]	[illegible]	[illegible]
[illegible]	[illegible]	[illegible]	[illegible]	[illegible]		[illegible]	[illegible]
[illegible]	[illegible]	[illegible]	[illegible]	[illegible]		[illegible]	[illegible]
[illegible]	[illegible]	[illegible]	[illegible]	[illegible]	[illegible]	[illegible]	[illegible]
[illegible]	[illegible]	[illegible]	[illegible]	[illegible]	[illegible]	[illegible]	[illegible]
[illegible]	[illegible]	[illegible]	[illegible]	[illegible]		[illegible]	[illegible]
[illegible]	[illegible]	[illegible]	[illegible]	[illegible]	[illegible]	[illegible]	[illegible]

Table 4: 12 common deregulated genes identified in NB1-T, NB1-NBM and NB2-T spheres

Foldchange of up-regulated (red) or down-regulated (blue) genes as measured by the microarray analyses are shown for the NB1-T, NB2-T and NB1-NBM experiments. The overlapping results with published lists of NCSC and NDCD (218), neural stem cells (219), iPS (220), and NB-TICs (203) expressed genes are mentioned in the "Other list" column.

Canonical pathways and biological functions enrichment

To investigate whether any biological functions were over-represented in the combined gene expression profiles of NB1-T, NB2-T, NB4-T and NB1-NBM spheres, we analyzed the enrichment of canonical signaling pathways and Gene Ontology annotations for biological processes in these four lists.

As shown in figure 16A, an enrichment of genes involved in canonical signaling pathways such as epithelial-mesenchymal transition (EMT), AP-1 pathway, VEGFC cascade, WNT pathway and cell adhesion was found. Moreover, the Gene Ontology annotation analysis revealed an over-representation of genes playing a key role in several **developmental processes** such as embryonic development, nervous system development and cell differentiation (Figure 16B), comforting the stem-like phenotype of these self-renewing cell populations.

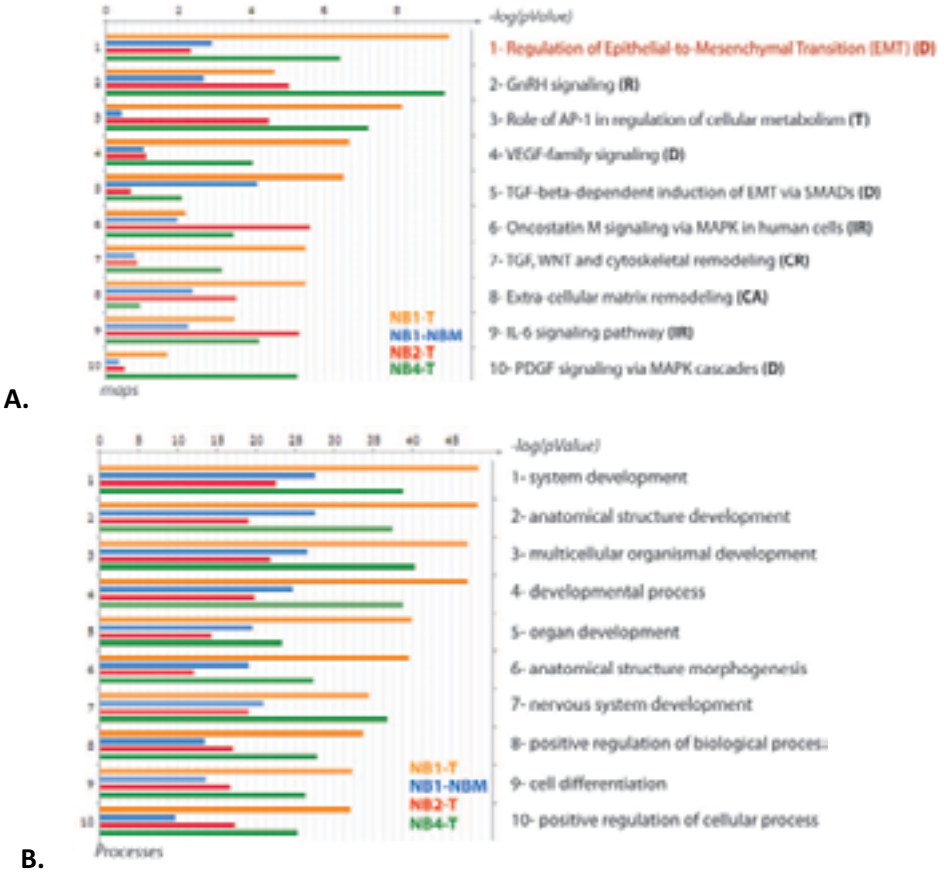

Figure 16: GeneGo enrichment analysis for canonical pathways and Gene Ontology processes in the lists of sphere-associated genes

The canonical pathways (**A**) and Gene Ontology processes (**B**) that were significantly enriched in NB1-T, NB1-NBM, NB2-T and NB4-T spheres expression profiles are reported. The quoted maps (in red) of canonical pathways involving genes of the sphere s are shown in Appendix 2. The so-called maps correspond to graphic reprentation of the molecular pathway provided by the GeneGo portal. D: Development, R: Reproduction, T: Transcription, IR: Immune Response, CR: Cytoskeleton Remodeling, CA: Cell Adhesion.

Enrichment of biological processes in the NB1-T model

The NB1-T and NB1-NBM profiles seemed more relevant for the identification of a self-renewing associated as they were established from quaternary spheres. Indeed, it is generally accepted that long-term passages are more representative of self-renewal capacity. We thus considered that the self-renewing population was stable at the fourth sphere passage and focused the analysis of canonical pathways enrichment on the NB1-T derived spheres expression profile (Figure 17).

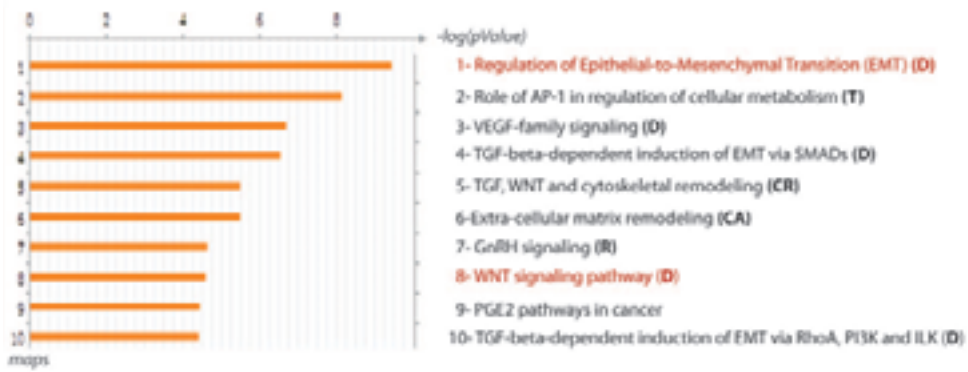

Figure 17: GeneGo enrichment analysis for canonical pathways and Gene Ontology processes in the list of NB1-T sphere associated genes

Gene Ontology processes that were significantly enriched in NB1 spheres expression profile only are shown. The quoted map (in red) of canonical pathways involving genes of the sphere s are shown in Appendix 2. The so-called maps correspond to graphic reprentation of the molecular pathway provided by the GeneGo portal. D: Development, R: Reproduction, T: Transcription, IR: Immune Response, CR: Cytoskeleton Remodeling, CA: Cell Adhesion.

The first ten more significant key pathways were found to be similar with the enrichment analysis of the four combined experiments of Figure 16A and underlined the over-representation of genes involved in EMT (maps 1, 4 and 10), Wnt signaling (maps 5 and 8) and interactions with the micro-environment (maps 3, 6 and 7) in the sphere expression profiles. Detailed maps with the gene expression fold-change observed in spheres of the four experiments are shown in Appendix 2.

We next addressed the enrichment in NB1-T spheres of genes involved in known essential attributes of stemness including the TGFβ, JAK/STAT, NOTCH, WNT and YES signaling pathways, the capacity to sense growth hormone and the interaction with the extracellular matrix via integrins (219) or in the neural crests development and NB tumorigenesis. These genes are listed in Table 5. Several of these genes were also deregulated in NB2-T and/or NB4-T spheres.

So, the gene expression analysis of NB1-T spheres supported by three other experiments in NB1-NBM, NB2-T and NB4-T spheres provided a list of genes involved in key pathways such as EMT and Wnt signaling, extracellular matrix remodeling and immune response modulation.

Category	Genes
I-Signaling	
active JAK/STAT (Janus kinase/signal transducers and activators of transcription)	↑ ***IL10 receptor beta (x2.3), IL6 signal transducer (x2.4), STAMBPL1 interacting with the adaptator STAM (x2.3)*** ↓ *STATIP1(x2.2) interacting with STAT3 (x5.2), PIAS(x3.2) inhibitor of activated STAT3, AKT2 (x2.4), SOS2 (x3.5) activator of MAPK, MYBP2 (x2.7) interacting with c-Myc, PIM genteic target (x2.6)*
TGF-β	↑ ***TGF-β induced transcript (x3.5), TGF-β receptor 2 (x4.7), SMAD6 (x2.6), SMAD3 (x2.7), BMP5 (x7.3), ID4 (x14.4)*** ↓ *SMAD2 (x2.0), SMURF2 (x2.1), ACVR2B (x2.3), ROCK (x2.2)*
Notch	↑ ***NOTCH2 (x14.5), NOTCH3 (x6.8), HES1 (x2.8), HEY1 (x2.8), JAG1 (x2.3), MEGF10(x8.3), MAML2 (x3.8)*** ↓ *HDAC9 (x24.8), MAML3 (x5.5), RBPSUH (x2.2)*
Wnt	↑ ***WNT5A (x25.0), FZD2 (x2.5), FZD7 (x3.1), FZD6 (x3.2), SNAI2 (x9.6), GPR177 (x10.2), DKK2 (x2.6), TCF7L1 (x14.0), TCF7L2 (2.1), BMP4 (x4.0), PPARD (x2.4)*** ↓ *cyclinD1 (x4.2)*
II-Capacity to sense growth hormone	
IGF	↑ ***IGFBP3 (x10.8), IGFBP5 (x8.1), IGFBP7 (x9.0), IGF2BP2 (x18.6), IGF2R (x2.3)*** ↓ *IGF2BP3 (x2.2)*
FGF	↑ ***FGFR1 (x2.7), FGFR2 (x2.7)*** ↓ *FGF9 (x2.1)*
EGF	↑ ***EGFR (x7.2)***
VEGF	↑ ***VEGFC (x8.6)*** ↓ *VEGFD (x8.3)*
PDGF	↑ ***PDGFRL (x3.1), PDGFRA (x3.2), PDGFD (x16.0), PDGFC (x5.0)***
PGF	↓ *PGF (x2.0)*
III-Integrin signaling pathway	↑ ***ITGAV (x2.9), ITGA9 (x9.6), RHOJ (x61.3), RELN (x3.3)*** ↓ *ITGA8 (x2.9), JUND (x2.1), JUNB (x2.6), MAPK8 (x2.5), ROCK1 (x2.2)*
III-Neural crest development and NB tumorigenesis	↑ ***EPHA4 (x3.5), EPHA5 (x25.6), EPHA6 (x2.7), EFNB2 (x2.6), EFNA4 (x9.3), SEMA3C (x29.0), SPON1 (x24.4), COL5A3 (x2.5), COL12A1 (x2.5), FOXO1A (x3.2), FOXP4 (x3.2), FOXC1 (x9.4), ETS1 (x3.5), SOX9 (x4.8), RET (x4.4), NTRK2 (x13.5), LAMA1 (x12.8), LAMA2 (x5.2), LAMC1 (x2.8), ABCB1 (x6.4), ABCA1 (x16.6), ABCB4 (x9.2), CASP8 (x2.0)*** ↓*EPHA5 (x9.2), EFNA5 (x4.3), SEMA3E (x4.4), FOXP1 (x3.1), FOXO3A (x3.0), CXCR4 (x2.4), NTRK3 (x2.0), PHOX2A (x3.5), CD44 (x3.6), BCL2 (x2.3)*

Table 5: List of genes up- or down-regulated in the NB1-T spheres and involved in stem-cell physiology

Foldchanges measured in the microarray analysis of NB1-T sphere gene expression profile are indicated for the up-regulated (in bold) and down-regulated genes.

Characterization of a Neurosphere Expression Profile (NEP)

In order to determine the most relevant list of genes associated with the self-renewing phenotype of NB cells, we annotated the deregulated genes in NB1-T quaternary spheres for their characterization in previous published gene expression profiling. Thus, the list of 901 over-expressed genes in NB1-T spheres have been crossed with five lists of published genes over-expressed in neural crest stem cells (NCSC), neural crest derived progenitor cells (NCDC), neural stem cells, NB-TICs and induced pluripotent stem cells (iPS) (203, 218-220). Indeed, those five gene expression profiles were considered particularly relevant in the quest of self-renewing NB cells markers. Induced-PS (iPS) up-regulated genes were added to the analysis as NB1-T cells over-expressed c-MYC which is one of the inducer for the re-programming of human fibroblasts into pluripotent cells.

Common genes were summarized in Appendix 3 and referred below as the Neurosphere Expression Profile (NEP). In particular, 20 genes were found commonly up-regulated in NCSC and NB1-T spheres. Interestingly, the receptor ***PROM1*** (***CD133***) was expressed with a 29-fold increase in NB1-T spheres expression profile. Expending evidence highlighted the role of CD133 as a marker of CSCs in various human tumors (221) such as brain and colon cancer stem cells (49, 55, 56, 222). In addition, CD133 expression was reported to be induced in iPS cells (220). Among the genes with the highest fold-change in NB1-T spheres, this overlap also identified the ***VEGFC*** growth factor (9x) involved in angiogenesis of the venous and lymphatic vascular systems during embryogenesis and nervous system development, the axon guidance receptor ***ROBO1*** (6x) and the FGF receptor ***FGFR2*** (3x) present on the iPS cell membrane.

In addition, 13 genes were identically over-expressed in NCDC and NB1 spheres such as the ***GPR177*** gene that regulates WNT proteins sorting and secretion (223) and the receptor ***NOTCH3*** which promotes cell self-renewal and tumor formation (224-226).

Finally, a list of 100 up-regulated genes was identified in both NB1-T spheres and NSC gene expression profiles, among which two particularly relevant genes emerged: the ***EDNRB*** and ***ABCA1*** genes which showed 33- and 17-fold respective changes in NB1-T spheres. Indeed, the endothelin receptor B (EDNRB) located in 13q22, and its ligand, the endothelin 3 (EDN3), are involved in the neural crests development during embryogenesis, and promote cell growth and normal formation of peripheric nerves and melanocytes (227-229). EDNRA, receptor for endothelin-1 (EDN1), has also been found 11-fold over-expressed in NB1-T spheres. On the other hand, the ABCA1 transporter mediates the efflux of cholesterol and phospholipids.

NB1-T tumor vs. NB1-NBM cell line sphere gene expression profiling

Interestingly, a significant smaller number of up- or down-regulated genes was observed in spheres derived from NB1-NBM compared to NB1-T. We then reported the genechip signal for *EDNRB*,

CD133, *ABCA1* and *GPR177* genes described above. All transcripts were found to be over-expressed in NB1 spheres but not in NB1-NBM spheres (Figure 18). However, the expression level of these genes was already high in NB1-NBM-C0 whereas it was low in NB1-T0. This observation explained the lower number of upregulated genes in NB1-NBM spheres. Interestingly, a number of highly expressed genes in NB1-NBM are progressively increased in T1 to T4 NB1-T spheres up to the NB1-NBM C4 level. These results indicate that the culture conditions for establishment of the NB1-NBM either selected a cell population with CSCs characteristics, or induced the expression of self-renewal genes.

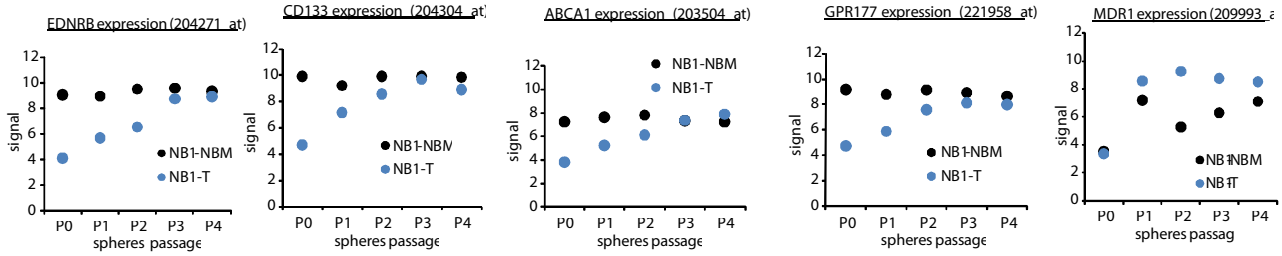

Figure 18: Genechip signals of five NEP selected genes in the NB1-T derived spheres: EDNRB, CD133, ABCA1, GPR177, and MDR1

Expression profiles for a few selected genes overexpressed in the time-course micro-array analysis of NB1 sphere. For EDNRB, CD133, ABCA1, GPR177, and MDR1 genes, the signal levels of mRNA hybridization on the genechips are represented for the NB1-NBM (blue) and NB1-T (black) experiments.

The seven ***CD133*, *MDR1*, *EDNRB*, *NOTCH3*, *ABCA1*, *GPR177*** and ***ROBO1*** genes were identified from the first series of gene data (NB1-T and/or NB1-NBM) which was crossed with the list of neural crest stem cells and neural stem cells associated genes, further reduced by the enrichment analysis thus releasing this set of **representative NEP markers** to characterize their associated functional properties.

Validation of the NEP in a panel of NB secondary spheres

To validate the micro-array results, and confirm that such self-renewal phenotype was not specific of the NB1 patient tumor, the up-regulated expression of CD133, MDR1, EDNRB, NOTCH3, ABCA1, GPR177 and ROBO1 in the NB1-T and NB1-NBM spheres was checked on spheres derived from other patient tumors and cell lines by real-time PCR and/or FACS.

Messenger RNA was extracted from available NB1, NB2, NB4 and NB5-T xenograft tumors, and from SK-N-Be2C, LAN-1 and NB1-NBM cell lines and their derived secondary spheres (Table 6). The transcript levels of CD133, MDR1, EDNRB, GPR177, ROBO1, NOTCH3 and ABCA1 were measured by real-time PCR.

Interestingly 4/7 NEP genes, CD133, MDR1, GPR177 and ROBO1, were significantly up-regulated or already highly expressed in 70-100% of the tested tumors and cell lines respectively. EDNRB and NOTCH3 highly expressed in NB1-NBM were also over-expressed in 2/7 NB samples with a high expression in NB1-NBM. ABCA1 over-expression was restricted to NB1-T and NB1-NBM secondary spheres.

Sample	CD133 expression		MDR1 expression		EDNRB expression		GPR177 expression		ROBO1 expression		NOTCH3 expression		ABCA1 expression	
	Fold change	P-value	Fold change	P-value	Fold change	P-value	Fold change	P-value	Fold change	P-value	Fold change	P-value	Fold change	P-value
NB1-T	**37.21 ± 7.73**	*p<0.0002*	**100.5 ± 7.0**	*p<0.0001*	**72.42 ± 15.29**	*p<0.0001*	**76.04 ± 20.39**	*p<0.002*	**6.76 ± 1.37**	*p<0.0004*	**12.48 ± 0.99**	*p<0.0001*	**9.89 ± 0.98**	*p<0.0001*
NB2-T	**10.14 ± 2.99**	*p<0.0001*	**37.38 ± 5.74**	*p<0.0001*	**10.09 ± 2.08**	*p<0.0001*	**5.05 ± 1.29**	*p<0.0083*	0.55 ± 0.06*	*p<0.0001*	0.60 ± 0.15	*p<0.0246*	0.44 ± 0.06	*p<0.0054*
NB4-T	nd		**2.86 ± 0.50**	*p<0.0077*	nd		37.16 ± 17.05	*p<0.0667*	0.50 ± 0.16*	*p<0.0163*	**5.21 ± 0.92***	*p<0.0469*	1.316	
NB5-T	**13.49 ± 1.53**	*p<0.0101*	**5.04 ± 0.25**	*p<0.0001*	nd		**3.79 ± 1.44**	*p<0.0264*	**2.08 ± 0.06**	*p<0.0026*	1.15 ± 0.50	*p<0.8375*	0.42 ± 0.05	*p<0.001*
NB1-NBM	**1.49 ± 0.18***	*p<0.0129*	**29.09 ± 9.56**	*p<0.0096*	1.39 ± 0.25*	*p<0.1609*	1.17 ± 0.19*	*p<0.8232*	**2.34 ± 0.53***	*p<0.0226*	0.86 ± 0.12*	*p<0.2873*	**1.97 ± 0.40**	*p<0.0297*
LAN1	**6.28±1.25**	*p<0.0002*	**39.28 ± 13.68**	*p<0.0129*	6.14 ± 3.27	*p<0.13*	0.79 ± 0.14*	*p<0.0804*	1.13 ± 0.19*	*p<0.5461*	*0.81 ± 0.14*	*p<0.2585*	1.29 ± 0.26	*p<0.5420*
SK-N-BE(2)C	23.91 ± 10.36	*p<0.1258*	1.28 ± 0.19*	*p<0.1735*	2.99 ± 1.39	*p<0.0896*	1.23 ± 0.18	*p<0.2846*	1.53 ± 0.33*	*p<0.1863*	15.70 ± 7.06	*p<0.0899*	11.47 ± 5.49	*p<0.0759*

Table 6: NEP validation in NB patient and cell lines by real-time PCR

The over-expression of selected NEP genes in the secondary spheres derived from the four stage4 NB samples NB1-T, NB2-T, NB4-T and NB5-T, and the NB cell lines has been validated by real-time PCR. The relative expression was expressed by the mean ± SEM of measures from three independent experiments for NB1-T and cell lines, two for NB2-T and 1 for NB5-T. * indicates samples where the measured transcripts were already highly expressed in the tumor or the cell line. In three cases with the mention “nd” (i.e. no detection), the amount of total synthesized cDNA and the level of the transcript extracted from secondary spheres were too low to be detected and amplified in the experiments.

As CD133 and MDR1 proteins appear to be almost universally increased in NB samples-derived spheres, their surface expression was checked by flow cytometry in several samples and derived spheres (Figure 19).

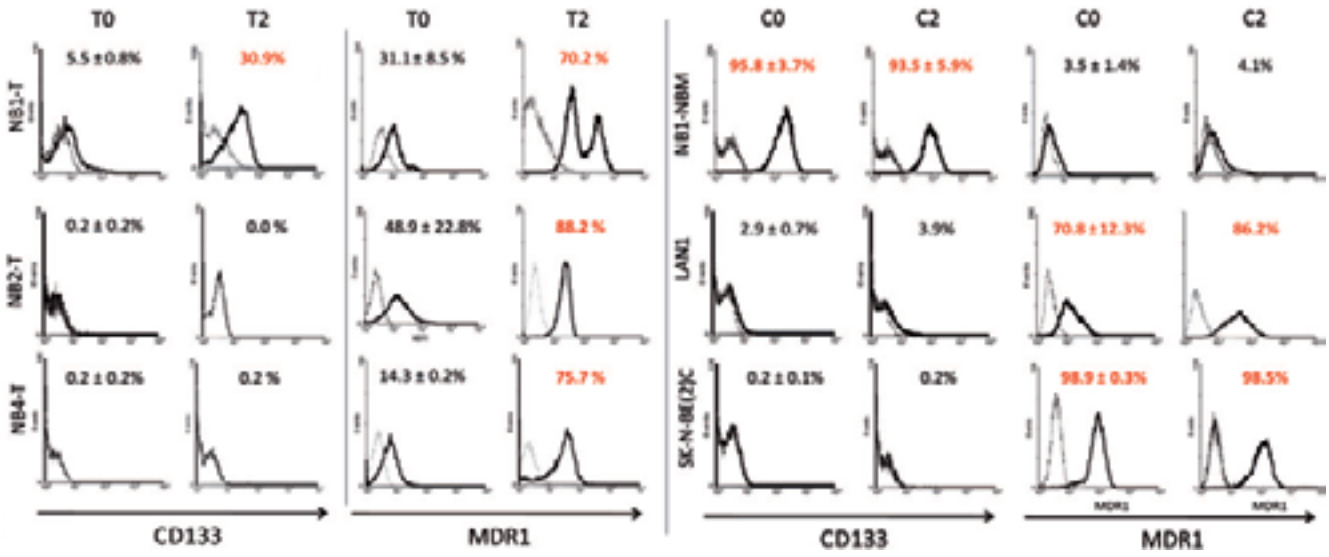

Figure 19: CD133 and MDR1 expression in NB patient and cell lines by FACS analysis
Flow cytometry analysis of the CD133 and MDR1 expression in secondary sphere (T2 and C2 in tumors and cell lines respectively) derived from the NB1, NB2 and NB4-T (T0, left panel) and cell lines (C0, right panel). The percentage of positive cells for each marker is indicated by the mean ± SEM of three independent measures and is illustrated by a representative graph.

CD133 was detected on 5% of NB1-T cells, but undetectable on NB2-T or NB4-T cells (left panel), whereas MDR1 was highly expressed by NB1, NB2 and NB4-T tumors with 31.1%, 71.6% and 27.2% of positive cells respectively. CD133 (30.9%) and MDR1 (70.2%) positive cells were found in NB1 secondary sphere cells, confirming the transcript up-regulation of these markers.

In cell lines, CD133 was highly expressed on the serum-free cultivated NB1-NBM cells (95.8%±3.7% positive cells), whereas it was almost nonexistent at the surface of LAN1 (2.9%) and SK-N-Be(2)c (0.2%). The mean of CD133 expression in NB1-FCS was 64.7±12.4% (5 independent experiments with 1<P<40) but we observed a consistent decrease of CD133 positive cell percentage with the passages; at early passages (P<5) over 90% cells were CD133 positive whereas the number of positive cells dropped down to only 46% at P>20 in 10% serum-supplemented medium (data not shown). The up-regulation of CD133 mRNA was confirmed by up-regulation of CD133 protein in LAN1 spheres, but not in NB1-NBM which already highly expressed this marker. No significant over-expression of CD133 between C0 and C2 has been detected in SK-N-Be(2)c, neither at the RNA or protein level.

In contrast, MDR1 transporter was consistently detected on all cell lines, with up to 70.2% positive cells in LAN-1 and 98.9% in SK-N-Be(2)c. LAN1 spheres over-expressed MDR1 detected by FACS at C2 (86.2%) confirming the real-time PCR analysis. In contrast, only 3.5% NB1-NBM cells were MDR1 positive and no significant increase between C0 and C2 was detected, as opposed to the observed mRNA up-regulation.

Genes such as MDR1 which expression is not elevated in the NB1-NBM, but increase in spheres, may be particularly relevant to further investigate, as the effect of the serum-free, growth factors and B27-supplemented medium can be excluded, and their increase may specifically reflect the increase in self-renewing cells.
These findings validated the use of CD133, MDR1, GPR177 and ROBO1 as the restricted list of genes to further analyze the sphere cell population.

The Neurosphere Expression Profile is associated with tumor microenvironment-related tumorigenic characteristics

In the above section, we have analyzed the gene expression profile of tumors and neurospheres, and proposed a gene expression profile associated to NB sphere-forming cells, and hence to a self-renewal property.
We then investigated the capacity of different samples, NB1-T and derived secondary (T2) or tertiary (T3) sphere-forming cells, NB1-NBM and NB1-FCS, to induce tumors *in vivo* in either heterotypic (subcutaneous injections) or orthotopic (intra-adrenal injections) conditions as described (209).

In vivo heterotopic tumor development and growth of NB1-T sphere cells

To address the *in vivo* tumorigenicity of the self-renewing NB1-T cell population in a heterotopic model, groups of 6-10 nude mice were subcutaneously engrafted with decreasing amounts of NB1-T, NB1-T3, NB1-NBM and NB1-FCS cells (10^5 to 10) in the presence of 50% Matrigel. Tumor development and growth were followed every 3-4 days using calipers.
When 10^5 cells were engrafted, tumor growth of NB1-T3 cells was significantly faster than NB1-T cells. The growth of NB1-NBM tumors was faster and animals were sacrificed earlier, at 40 days already, considering the big size of 3/6 tumors. However the observed difference of tumor growth was not significant between NB1-NBM group and the others. The NB1-FCS cells, in contrast did not initiate any tumor after injections of less than 10^5 cells (Figure 20).

In the groups implanted with lower number of cells (10^4, 10^3 and 10), no difference was observed between the different groups except for the group injected with 10^4 cells, at day 48 (*p=0.03*) where the mean of NB1-T tumor volume was bigger than NB1-T3 tumor volume (Figure 20).

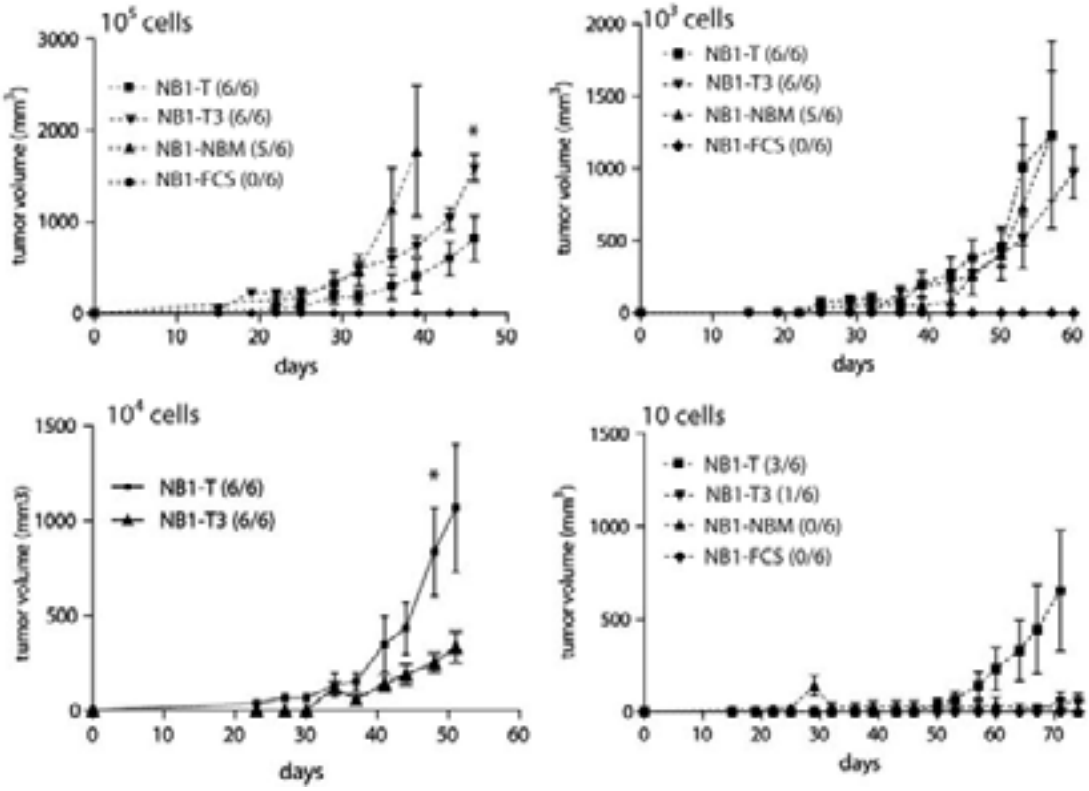

Figure 20: *In vivo* subcutaneous growth and tumor take of NB1-T tumor and spheres
Mean and SEM tumor volumes has been measured every three days after subcutaneous implantations of 10^5, 10^4, 10^3 and 10 NB1-T, NB1-T tertiary spheres (NB1-T3), NB1-NBM and NB1-FCS cells. The number of observed tumor takes is expressed as number of mice with tumor/total mice for each sample. * indicate p<0.05 (One-way ANOVA).

In addition, a mean of 5.6±0.4 (N=6) weeks for the first detection was observed in NB1-T group and was significantly higher than the detection in the NB1-T3 (3.8±0.4 weeks) and NB1-NBM groups (4.1±0.4 weeks). In the group of 10^4 cells, no significant difference for the first detection was observed; the tumors were detected in NB1-T and NB1-T3 groups at 6.1±0.3 and 6.4±0.4 weeks respectively (Figure 21).

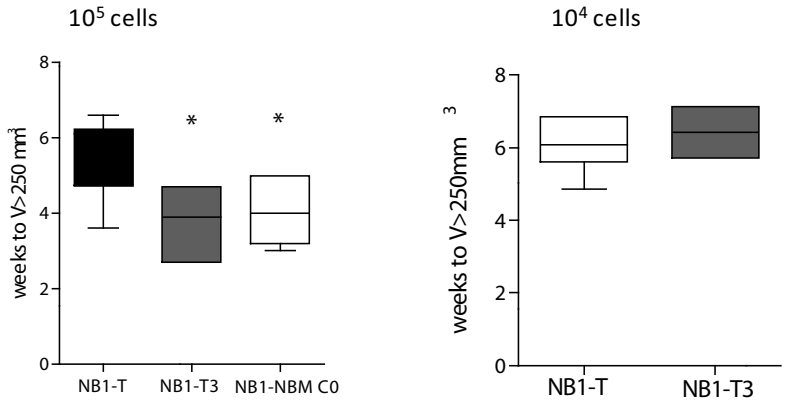

Figure 21: *In vivo* subcutaneous tumor detection after grafting of NB1-T tumor and spheres
Mean and S.E.M. of detection date of tumors with a volume exceeding 250mm^3 are represented for mice groups injected with 10^5 (left) and 10^4 (right) cells of the indicated samples. *indicate $p<0.05$ (Mann-Whitney test).

Thus, in heterotopic implantations, significant differences in tumorigenicity between NB1-T and NB1-T3 cells were only observed when a high cell number, superior to 10^5, was implanted.

NB1-T sphere cells tumorigenicity in orthotopic microenvironment

We next addressed the question of the effect of the micro-environment on the NB1-T2 cell tumorigenicity. In this model, 10^4 cells of NB1-T and NB1-T2 cells in PBS, without matrigel, were implanted in the adrenal gland of 10 to 14 nude mice respectively. Measures of tumor volumes were performed every 2 weeks by ultrasound imaging to assess tumor burden and growth (Figure 22).

The observed tumor take was 40% (4/10) vs. 79% (11/14) for NB1-T and NB1-T2 respectively, and the mean detection time (defined as disappearance of the adrenal gland structure) was 65.5±6.7 vs. 61.4±4.5 days. In addition, 5/14 tumors exceeded 100 mm^3 at 100 days in the NB1-T2 group vs. 1/10 in the NB1-T group. These data indicate that NB1-T2 cells displayed significant enhanced tumor take and growth when implanted in an orthotopic environment, and also produced larger tumor volumes as compared with the NB-T cells.

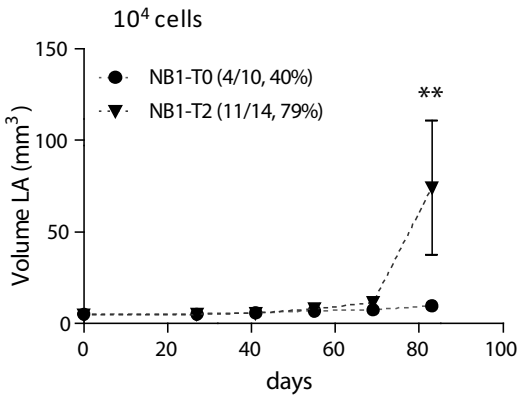

Figure 22: *In vivo* orthotopic tumor detection after grafting of NB1-T tumor and spheres in nude mice
Mean volumes of tumor and normal adrenal gland as measured are represented at the indicated days after implantation of 10^4 cells of NB1-T and derived secondary spheres (NB1-T2) in PBS into the adrenal gland of nude mice. The number of developed tumors is expressed as number of mice with tumor/total mice and percent mice with tumor. ** indicate $p<0.01$ (Two-way ANOVA).

Heterotopic and orthotopic NB1-T tumors histology

The histology of original patient tumor, NB1-T and NB1-T2/3 derived, subcutaneously or orthotopically grown tumors, was examined. The histology of all tumors with undifferentiated small blue round cells and large vascularized regions was very similar in either injection sites (Figure 23).

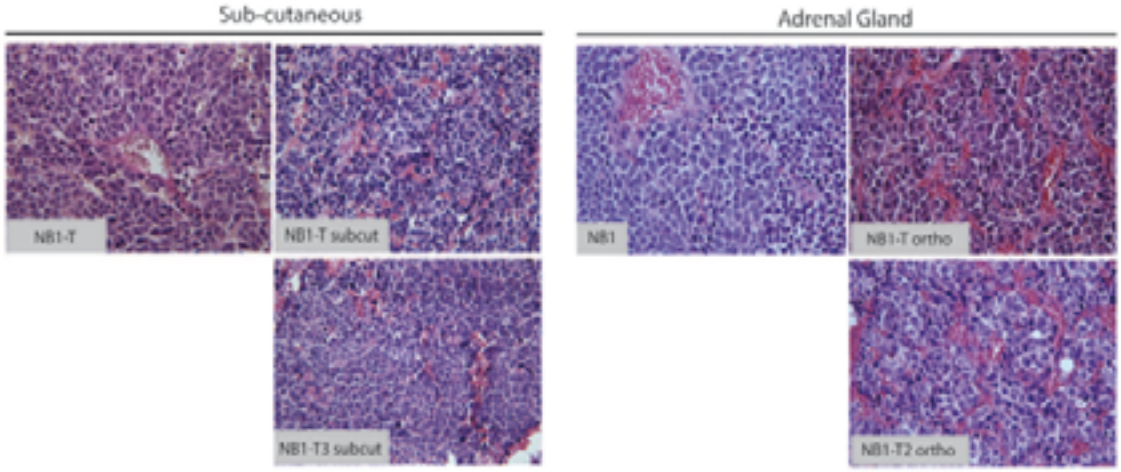

Figure 23: Histology of the *in vivo* subcutaneous and orthotopic tumors derived from NB1-T tumor and spheres in nude mice
The tumor micro-environment organization was evaluated by H/E staining on paraffin sections of the NB1, subcutaneous (left) and orthotopic (right) tumors obtained after implantation of 10^4 NB1-T ("NB1-T subcut" and "NB1-T ortho") and NB1-T2 cells ("NB1-T3 subcut" and "NB1-T2 ortho").

Subcutaneous engraftments of NB1-T/T2 cells without Matrigel

To better address the influence of the medium and environment on tumor growth, the subcutaneous implantations were repeated without Matrigel, in similar conditions as for orthotopic engraftment. Indeed Matrigel contains growth factors which could influence the tumor cell growth and divert them from the original microenvironment pressure.

Ten nude mice/group were therefore s.c. injected with 10^4 NB1-T and NB1-T2 cells respectively in PBS. Five mice died from independent causes in the 10^4 NB1-T cells group. In these conditions, no growth was observed in both groups up to 133 days, indicating that factors present in the Matrigel solution, and/or in the mouse adrenal tumor environment are essential to induce NB growth.

So, the adrenal environment seemed to specifically support the growth of NB-CSCs. Orthotopic conditions may thus highlight the tumorigenic properties of the NB-CSC population.

The above-described findings also suggested that serial NB sphere formation results in a progressive enrichment in cells with essential characteristics of cancer stem cells such as normal stem cells markers expression, self-renewal and tumorigenicity. In particular, the NB1-T model allowed us to define a neurosphere expression profile associated with enhanced microenvironment-related tumorigenic properties.

Phenotypic heterogeneity of NB-CSCs

The previous results allowed us to identify a self-renewing and tumorigenic population of cells defined by the specific NEP expression. In order to further characterize such cell sub-population responsible for NB1 tumorigenicity, we next addressed its putative heterogeneity. The functional relationship between cell subsets selected by differential NEP genes expression was investigated.

Characterization of CD133 positive cells in NB1 tumor and spheres

CD133 has been described for several adult tumors (brain, colon, pancreatic, Ewing) as a marker for cancer stem cells, capable to select for a tumorigenic sub-population (48-50, 52, 55, 56). CD133 expression was very low or undetectable in all analyzed patient tumors: NB1 (5.5±0.8 % positive cells), NB2 (0.8±0.0%), NB3 (≤0.5%) and NB4 (0.8%) (Figure 19). In our NB1 model, CD133 was found to be over-expressed in NB1-T2 (30.9% positive cells) and NB1-NBM (95.8±3.7% positive cells) but significantly lower in NB1-FCS (64.7±12.4% positive cells) (Figure 19). Moreover, as shown in Table 6, CD133 expression was significantly increased in spheres derived from a majority of analyzed stage4 patient tumors.

CD133 expression was highly variable in these different samples and cell lines, and dependent on the culture conditions. We therefore attempted to determine whether the cells expressing CD133 and the other NEP-associated genes corresponded to a single homogeneous CSC population, gradually selected by the serial sphere culture, or if CD133 and the other NEP genes could be independently induced in selected cells within the sphere population.

$CD133^{high/low}$ cell sorting in NB1-T

In this aim, $CD133^{high}$ and $CD133^{low}$ populations were sorted from dissociated NB1-T tumor and the expression of CD133, GPR177, EDNRB, MDR1 and ABCA1 NEP-genes was measured by real-time PCR (Figure 24A). GPR177, IGFBP5 and EDNRB transcripts were found co-expressed with CD133 gene in NB1-T cells whereas MDR1 and ABCA1 were equally expressed in both sub-populations.

The same CD133 cell sorting experiment was carried out with the NB1-T2 cells. A similar heterogeneity in sphere genes expression was found, with the significant anti-correlated expression of CD133/GPR177/EDNRB and MDR1 genes. In these cells, ABCA1 was shown to be co-selected with the $CD133^{high}$ cells although the measured difference was not significative (Figure 24B). These results indicate that in NB1-T sample, at least two distinct cell sub-populations able to survive in sphere culture conditions could be identified, which were characterized by either CD133 or MDR1 expression.

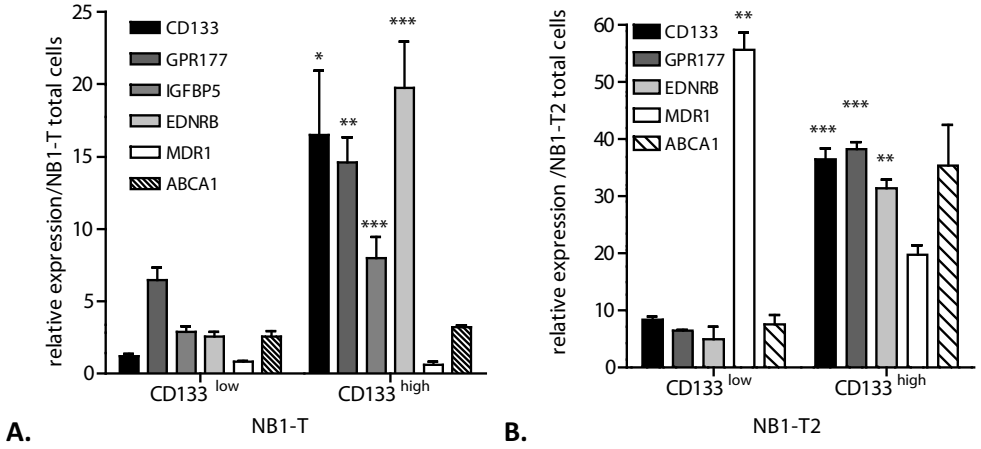

Figure 24: NEP gene expression in $CD133^{high/low}$ sorted cell populations in NB1-T and NB1-T2

A. Expression level of the CD133, GPR177, IGFBP5, EDNRB, MDR1 and ABCA1 NEP associated genes were analyzed by real-time PCR in $CD133^{high/low}$ sorted cells from dissociated NB1-T tumor. **B.** Expression level of the CD133, GPR177, EDNRB, MDR1 and ABCA1 NEP associated genes were analyzed by real-time PCR in $CD133^{high/low}$ sorted cells from dissociated NB1 secondary spheres (NB1-T2). Two independent experiments were performed. *, ** and *** indicate $p<0.05$, $p<0.01$ and $p<0.001$ respectively (Student's t-test).

Characterization of MDR1 positive cells in NB1 tumor and spheres

The MDR1 transporter (also called ABCB1), responsible for multi-drug-resistance in NB cells, was another strongly and gradually increased gene in NB1-T spheres as shown in Table 4, Table 6 and Figure 19. Whereas its surface expression level in NB tumors and cell lines was variable (31.1±8.5%, 71.6% and 0.3% positive cells in NB1, NB2 and NB4-T samples respectively), MDR1 transcripts level was uniformly enhanced in the spheres derived from all patient samples analyzed. This enhancement was confirmed by FACS analysis of NB1-T derived spheres with an increase up to 70% positive cells (Figure 19). In addition, while micro-array analysis showed a "linear" increase evolution of CD133 expression, MDR1 expression in contrast showed a "step" increase evolution along serial sphere passages of NB1-T and NB2-T samples (Figure 18).

$MDR1^{high/low}$ cell sorting in NB1-T and LAN-1 cells

To confirm the mutually exclusive expression of the CD133 and MDR1 NEP genes, $MDR1^{high}$ and $MDR1^{low}$ expressing cell subsets were selected from LAN-1 and NB1-T cell populations. Data showed that CD133 and GPR177 expressing cells were indeed enriched in the NB1-T $MDR1^{low}$ subset whereas ABCA1 appeared to be co-expressed with MDR1 (Figure 25).

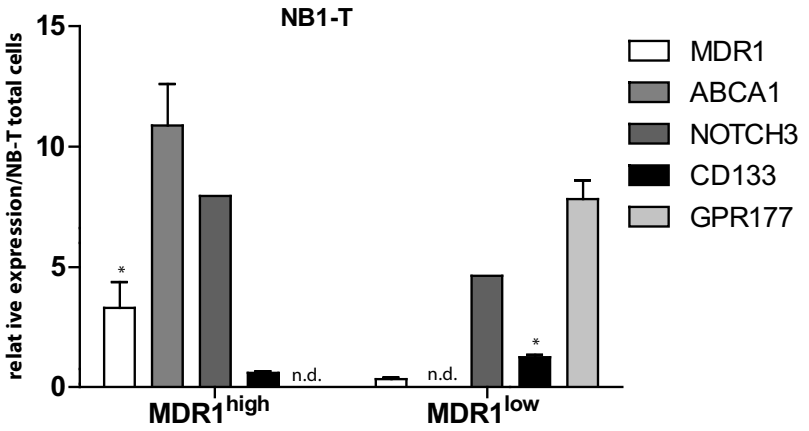

Figure 25: NEP gene expression in $MDR1^{high/low}$ sorted cell populations in NB1-T

Expression level of MDR1, ABCA1, NOTCH3, CD133, and GPR177 genes were analyzed by real-time PCR in $MDR1^{high/low}$ sorted cells from dissociated NB1-T tumor. "n.d." stands for "non-detected". * indicates $p<0.05$ (Student's t-test).

The same experiment performed with LAN-1 cells indicated a significant anti-correlation between the expression of CD133/NOTCH3 and MDR1 as illustrated in Figure 26.

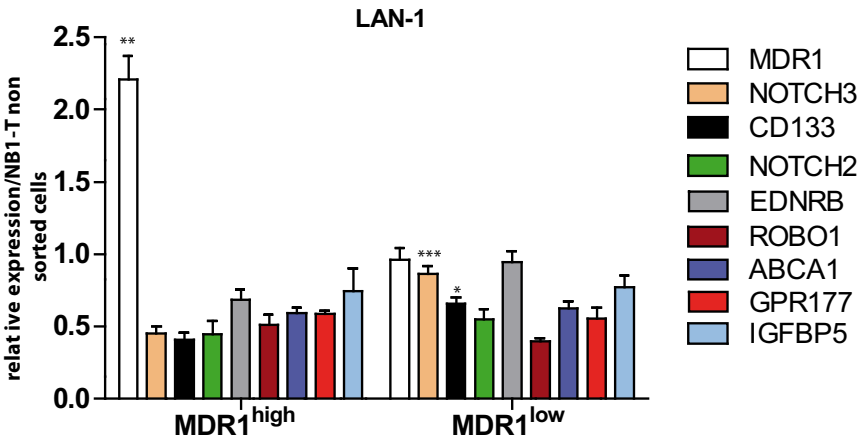

Figure 26: NEP gene expression in MDR1$^{high/low}$ sorted cell populations in LAN-1 cell line
Expression level of MDR1, NOTCH3, CD133, NOCTH2, EDNRB, ROBO1, ABCA1, GPR177 and IGFBP5 genes were analyzed by real-time PCR in MDR1$^{high/low}$ sorted cells from LAN1. *, ** and *** indicate $p<0.05$, $p<0.01$ and $p<0.001$ respectively (Student's t-test).

To support these data, double MDR1/CD133 cell sorting of NB1 tumor was carried out. Three sorted CD133^{high}MDR1^{low} (1.2±0.2% gated cells), CD133^{low}MDR1^{high} (15.4±1.2% gated cells) and CD133^{high}MDR1^{high} (0.4±0.0% gated cells) cell populations were obtained (Figure 27A). The expression of MDR1, CD133, EDNRB and GPR177 was measured by real-time PCR on the selected populations and on the unsorted population (Figure 27B). CD133/EDNRB/NOTCH3 expressing cells were clearly co-selected in the same sub-set, while MDR1 gene was selected in the MDR1^{high}CD133^{low} population. These data confirmed the anti-correlated expression of MDR1 and CD133 NEP genes.

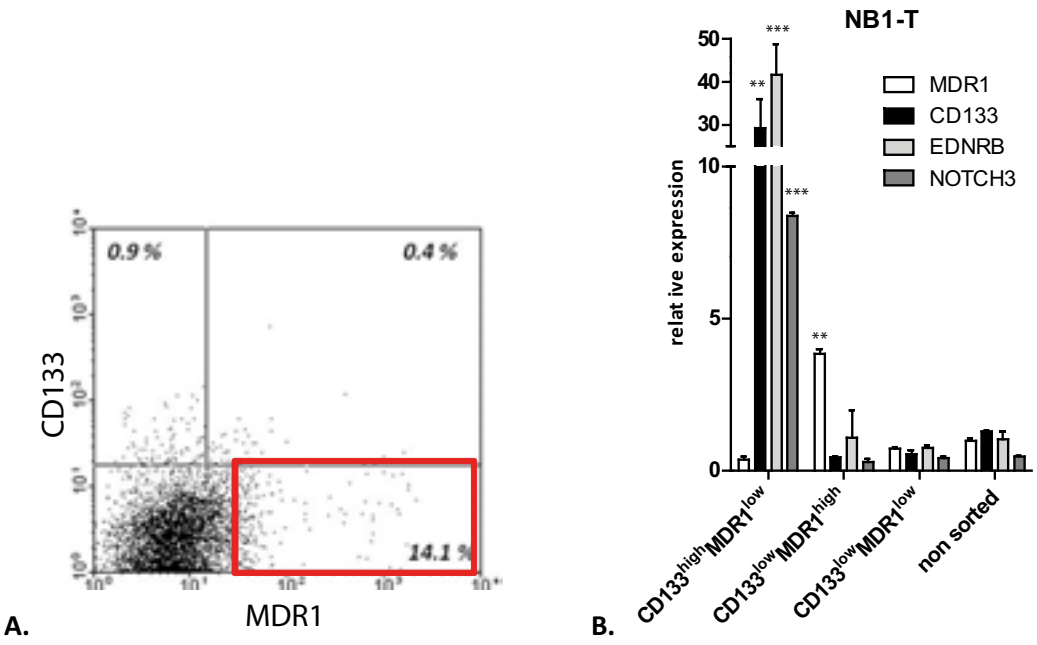

Figure 27: NEP gene expression in MDR1$^{high/low}$ sorted cell populations in LAN-1 cell line

A. CD133/MDR1 FACS analysis on dissociated NB1-T tumor. The displayed dotplot is representative of the two independent experiments. **B.** Expression level of MDR1, CD133, EDNRB, NOTCH3, NOTCH2, ABCA1, GPR177, ROBO1 and IGFBP5 genes were analyzed by real-time PCR in MDR1$^{high/low}$ sorted cells from NB1-T. *, ** and *** indicate p<0.05, p<0.01 and p<0.001 respectively (Student's t-test).

All together, these results supported the pre-existence in NB1-T of at least two cell subsets selected in the sphere culture: the CD133^{high}MDR1^{low} cells co-expressing EDNRB, GPR177 and IGFBP5, and the CD133^{low}MDR1^{high} cells, co-expressing ABCA1. In addition, these results identified on the basis of the NEP expression profile, the existence of at least 2 distinct cells subsets with putative CSC characteristics in NB.

Tumorigenic properties of the CD133$^{high/low}$ and MDR1$^{high/low}$ sphere cell populations

To further address the functional heterogeneity of the cell populations enriched in NB1-T spheres, CD133 or MDR1 high and low expression subsets were isolated from NB1-T and their tumorigenic properties evaluated *in vivo,* in orthotopic conditions.

Tumorigenic properties of the CD133$^{high/low}$ NB1-T cell populations

The *in vivo* tumor growth of sorted CD133^{high} and CD133^{low} NB1-T cell populations was measured by orthotopic implantation of 10^4 cells in PBS, in the adrenal gland of nude mice (6 animals/group).

As shown in Figure 28, tumors were found in 2/6 ($CD133^{high}$) vs. 1/6 ($CD133^{low}$) mice after 110 days, revealing no significantly different tumor growth and take between $CD133^{high}$ and $CD133^{low}$ populations. One mouse in the $CD133^{low}$ group presented a big adrenal tumor which was detected as early as 34 days after implantation. Among the two adrenal tumors which developed in the $CD133^{high}$ group, one was rapidly invasive. Cells infiltrating the adrenal vessel could be detected by ultrasound imaging and led to the growth of a big ovarian tumor at 100 days. The NB origin of $CD133^{high}$ and $CD133^{low}$ grown tumors was confirmed by IHC and FACS analyses with an anti-GD2 antibody, which stained over 90% of cells. CD133 expression in tumors grown from $CD133^{high}$ and $CD133^{low}$ subsets was 5-7.5% and 20.5% positive cells respectively (Figure 28, right panel). Surprisingly, the tumor grown from $CD133^{low}$ subset contained more $CD133^{+}$ cells than tumors grown from $CD133^{high}$ subset, confirming the high heterogeneity and plasticity of these cells.

Histology of tumors developed from $CD133^{high}$ and $CD133^{low}$ populations did not reveal differences in morphology, vascularization or differentiation from the original NB1-T tumor (Figure 28, middle panel).

These observations showed that CD133 expression was not able to select NB1-T cells with enhanced tumorigenic property. Therefore, although CD133 was included in the NEP, this marker did not alone represent a specific marker to identify NB-TICs. However, the infiltrative phenotype of $CD133^{high}$ cells observed in one mouse suggested a possible implication of the CD133 transmembrane protein or the specific CD133-associated cell subset in the observed pro-invasive behavior. This assumption would need further analyses to be validated with a greater number of mice per group and the orthotopic injection of the original NB1-T cells.

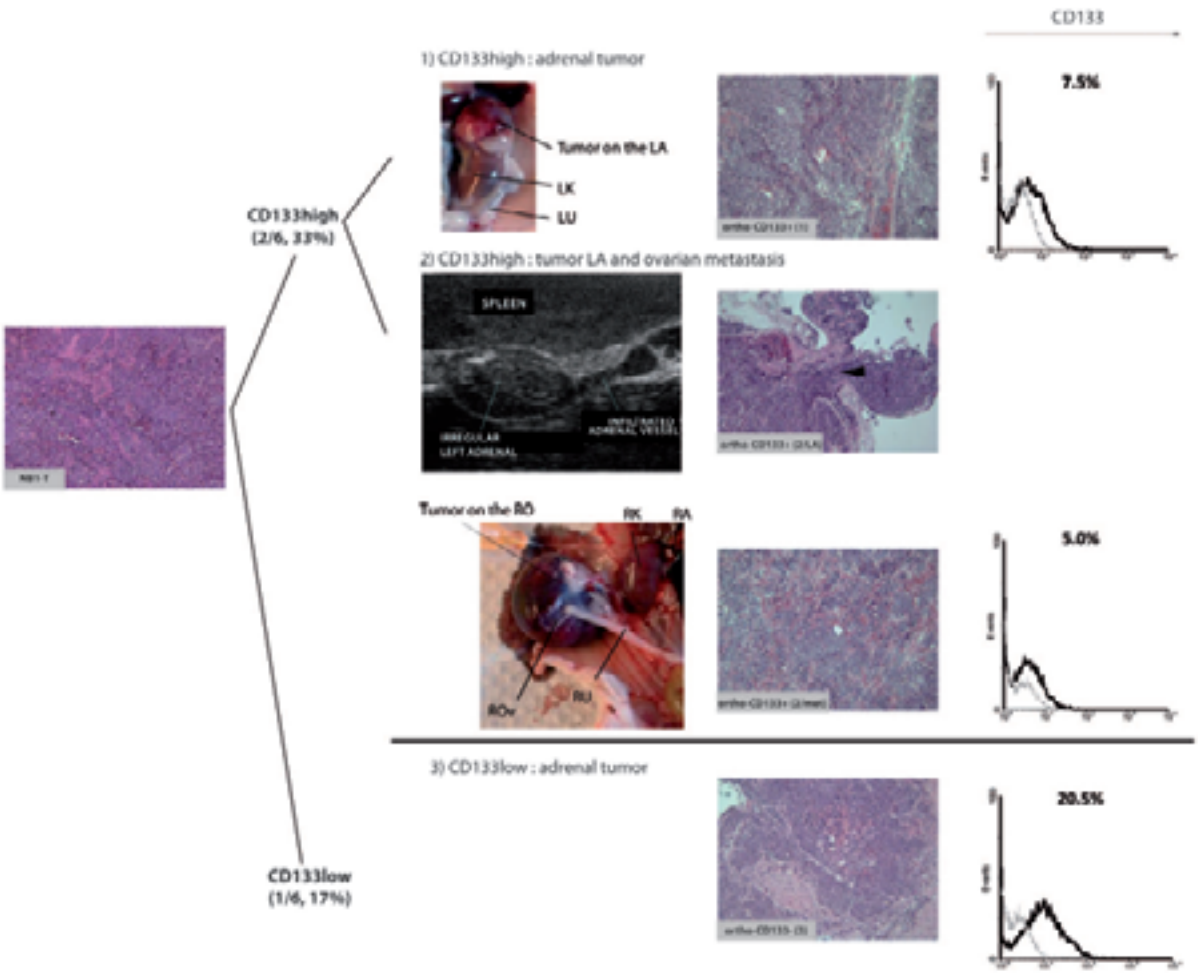

Figure 28: Orthotopic injections of CD133^{high} and CD133^{low} NB1-T cell populations

Dissociated NB1-T tumor (IHC on the left) was sorted in CD133^{high} and CD133^{low} population and orthotopically injected into the adrenal gland of nude mice (6 mice per group). 2/6 and 1/6 tumors developed from the two former populations respectively. Middle panels show for each following tumor the macroscopic picture or the ultrasound imaging of the primary tumor and the metastasis and the H/E staining on paraffin section. The right panel indicates the CD133 expression level (% gated cells) measured by FACS on the dissociated samples:

(1) Macroscopic adrenal tumor derived from the CD133^{high}.

(2) Microscopic primary tumor derived from the CD133^{high} NB1-T cells on the left adrenal and the associated contralateral ovarian metastasis.

(3) Macroscopic adrenal tumor derived from the CD133^{low}.

LA: Left Adrenal, LK: Left Kidney, LU: Left Uterus, RO: Right Ovary, RK: Right Kidney, RA: Right Adrenal, ROv: Right Oviduct, RU: Right Uterus. Black arrow head on the H/E staining of (2) shows invasive NB cells expanding out of the adrenal gland.

Tumorigenic properties of the MDR1$^{high/low}$ NB1-T cell populations

To assay the tumorigenicity of the NB1-T MDR1 expressing cells, corresponding to the alternative sub-population enriched in NB spheres, 5.10^3 MDR1^{high}, MDR1^{low} and unsorted NB1-T cells were orthotopically injected in the mice adrenal glands (Figure 29).

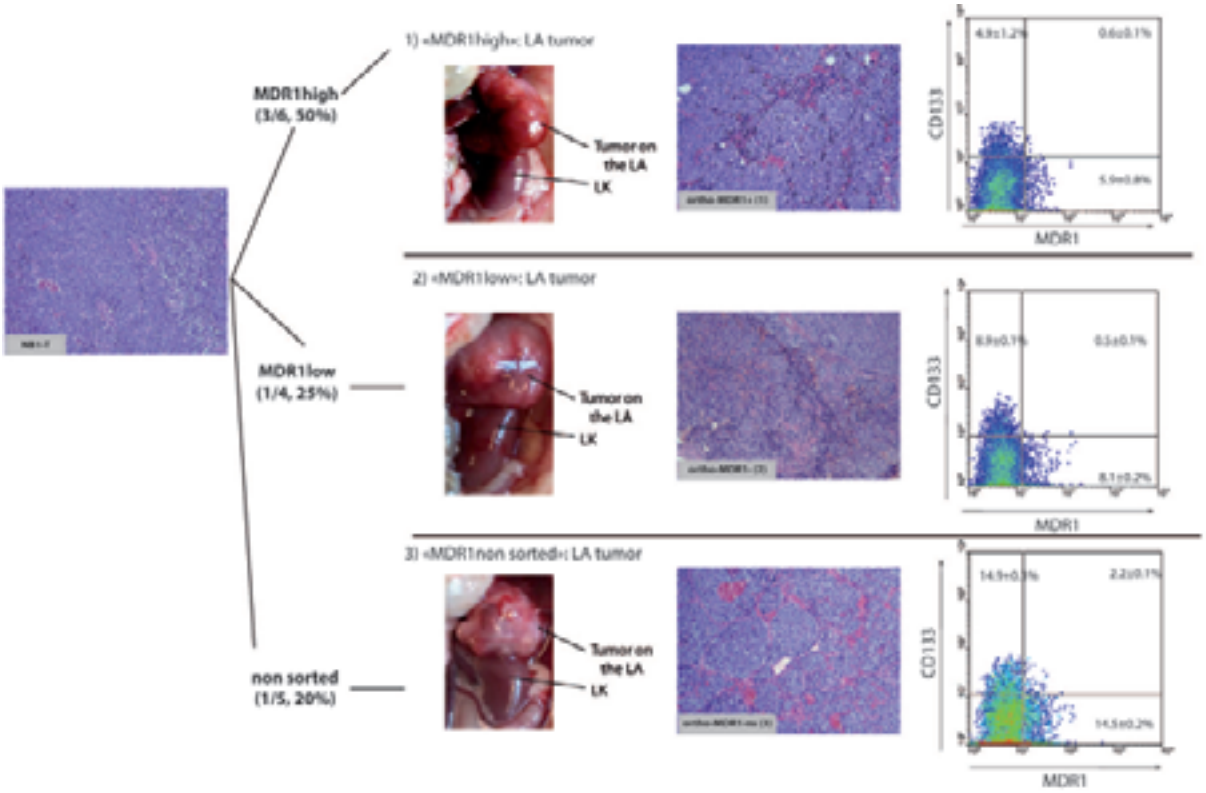

Figure 29: Orthotopic injections of MDR1^{high}, MDR1^{low} and non sorted NB1-T cell populations

Dissociated NB1-T tumor (IHC on the left) was sorted in MDR1^{high}, MDR1^{low} and non sorted populations.

5.10^3 cells of each population were orthotopically injected into the adrenal gland of nude mice (6, 4 and 5 mice respectively). 4/6, 1/4 and 1/5 tumors developed respectively from the three former injected populations.

Middle panels show for each following tumor the macroscopic picture of the orthotopic tumor and the H/E staining on paraffin sections. Right panel indicates the CD133/MDR1 expression level (% gated cells) measured by FACS on the dissociated samples:

1) «MDR1high» macroscopic adrenal gland tumor (pictures representative from the three tumors of this group).

2) «MDR1low» macroscopic adrenal gland tumor.

3) «non sorted» macroscopic adrenal gland tumor.

The percentage of CD133$^+$MDR1$^-$, CD133$^+$MDR1$^+$ and CD133$^-$MDR1$^+$ is indicated in each quadrant by the mean ± SEM measured in the orthotopic tumors. LA: Left Adrenal, LK: Left Kidney

The follow-up showed an increased tumor take at 105 days post-injection in the MDR1^{high} group with 67% of mice bearing adrenal tumors, compared to the MDR^{low} and non sorted group showing 25% and 20% of mice with adrenal tumors respectively (Figure30 A). Likewise, tumor volumes were higher in the MDR1^{high} group as compared with the MDR^{low} or unsorted groups (Figure30 B). Although these data did not reach significance due to the low number of animals, it nevertheless suggested that highly tumorigenic cells were mostly included in the MDR1^{high} group.

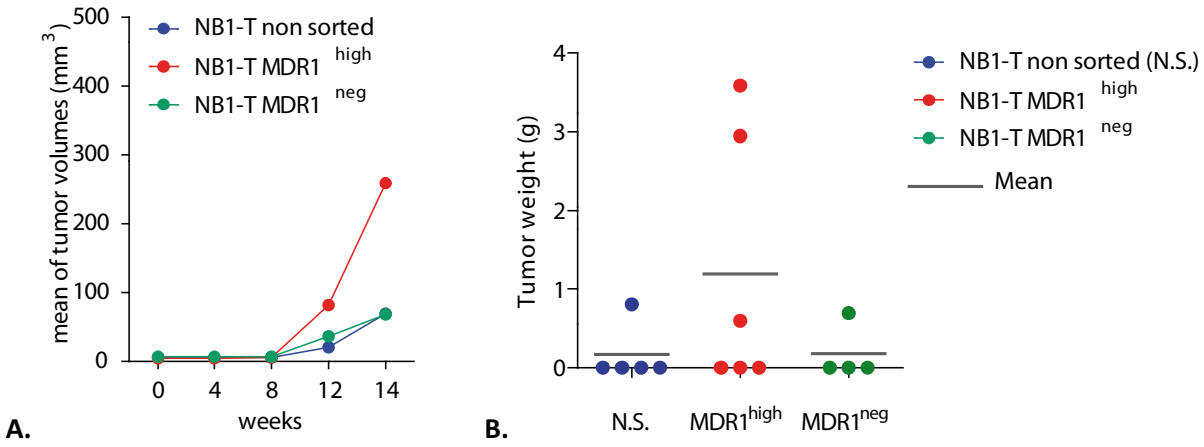

Figure 30: *In vivo* orthotopic tumor growth and volume derived from the MDR1^{high} and MDR1^{low} and non sorted populations

A. Mean volumes of tumor and normal adrenal gland as measured are shown at indicated days after implantation of 5.10^3 cells of in PBS into the adrenal gland.

B. Weights of tumors and normal adrenal gland at 105 days post injections of 5.10^3 cells NB1-T non sorted, MDR1^{high} and MDR1^{low} cells. Grey bars indicate the mean of weights in each group of injected mice.

Phenotype of orthotopic tumors derived from the MDR1$^{high/low}$ NB1-T cells

The dissociated orthotopic derived tumors (MDR1^{high}, MDR1^{low} and MDR1^{unsorted}) were analyzed by FACS for cell surface expression of MDR1 and CD133 (Figure 29, right panel). Three different cell populations regarding their combined expression of the two markers: CD133$^+$MDR1$^-$, CD133$^+$MDR1$^+$ and CD133$^-$MDR1$^+$ cells were identified. In all groups of orthotopic tumors, the double positive cells were the smallest represented sub-population with a percentage of 0.6%, 0.5% and 2.2% of gated cells respectively. The majority of stained cells corresponded to CD133$^+$MDR1$^-$ and CD133$^-$MDR1$^+$ cells. Interestingly, the orthotopic tumors reproduced the CD133/MDR1 initial expression phenotypes observed in the NB1-T injected cells except for the CD133$^+$MDR1$^-$ sub-population which is almost absent in NB1-T (Figure 27A). Indeed less than 1% of the NB1-T cells were CD133$^+$MDR1$^-$ whereas this subset represented between 5 and 15% of the MDR1^{high}, MDR1^{low} and MDR1^{unsorted}

orthotopic derived tumor cells as shown in Figure 29. The variable CD133 expression observed in the $CD133^{high/low}$ orthotopic derived tumor was comforted by these data in $MDR1^{high/low}$ orthotopic tumors, and suggested a micro-environmental regulation of CD133 expression.

In addition, the above observations support the $CD133^{low}/MDR1^{high}$ cells as the most representative CSC population.

Trails for therapeutic uses of NEP markers

In our study, the NEP genes have been associated with self-renewal and tumorigenic property in the NB1 model and as such may represent a panel of potential therapeutic targets.

Specific inhibition of the endothelin pathway in NB-CSCs

The microarray analyses of NB spheres identified several upregulated NEP genes involved in the endothelin axis, including the endothelin receptors A (EDNRA) and B (EDNRB) as shown by the genechip signals of figure 31. The up-regulation of EDNRB gene in NB spheres has been validated in 43% of analyzed NB samples (Table 6). In contrast, EDN ligands were not found to be deregulated in NB1-T, NB1-NBM, NB2-T or NB4-T spheres except for EDN3 which was weakly upregulated in the NB1-T spheres (Figure 31).

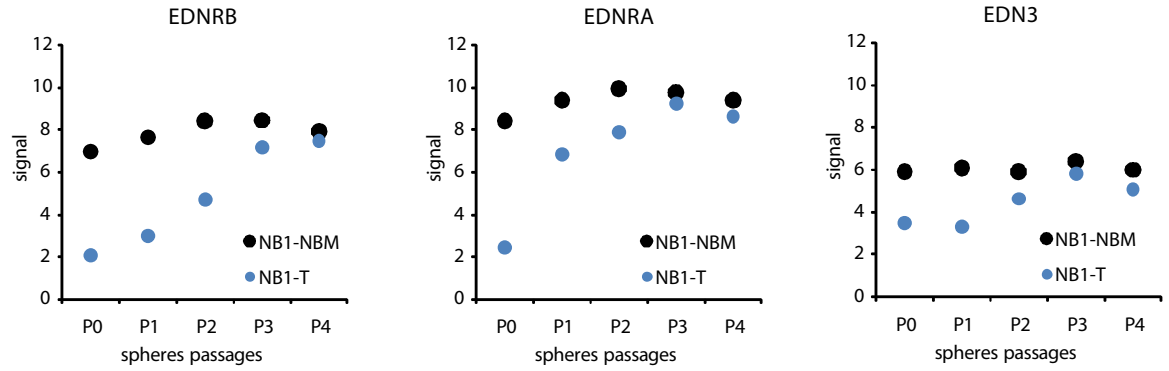

Figure 31: Microarray gene expression profiles of EDNRA, EDNRB receptors and endothelin-3 (EDN3) genes in the NB1-T and NB1-NBM derived spheres

The signal levels of mRNA hybridization on the GeneChips are represented for the NB1-NBM (blue) and NB1-T (black) experiments from the parental cells (P0) to their derived quaternary spheres (P4). The most relevant probe-set for each gene has been selected. EDN1 and EDN2 associated probe-sets showed neither any significant signal nor any variable expression in all the micro-array experiments (data not shown).

Endothelin receptors are G-protein coupled receptors which have different affinity for their three ligands endothelin 1, 2 and 3 (EDN1, 2 and 3): EDN1 and EDN2 bind preferentially EDNRA with similar affinity, while EDN3 has a low affinity for EDNRA. EDNRB binds all three ligands with equal affinity (230). EDN1 is primarily expressed by endothelial cells, EDN2 in kidney and intestine, and EDN3 is found mainly in the brain (231). Endothelin axis has been implicated in the regulation of proliferation, differentiation and angiogenesis in a number of normal and cancer cell types (232-234). In particular, EDNRs and their ligands play a key role during neural crest development (171, 172, 227, 228).

In order to further investigate the implication of this pathway in the NB1-T sphere, we determined the expression of endothelin axis actors in NB samples. The expression of EDNRA, EDNRB, EDN1, EDN2 and EDN3 in eight NB cell lines was measured by PCR (Figure 32). NB cell-lines were shown to express high level of one or both endothelin receptors and at least one ligand was detected in all the NB cell lines. EDN1 was almost consistently expressed whereas EDN3 was detected only in 2/8 NB cell lines.

These observations lead us to postulate that entothelin axis could represent a suitable therapeutic target for NB.

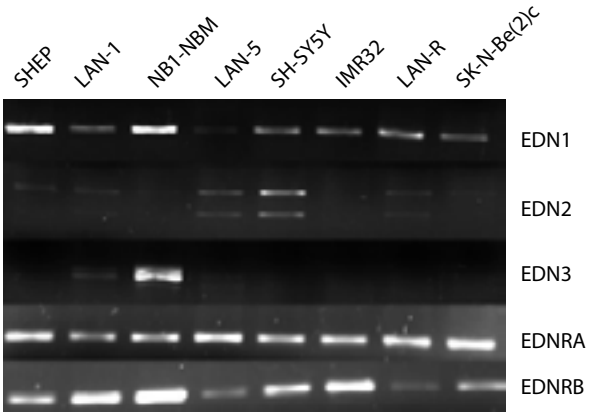

Figure 32: Endothelins (EDN1, 2 and 3) and endothelin receptors (EDNRA and B) expression analysis by RT-PCR in eight NB cell lines.

GAPDH expression was used as a control in all NB samples (data not shown).

It has been recently shown that EDNRA and EDNRB antagonists can have antitumor activity in human melanoma and ovarian cancer cells (235-237).

Bosentan, a mixed EDNRA/B receptor antagonist has been shown to potentiate Fas-L-induced apoptosis in rat colon carcinoma cells (207). To address the sensitivity of NB cells to Bosentan, NB1-NBM, LAN-1, SK-N-Be(2)c, SH-SY5Y, SH-EP, and LAN-5 NB cell lines were exposed to gradually increased doses of Bosentan (Figure 33). All tested NB cell lines were sensitive to Bosentan except SHEP and LAN-5 which showed a significant resistance to this drug. Interestingly, the NB cell lines showing higher sphere-forming capacity (LAN-1, SK-N-Be(2)c and NB1-NBM) were the most sensitive to Bosentan.

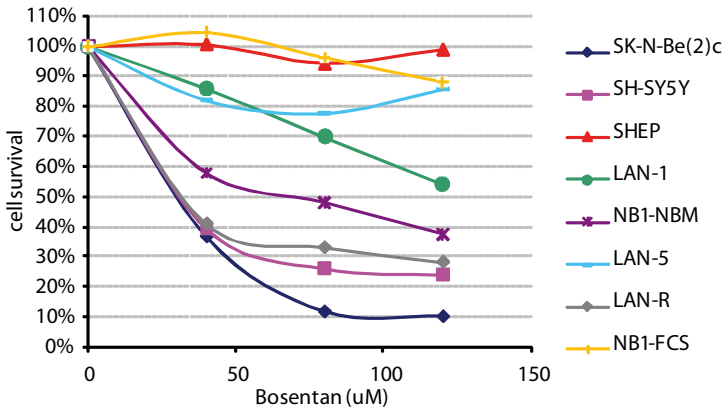

Figure 33: Cell survival capacity analysis in a panel of NB cell lines in presence of Bosentan
Bosentan cell cytotoxicity has been measured in 9 NB cell lines, in NB1-NBM and NB1-FCS which have been established in the lab by propagating NB1-T cells in serum-free and 10%serum medium respectively. LAN-R is a multi-drug resistant cell line derived from LAN-1 and previously described by Flahaut et al. (217).

NB1-NBM cell line has previously been shown to express high level of both EDNRA and EDNRB (Figure 31) and to have a high capacity to form spheres (Figure 8 and 10). To test the effect of Bosentan on NB cell sphere-forming capacity, NB1-NBM cells were therefore seeded in sphere culture and exposed to 80 µM of Bosentan. As shown in Figure 34, after one week of exposure to Bosentan, a drastic decrease of the NB1-NBM sphere number was observed compared to the control.

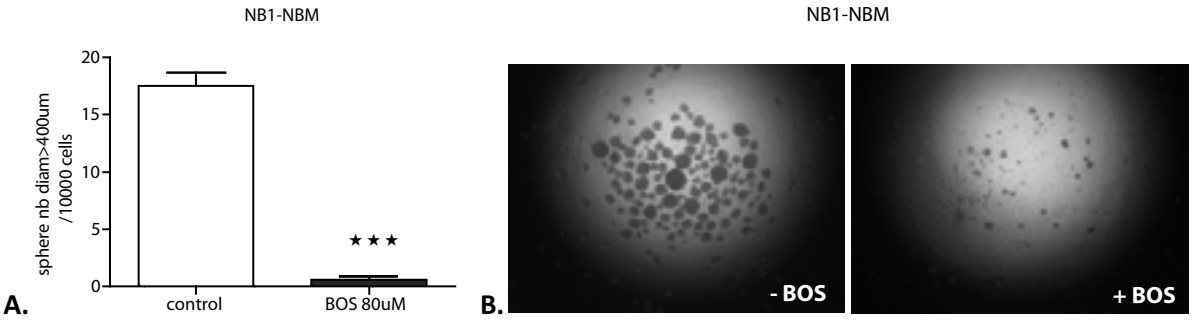

Figure 33: Bosentan inhibited the sphere-forming capacity of the EDNRA/B expressing NB1-NBM cells

A. The Bosentan (BOS) inhibiting effect on the sphere-forming capacity of NB1-NBM cell line has been measured by self-renewal assay in sphere culture conditions. **B.** Pictures show self-renewal assay without (-BOS) or with (+BOS) Bosentan in the culture medium. Cells were plated in triplicates and for each well, only spheres with a diameter > 400 µm were counted. *** indicate $p<0.001$ (Student's t-test).

In consequence, due to its essential role in neural crest development, its enrichment in NB1-T spheres and the availability of specific inhibitors, the endothelin axis constitutes a relevant biological target that would need further investigations for targeted NB treatments.

DISCUSSION

Context of the project

The present project was initiated in 2006, when we proposed to address the contemporary questions on the adult cancer stem cell (CSC) concept in neuroblastoma (NB), a model for pediatric solid tumors. The main goal was to first determine if CSC concept could have been applied to NB tumors and if so, to characterize specific cell surface markers and gene activity profiles that can reliably be used to identify these CSC. The intratumoral cell hierarchy observed in NB has comforted us in the hypothesis of the NB-CSC existence and led us to address the mechanisms of its origin. These investigations had to be accompanied by the development of *in vivo* and *in vitro* functional assays that confirmed the different properties of the CSC subset as tumorigenicity, self-renewal, cell differentiation and resistance to cytotoxic agents.

Definitions in the CSC concept

Genetic and phenotypic cell heterogeneity in neoplasms have long time been recognized (238-240), but has only recently been systematically investigated (241-243). In particular, the origin of the cell phenotypes diversity observed in many cancers was first explained by the accumulation of genetic and epigenetic changes occurring in tumor cell genome and leading to the selection of tumorigenic clones (25). However with the emergence of the cancer stem cell concept, it was then thought that the observed heterogeneity of cancer cells, and in our case NB cells, could be explained by the existence in tumors of a hierarchical cellular organization, including a subset of so-called cancer stem cells that « constitutes a reservoir of self-sustaining cells with the exclusive ability to self-renew and maintain the tumor ». These terms constituted the rigorous definition established after a critical discussion during the American Association for Cancer research (AACR) workshop in 2006 by the scientific community having faced the need for a semantics agreement (41).

CSC hypothesis in NB

In this context, we were interested in addressing the existence of a NB stem cell subset in the aggressive NB tumors. Indeed, NB seemed good models for CSC study as they are embryonic especially aggressive tumors which display great inter- and intra-tumoral heterogeneity.

We studied a panel of NB samples of different stages, from differentiated benign phenotypes to more invasive and metastatic ones. The histological examination of the tissues confirmed the heterogeneous nature of NB tumors, with the coexistence of an array of different cell types. Indeed, in addition to the tumor stroma composed of immune cells, various mesenchymal and endothelial

cells, the malignant compartment included a variety of cells expressing specific neural crest lineages markers. These findings supported our hypothesis that cancer stem cells could exist in NB.

Experimental model

Therefore, among NB patient tumors and cell lines available in the pediatric oncology research laboratory, we selected samples which showed a high capacity to form xenograft tumors in immunocompromised mice and to grow as spheres in a serum-free medium, two experimental assessments of cell tumorigenicity and self-renewal respectively. A significant correlation between the stage of tumor aggressiveness in the patient and the stem-like phenotypes of the tumor cells was established. For most aggressive NB, stage4 NB1 tumor, as well as NB2 and NB4 samples, metastatic cells of the patient infiltrated bone marrows were primarily injected in the flanks of nude mice, and generated NB xenograft tumors recapitulating the primary tumor phenotype. NB xenografts were validated as NB study models and were preferentially chosen to identify NB tumorigenic cells.

Indeed, genetic and biological cell phenotypes were conserved between the primary tumors and their derived xenografts. Other model previously applied for NB-TICs study have been proposed (Hansford et al 2007), isolating sphere forming cells from NB patient bone marrows cultivated after weeks even months in *in vitro* conditions. Genomic alterations of the NB sphere cell lines were determined and in some cases lacked the typical NB chromosomic alterations. Moreover, in a recent communication (ANR 2010), the author reported the CD20 expression for some derived NB sphere cells suggesting their pre-B cell phenotype. Thus, the biological relevance of their NB-TICs model needs to be discussed as compared to the use of NB derived tumors maintained *in vivo*.

Neurosphere Expression Profile (NEP) characterization

In the attempts to identify in NB tumors the putatively rare population of cells with TIC properties, we cultured the NB1-T tumor in specific sphere-forming conditions, as a representative assay for self-renewal. Then, we performed a microarray analysis of the *acquired* sphere-forming cells expression profile to establish a sphere expression profile. We next functionally validated this sphere expression profile.

To limit the bias of interpretation due to self-renewing cell population purity, we considered that the significant selection of cells capable of self-renew occurred at the fourth passage of spheres based on the accepted idea that stem cells have a long-term self-renewal capacity. The gene expression profile study of NB sphere cells provided, by an objective and original approach, a panel of up- and down-regulated genes at the fourth generation of self-renewing cells that were subsequently termed **“Neurosphere Expression Profile”** (**NEP**).

A specific biological process enrichment analysis showed different families of genes specifically expressed in spheres and involved in molecular cascades important during embryogenesis, cell differentiation and stem cell homeostasis.

Moreover, several genes that were previously shown to be associated to CSC phenotype were found in the NEP. For instance, the aldehyde deshydrogenases (ALDH) used as breast tumor (47, 244) and human thyroid (245) cancer stem cells markers, were over-expressed in most of the NB sphere cells. Likewise CD133, strongly over-expressed in the NB spheres, has been recognized in the literature as the most important marker inherent to a number of CSC identified to date (48, 55, 56, 246), although its physiological role is presently unknown, leading to focus on its potential use as a NB CSC marker.

But most importantly, by overlapping our NB spheres micro-array analysis data with other published list of neural crest stem cells and progenitors markers, we were able to identify a new combination of neurosphere associated genes in aggressive NB cells. Among those candidates, we selected a combination of several transmembrane proteins that could be easily studied and characterized by experimental procedures such as fluorescent flow cytometry.

Three ATP-binding cassette (**ABC**) transporter genes were found over-expressed in NB sphere cells: ABCB1 (MDR1) in NB1- and NB2-T spheres, ABCB4 and ABCA1 in NB1-T spheres were identified with a 6-fold, 9-fold and 17–fold increased expression respectively. In normal physiology, MDR1 is considered as a specific marker for early neural stem/progenitor cells and hematopoietic stem cells (247-249) and was found over-expressed in the “universal stem-cell ” (219). In disease, ABC transporters play major roles in the development of drug resistance in cancers (250, 251).

The CSC hypothesis states that CSC possess some of the biological properties of normal stem cells including resistance to toxic agents, owing, in part, to elevated expression of ABC transporters. Drug resistance has thus been reported to be associated with stem-like features of the cancer cells (252, 253). In melanoma, MDR1 and ABCB5 transporters have been described as markers identifying melanoma initiating cells (61, 254), and ABCB5 was shown to mediate doxorubicin transport and chemoresistance in this human malignant neural crest derived tumor (59).

In NB, MDR1 was associated with multidrug resistance in NB cell lines and patient tumors at relapse after chemotherapy (217, 255, 256), whereas the expression level of the multidrug resistance genes MDR1, MRP1, MRP5 and LRP in advanced NB samples was not predictive of response, relapse or survival (257). Taken together, these data encouraged us to focus on the MDR1 transmembrane transporter as a potential functional NB-TICs marker.

Moreover, the canonical pathway enrichment analysis, revealed two principal signaling pathways involving many NEP genes.

First, in addition to the **NOTCH2** and **NOTCH3** receptors, the ligands JAG1 and DLL1, the down-stream transcription factors HEY1 and HES1 found over-expressed in the NB1-T spheres, other Notch pathway regulators were also detected in the sphere gene expression profiling experiments such as MAML2 in NB2-T and DTX3L in both NB2-T and NB4-T experiments.

In normal tissues, Notch regulates the cell-lineage decisions during embryogenesis (258), promotes the proliferation of non-neoplastic neural stem cells and inhibits their differentiation (259-261). NOTCH cascade is initiated when transmembrane ligands, on one cell, bind NOTCH receptors on an adjacent cell and cause γ-secretase-mediated proteolytic release of the NOTCH intracellular domain (NICD). NICD then translocates into the nucleus and activates targets such as the HES and HEY genes (262). In a wide range of neoplasms including lung, breast, myeloma and melanoma, the Notch pathway has been implicated in the regulation of the main cellular functions associated with tumorigenesis, such as proliferation, angiogenesis, and cell migration (263-269).

Recently, NOTCH signaling has also been related to the cancer stem cell phenotype. For instance, in breast tumors, it has been reported that breast cancer stem cell activity was governed specifically through NOTCH4 receptor signaling, offering new approaches to treat breast cancer recurrence (270, 271). Moreover, Notch pathway inhibition in embryonal brain tumors, such as medulloblastoma, and in glioblastoma tumors lead to the depletion of the CD133-positive stem-like cell subpopulation preventing tumor spheres and xenograft (272, 273).

In NB, activated Notch pathway was shown to prevent neuronal differentiation (274) and to induce dedifferentiation accompanied by more aggressive stem-cell phenotype characteristics under hypoxic conditions (275, 276). So, all these results seem consistent with our gene expression profiles of NB spheres that can be functionally considered as a stem-like subpopulation over-expressing development-involved pathways such as Notch signaling. In particular, specific Notch blocking in the NB stem-like cells could constitute a promising complementary therapy in NB (277).

Wnt pathway key actors were significantly represented among the NEP. Interestingly, Wnt signaling cascades are involved in a variety of cellular processes during embryogenesis and their sustained activation is a major factor of oncogenesis in many cancers (278-280). This aberrant activation is often due to mutations in regulators such *APC* or *AXIN* genes and effectors like β-catenin gene (281), or to an overexpression of the FZD family members which are specific Wnt ligand receptors (282-284). In NB, β-catenin has been shown to be strongly expressed and aberrantly localized in the nucleus in highly aggressive NB cells without MYCN amplification, whereas no β-catenin-specific mutations were identified (285). In the NB NEP, we observed, in addition to FZDs receptors and WNT

chaperon protein, an over-expression of the WNT5A gene (chr3p14) and of the WNT5B paralog gene (chr12p13). The WNT5A non-canonical signaling map and its legend are shown in the Appendix 2. The transcriptional mechanisms of WNT5A have recently been shown to be based on NF-κB, Hedgehog, TGFβ and Notch signaling cascades (286) and expressed in a variety of human tumors (287). In normal cells, WNT5A is an important regulator of morphogenetic movements during embryonic development of neural crest stem cells (288), whereas in malignant cells it is involved in invasion, peritoneal dissemination, and distant metastasis via RhoB and Snail (289, 290). In particular WNT5A initiates EMT in melanoma cells and promote metastases in this tumor (291, 292). Only one study addressed the function of WNT5A in NB tumors; WNT5A was found to be under-expressed in a model of xenograft primary tumor and metastasis derived from the human IGR-N91 NB cell line (293). Their results are consistent with the potential tumor suppressor function of WNT5A reported previously (294), although its pro-invasive activity has also been shown in many tumors. Thus, it is still unclear whether or not WNT5A signaling is involved in NB tumor progression. The microenvironment of the tumor cells could be one modulator of the different observed effects.

Finally, the analysis of signaling pathways over-represented in sphere cells revealed a strong enrichment of **EMT**-associated genes. EMT takes place during embryogenesis, wound healing, carcinogenesis and metastatic process. It groups together complex signaling pathways which drive a series of events during which epithelial cells lose many of their epithelial characteristics and take on properties that are typical of the mesenchymal cells (295, 296). EMT is one of the processes usurped by oncogenically transformed cells during tumorigenesis (78).

Interestingly, several recent studies showed that EMT can trigger reversion to a cancer stem cell-like phenotype (297, 298), providing an association between EMT and CSC. EMT mechanism is particularly interesting in the context of CSC given that it covers at the same time intracellular control of stem-like properties and extracellular influences on stem-like phenotype in response to micro-environmental changes. Indeed, several well known EMT actors such as WNT ligands (299-301), Frizzled receptors, TGF-β receptor (302-304), endothelin receptors (305), vimentin (306), SLUG and SNAIL (307-309), NOTCH3 (310, 311) and HEY1 (312) have been found to be overexpressed in the NB sphere cells. Internal cascades involving these genes constitute direct response of extrinsic cues such as HGF signaling via c-MET binding, TGF-β1, 2 and 3-mediated pathways or NOTCH activation by secreted JAGGED1 (78).

Thus, the NEP characterization highlighted genes associated with cell self-renewal in NB tumors involving a cross-talk between NOTCH, WNT, TGF-β signaling cascades which are physiologically involved in the stem cell signaling network and playing a key role in the EMT regulation (313, 314). In the context of CSCs to be potentially conditioned by their micro-environment, the NB neurosphere

expression profile (NEP) will be very useful to identify both intrinsic and extrinsic key actors playing a key role in the self-renewing and tumorigenic phenotype of NB-CSCs. For instance, HGF secreted by myofibroblasts in colon cancers have been shown to activate WNT signaling via its c-MET receptor binding and to lead to a subsequent increased clonogenicity of colon cancer stem cells (315).
Moreover, as it seems important to consider each cancer type separately to define specific targeted treatment, our findings provided an objective characterization of NB-specific expression profile of CSCs cells that could further provide new potential targets for complementary therapies.

NEP Validation in NB patients and cell lines

NEP was identified in quaternary NB spheres in one aggressive cell sample from a stage 4 patient. We therefore needed to validate the over-expression of several NEP gene candidates in spheres derived from the other available NB samples (Figure 5). Among the seven analyzed NEP markers, four of them, CD133, MDR1, GPR177 and ROBO1 were consistently over-expressed, already in secondary NB spheres derived from stage 4 tumors and NB cell lines. In contrast, EDNRB, NOTCH3 and ABCA1 were either stably expressed or even decreased. However, in these cases, the passage 2 rather than passage 4 spheres could represent too early passages to detect some gene expression increase.
Moreover, due to their limited tumorigenic capacity, primary NB cells display a limited ability to grow as spheres, resulting in a low cell yield after sphere dissociation, leading to a small amount of extracted RNA. Indeed, except for NB1 and NB1-NBM, LAN1 and SK-N-BE(2)C cell lines, the yield of sphere cells after several passages was limiting. This observation confirmed the heterogeneity in the proportion of self-renewing cells between the different NB cell samples. Nevertheless, it is difficult to establish a correlation between the sphere-forming capacity of the NB cells and the CD133/MDR1 expression, as shown by the fluorescent flow cytometry analyses. Although NB1 and NB1-NBM, LAN1 and SK-N-BE(2)C cell lines showed the highest self-renewal capacity, there is no relationship with an increased CD133 and MDR1 combined expression. In the other way, NB2 and NB4 didn’t show an extended sphere-forming ability but they both expressed a relatively important amount of MDR1 transporter.
Therefore, although an increase in the sample panel size would release stronger results, our validation showed an enrichment of NEP candidates in spheres derived from several NB cell samples.

Enhanced tumorigenicity of the NB sphere cell populations

In many studies, CSCs are referred to the tumor-initiating cell (TIC) population as these cells are experimentally identified by their ability to seed tumors in animal hosts and to recapitulate the cellular hierarchy of differentiated progeny observed in the parental tumor.

In order to isolate the NB-TIC population, we addressed the *in vivo* tumorigenicity of NB sphere cell populations in a heteropic model of subcutaneous injections in nude mice in the presence of Matrigel^{TM} (BD), a reconstituted basement membrane matrix (Figure 6). Matrigel, used to enable cell grouping and attachment for *in vivo* engraftment, contains extra-cellular matrix components and non-specific growth factors (see Material and Methods).

Subcutaneous tumors were observed when 10^5 to as few as 10 dissociated NB1-T cells were injected. A significant increased tumor development was observed when 10^5 NB1-NBM and NB1-T3 cells were implanted, but when fewer cells were implanted, no significant difference in the tumorigenicity between these different cell populations was observed. Interestingly, NB1-FCS did not show any *in vivo* tumor-forming capacity, confirming the *in vitro* modifications that occurred in the presence of serum in this cell line. In all the cases, the derived subcutaneous tumors showed a similar histology and were identical to the parental tumor.

On the other hand, for subcutaneous and orthotopic injections of NB1-T and NB1-T2/3 cells, we injected tertiary sphere cells. The difference in tumorigenicity for the four cell populations could have been attenuated by a non-optimal selection of the self-renewing cells that might occur after passage 3. We assumed that the enrichment in NB-TICs would be important enough to see an effect *in vivo*.

So, the data obtained with 10^5 injected cells supported the hypothesis of NB-TICs enrichment in the NB1-NBM cell line and in the sphere cells derived from the dissociated NB1-T tumor. Most of the NEP genes identified in the NB1 spheres were shown to be already highly expressed in the serum-free established NB1-NBM cells which showed the most rapid tumor growth in subcutaneous implantation model, comforting the idea that this cell-line had conserved and enriched the stem-like phenotype in *in vitro* culture compared with its homologue NB1-FCS cell line which was grown in 10% serum and did not give any heterotopic tumor *in vivo* (even when up to 10^5 cells were injected).

In the CSC concept, the CSC population resembles the normal stem or progenitor cells of the corresponding tissue of origin and would therefore also be influenced by its immediate microenvironment, the “niche”. To address the question of a physiologic micro-environment effect on the tumorigenic phenotype, we orthotopically injected the NB1-derived cells and their corresponding secondary spheres directly in the adrenal gland of nude mice without any exogenous growth factor supply like Matrigel. We observed a significant increase in the tumor take of the

sphere cell group where 79% of the mice developed an adrenal tumor compared to 40% for the animals injected with the parental cells.

When the same amount of cells from both populations were injected in identical conditions, but in a heterotopic site, no tumor growth was observed up to three months post-injection.

These results allowed us to strongly associate the NEP with the two CSC functions: self-renewal and tumorigenicity. Moreover, we confirmed that the tumor-initiating capacity and growth of the putative NB-CSCs cells is directly influenced by their "niche" (i.e. their micro-environment).

However, it is still unclear to which extent the existence of a NB-CSCs niche is dependent on the presence of the NB-CSCs themselves. Indeed, the biochemical identity of the NB-CSCs may shift as the niche changes, and vice-versa making even more difficult the NB-CSCs identification. So, the correlation between the gene expression profile of *in vitro* selected self-renewing cells and the *in vivo* function of tumorigenicity seemed a relevant approach to search for a cell function associated to aggressiveness and not for an unstable cell entity.

NB sphere heterogeneity and plasticity

Intriguingly, when the NEP expressing cells were identified directly within the NB xenograft tumor, we were not able to identify a single cell population co-expressing all the NEP markers and exclusively recapitulating the functional CSCs features. Indeed, $CD133^{high}$ cells were positive for EDNRB, GPR177 and IGFBP5 but not MDR1 and ABCA1 expression. Conversely, sorted $MDR1^{high}$ cells coexpressed ABCA1 but not CD133 and GPR177, thus confirming an anti-correlation between CD133 and MDR1. Consequently, the different NEP markers were expressed within the tumor but were expressed on different cell sub-populations. This heterogeneity was likewise observed in the spheres derived from the same tumor. Indeed the sorting of $CD133^{high}$ cells included EDNRB/GPR177 positive cells with an $MDR1^{low}$ phenotype. The double CD133/ MDR1 sorting confirmed the existence in the xenograft tumor of different population of cells with either CD133/EDNRB/NOTCH3 expression or MDR1 exclusive expression. In summary, we identified in the NB1 tumor, at least two cell populations, $CD133^{high}MDR1^{low}$ and $CD133^{low}MDR1^{high}$, which were selected in the derived spheres.

It has already been shown that a panel of cell phenotypes can be identified in different culture conditions. For instance, a heterogeneous activation, i.e. nuclear translocation, of the β-catenin has been observed in the colon cancer sphere cell population (315). Concerning the normal breast stem cells, most of the cells of clonal mammosphere have been shown to express cytokeratin of either basal or luminal epithelium (297). A minority of bipotential precursor cells co-expressing both basal and luminal markers has also been found in these mammospheres.

In the context of neuroectodermic tumors, the $CD34^{+}p75^{-}$, $CD44^{-}p75^{+}$ and $CD34^{-}p75^{-}$ melanoma cell populations were shown to have distinct self-renewal and *in vivo* tumorigenicity capacities (316). In particular, $CD34^{-}p75^{-}$ subset was enriched for individual cell that could self-renew *in vitro* by forming spheres and reestablish cellular heterogeneity both *in vitro* and *in vivo*, whereas $CD34^{+}p75^{-}$, on the other hand, underwent self-renewal almost exclusively, *in vitro* and *in vivo*. A recent study proposed another model of melanoma-propagating cells where a temporarily distinct subpopulation of slow-cycling melanoma cells expressing the H3K4 demethylase JARID1B is essential for continuous tumor growth (317). They namely showed that JARID1B was dynamically regulated and that JARID1B negative cells could become positive and sustain tumor growth.

Finally, distinct pools of glioblastoma stem cells have been described on the basis of their CD133 expression (318). PTEN-deficient glioblastoma cells showed a high sphere-forming capacity and derived spheres constituted a mixed population of $CD133^{+}$ and $CD133^{-}$ cells that were equally clonogenic. It has been proposed that the different CD133 expression patterns in glioblastoma sub-population with diverse tumorigenic potential recapitulated hierarchical lineages of self-renewing cells. Thus, it is likely that NB-CSC population does not correspond to a single phenotypic subset but rather to a variety of NB cell sub-populations expressing different markers and able to self-renew.

These results strengthen our findings that either in a normal or a malignant context, a clonal sphere could support the expression of different early precursor cell markers and that the self-renewing properties are not characteristic of a unique sub-population. It also suggested that NB-CSC cells could constitute a dynamic heterogeneous population within a single tumor sample.

CD133 is not a NB-TIC marker, MDR maybe?

In order to address the tumorigenic capacity of the two cell populations $CD133^{high}$ and $MDR1^{high}$ found in NB1-T derived spheres, we measured their *in vivo* tumorigenicity by orthotopically implantation of both sorted populations in nude mice.

$C133^{high}$ and $CD133^{low}$ cells were isolated from NB1-T and did not reveal significantly different tumorigenicity (33% vs. 17% tumor takes respectively). Surprisingly, one animal in the $CD133^{high}$ group developed an ovarian metastasis, an atypical metastatic site in human NB. Furthermore, the single $CD133^{low}$ derived tumor grew much faster than tumors in the other group. Moreover the CD133 expression level measured in the orthotopic tumors was higher in the $CD133^{low}$ derived tumors compared to the $CD133^{high}$ derived tumor (20.5% vs. 5-7.5% of the tumor cells respectively) confirming the plastic behavior of CD133 expressing cells. We thus concluded that although CD133 was included in the NEP, it was not alone a reliable marker to select the tumorigenic NB cell subset.

This conclusion is comforted by recent progresses suggesting that CD133 was not restricted to somatic stem cells and cancer stem cells (319). Indeed CD133 expression did not always reliably

distinguish melanoma-initiating cells (316) or brain tumor stem cells (75, 320, 321) as opposed to older reported findings (48-50).

The observation in one animal of *in vivo* metastasis formation after injection of NB $CD133^{high}$ cells could eventually suggest that CD133 expression might be associated with an invasive cell phenotype rather than a strict tumorigenic capacity. In recent studies, $CD133^{+}$ glioblastoma stem-like cell lines selected *in vitro* have been shown to generate highly invasive orthotopic tumors *in vivo* whereas the selected $CD133^{-}$ cells, enriched for extracellular matrix-related genes, were far less tumorigenic and showed a more restricted differentiation capacity (322). In melanoma cells, CD133 expression has been associated with their metastatic potential and, in particular, the abrogation of CD133 expression at the cell surface of metastatic melanoma cell line resulted in the severe reduction of *in vivo* metastases (323-325). Finally, chemoresistant $CD133^{+}CXCR4^{+}$ melanoma cells were also shown to be stimulated and metastasize in presence of SDF1 secreted by lymphatic endothelial cells (326).

These published results together indicate that, in glioblastoma and in melanoma, CD133 might select for a small cell subset, or be itself, involved in rapid growth or/and cell dissemination to specific sites but not in specific tumor-initiating capacity. These findings could lead to new investigation trails for CD133 function in NB.

We therefore addressed the *in vivo* tumorigenicity of the alternative NB sphere cell subset expressing MDR1 but negative for CD133. 10^4 $MDR1^{high}$, $MDR1^{low}$ and $MDR1^{non\ sorted}$ NB1-T cells were orthotopically grafted and showed a difference in tumor take. 67% vs. 25% tumor takes were observed in the $MDR1^{high}$ and $MDR1^{low}$ groups respectively, while 20% of the mice injected with the $MDR1^{non\ sorted}$ developed an adrenal tumor detected by ultrasound imaging. As described above, CSCs may consist in a dynamic cell population expressing markers induced by the *in vitro* culture and/or the micro-environment. To determine whether we selected all the cells that could potentially express MDR1 transporter and be tumorigenic, it would be relevant to sort MDR1-positive and -negative cells from late passages NB spheres, such as the stable NB1-T4 cell population that already underwent self-renewal selection or “conditioning”.

Our results suggested that the direct selection, in NB primary tumors, of NB cell subset on the basis of a single marker may not be sufficient to isolate the NB cell population responsible for tumor initiation and growth even if MDR1 expressing NB cells were shown to be enriched for the putative NB-CSC population. **The functional study of NB sphere cells, selected from aggressive NB tumors by their ability to self-renew and the expression of a combination of NEP markers seems the most pertinent procedure to address the NB-CSCs biological characterization.**

Major impediments in NB CSC study

At this point, it is important to underline the pitfalls of the tumorigenic assay by *in vivo* implantation of sorted cells suspension. Indeed, for solid cancers, we faced the difficulty of getting a viable single-cell suspension as we observed the rapid death of the cells following the enzymatic and mechanical treatments. The duration of the sorting procedure, the pressure conditions and the effect of the antibody itself on the cell viability constitute parameters susceptible to alter the efficiency of the sorting and the purity of the sorted populations unevenly which was additionally compromised by the very low frequency of the $CD133^{high/\ low}$ cell populations. In consequence, to avoid such bias as much as possible, we increased the number of animals and injected sites to work with reliable statistics.

On the other hand, we discussed the essential role of the microenvironment in the observation of the TICs phenotype. In this purpose, it is essential to determine the more accurate host model for xenotransplantations. Indeed, a recent report addressed the host effect on the tumorigenicity of grafted tumor cells and concluded that as many as 25% of the cancer cells within certain tumors have properties of CSCs (327). They raised the question of the CSCs model applicability, although their choice of mouse model, the more highly immunocompromised NOD/SCID interleukin-2 receptor gamma chain null ($Il2rg^{-/-}$) mice, could have drastically influenced the CSC phenotype of the melanoma cells. Indeed, host biological characteristics such as vascularization at the site of implantation, extracellular matrix constitution, growth availability and host immunocompetence can affect cancer cell engraftment rate. Moreover, such model does not allow addressing the capacity of putative CSCs to escape from the immune response as it has been reported for glioma stem cells (328, 329). So, the lack of immune selective pressure in the $Il2rg^{-/-}$, as opposed to the less immunocompromised athymic nude mice, did not reproduce the cancer cell micro-environment observed in a human primary tumor and playing a key role in tumor progression. The most relevant model would be a syngenic model of mouse NB cells orthotopically engrafted in animals of the same strain. The use of Swiss nu/nu mice hosting model seemed to us the best compromise to allow the tumor growth of human NB cells *in vivo* and to conserve a minimal immune response in the tumor micro-environment. The residual immune system of nude mice did not interfere with the tumorigenicity efficiency as we were able to measure tumor propagation in this host after subcutaneous implantation of as few as 10 NB1-T cells.

In addition, when orthotopically injected in the adrenal gland of nude mice, NB1-T sphere cells over-expressing CD133 and MDR1 markers showed a significant increased tumor take compared to the NB1-T cells, whereas the CD133 and MDR1-positive NB1-T cells did not significantly reproduce the selection of the tumorigenic cell subset. This observation led us to question the effect of the cells

"conditioning" that occurs in the sphere culture conditions. We refer as a "conditioning" the serum-free medium exposure or the non-adherent sphere culture conditions as well as the tumor micro-environment in *in vivo* implantations. It remains unclear whether the sphere cells corresponded to selected cell populations among the bulk tumor cells or potential cells which were able to "turn on" intrinsic signaling pathway in adaptation to the external signals. For instance, it has been shown that sphere culture conditions activated the EMT leading to the TICs phenotype (297). So, the stem cell phenotype (function and not entity) may evolve with the changing cues in the *in vivo* microenvironment constituted by immune, mesenchymal and endothelial cells or the *in vitro* culture. We could tentatively define an aggressive tumor as a tumor that contains a high proportion of cells able to respond positively to extrinsic and intrinsic cues leading toward a stemness conversion.

However, whether acquired or induced in NB spheres, the sphere associated molecular signaling described in this study should be explored as potential targets for complementary therapies to prevent NB progression and relapse.

OUTLOOK

The stage 4 NB1 model presented in this study showed high sphere-forming and tumorigenic properties, and were used to define a neurosphere expression profile (NEP) associated to CSCs feature in this tumor. This has been compared with the gene expression analysis of two other NMYC non amplified NB tumors which provided secondary sphere cells. However, the self-renewal capacity of these two samples was more limited than NB1 model and did not allow us to define a reliable list of commonly expressed NB sphere associated genes. So, it would be relevant to increase the number of stage 4 NB derived spheres analyzed by time-course microarray profiling and especially samples that can produce long-term passaging spheres.

The NEP identified many candidates such as ABC transporters, endothelin ligands and receptors, and WNT actors that were found over-expressed in the NB spheres. The functional analysis of sphere cells would need further investigations to determine whether or not these signaling cascades are activated in NB spheres compared to the tumor bulk cells. For those which are activated, a targeted drug screening using specific inhibitors of the NB-CSCs associated markers, especially if they are more critical for self-renewal in NB-CSCs than in physiologic stem cells to spare the pool of normal stem cells, would be carried out to provide new potential therapeutic treatments against NB.

We have shown that ABC transporters, especially MDR1, could play an essential role in NB tumor initiation. They are known to be responsible for multidrug resistance in this malignant childhood tumor. The multimodal identification of the NB-CSCs via their drug resistance, self-renewal and tumorigenic capacities, in association with their gene expression profiles would be addressed in a panel of NB tumors and cell lines to narrow the net around the cellular culprit of NB progression and relapse. In order to avoid the risk to bias the enrichment of CSCs population by selecting cell with the tumor bulk on the basis of marker expression, we would propose to work with the “conditioned” NB sphere populations which have been propagated in serum-free medium from fresh NB tumor sample.

ACKOWLEDGMENTS

During my long time as a PhD student in Lausanne, in the laboratory of Dr. Nicole Gross, I was able to meet and work with people who had great humane and scientific qualities. I instinctively and naturally inclined towards this group for their generosity of spirit shown to me almost five years ago.

First, I would like to warmly thank my thesis director, Dr. Nicole Gross, with whom, beyond the scientific exchanges and intellectual support she brought to my work, I could develop a sincere friendly relationship and appreciate her example as of a strong and smart woman in research. She was also readily available and I found her guidance and support to me indispensable.

I sincerely acknowledge Prof. Ivan Stamenkovic, co-director of the project, for having opened the door of his lab to use a panel of highly modern technologies; Prof. Duchosal for his interested and pertinent remarks about my work, and the two experts of my thesis committee: Dr Olivier Delattre for his useful input and feedback in this project and Prof-Lukas Sommer. I would like to give a special thanks to Prof. Lukas Sommer who was a reference point, a scientific awakening and an intellectual stimulant at every discussion we had. He is a great scientist as well as a man with a developed personal sensitivity defining himself as a precious interlocutor.

I would also like to say thank you to my colleagues in the Oncology Hematology lab for their capacity to listen and the maternal care they gave during the difficult periods of my thesis.

Specifically, my gratitude goes to Dr. Marjorie Flahaut-Chételat, who is a great researcher, for her kindness, her patience, and her appreciable pedagogy, which is a rare element in scientific community. I also thank Dr. Annick Mühlethaler-Mottet who encouraged me and helped me a lot at the beginning of this project; Katia Bourloud-Balmas and Katya Nardou for their availability, their essential help in the realization of heavy experiments, for their precious practical advice and their support out of which developed a true friendship. I was also lucky to share some moments with Dr Emma Garcia about whom I appreciate the generosity and the light that she transmits to everyone. She helped me to make the bridge between the discreet world of research and the more applied practice of clinicians.

I'd like to thank Gilda Raguenez and Lucienne Lagopoulos who shared the neuronal boiling space of office 971 and provided numerous refreshing conversations.

I want to more particularly acknowledge the presence of Dr. Roland Meier and Julie Liberman who constituted until their own thesis defense, my true doctoral allies. Thanks to Roland for the support he gave me at the beginning: he assisted me, listened to me and gave me more self-confidence. Thanks to Julie who brought with her to the lab, smiles, good cheer and a joviality which mutually fed us, during this quite long period of our respective lives.

ACKNOWLEDGMENTS

Among all the people I've crossed during my researches and who helped me with their precious expert eye, I would like to mention and thank Dr. Jean-Marc Joseph for the *in vivo* procedures, Dr. Sarah Pernet-Fattet for her advice, Dr. Sylvain Pradervand and D. Thierry Sengstag for the gene expression statistics, Véronique Noguet for all the histology work, Miguel Garcia for the flow-cytometry experiments, Dr Maja Beck-Popovic and Dr Nicolas Van der Weid for their support in translational communication between clinics and research, Jean-Christophe Stehle at the mouse Pathology, and all people I have met in the Sommer's lab (Olga, Gianluca, Sebastien, Nessy, and Gregor).

Finally, I would like to thank the precious "Lausanners" with whom I became close and my former clan comprising family and friends who supported me at any moment during the up and downs and made it possible.

REFERENCES

(1) Hanahan D, Weinberg RA. The hallmarks of cancer. Cell 2000;100:57-70.

(2) Bhowmick NA, Neilson EG, Moses HL. Stromal fibroblasts in cancer initiation and progression. Nature 2004;432:332-7.

(3) Bissell MJ, Radisky D. Putting tumours in context. Nat Rev Cancer 2001;1:46-54.

(4) Mueller MM, Fusenig NE. Friends or foes - bipolar effects of the tumour stroma in cancer. Nat Rev Cancer 2004;4:839-49.

(5) Bussolino F, Mantovani A, Persico G. Molecular mechanisms of blood vessel formation. Trends Biochem Sci 1997;22:251-6.

(6) Folkman J. Angiogenesis in cancer, vascular, rheumatoid and other disease. Nat Med 1995;1:27-31.

(7) Carmeliet P. Angiogenesis in cancer and other diseases. Nature Insight 2000;407:249-57.

(8) de Visser KE, Eichten A, Coussens LM. Paradoxical roles of the immune system during cancer development. Nat Rev Cancer 2006;6:24-37.

(9) Pekarek LA, Starr BA, Toledano AY, Schreiber H. Inhibition of tumor growth by elimination of granulocytes. J Exp Med 1995;181:435-40.

(10) Pollard JW. Tumour-educated macrophages promote tumour progression and metastasis. Nat Rev Cancer 2004;4:71-8.

(11) Kalluri R, Zeisberg M. Fibroblasts in cancer. Nat Rev Cancer 2006;6:392-401.

(12) Walker RA. The complexities of breast cancer desmoplasia. Breast Cancer Res 2001;3:143-5.

(13) Karnoub AE, Dash AB, Vo AP, Sullivan A, Brooks MW, Bell GW, et al. Mesenchymal stem cells within tumour stroma promote breast cancer metastasis. Nature 2007;449:557-63.

(14) Provenzano PP, Eliceiri KW, Campbell JM, Inman DR, White JG, Keely PJ. Collagen reorganization at the tumor-stromal interface facilitates local invasion. BMC Med 2006;4:38.

(15) Somasundaram R, Herlyn D. Chemokines and the microenvironment in neuroectodermal tumor-host interaction. Semin Cancer Biol 2008.

(16) Seruga B, Zhang H, Bernstein LJ, Tannock IF. Cytokines and their relationship to the symptoms and outcome of cancer. Nat Rev Cancer 2008;8:887-99.

(17) Radisky D, Muschler J, Bissell MJ. Order and disorder: the role of extracellular matrix in epithelial cancer. Cancer Invest 2002;20:139-53.

(18) Barcellos-Hoff MH, Ravani SA. Irradiated mammary gland stroma promotes the expression of tumorigenic potential by unirradiated epithelial cells. Cancer Res 2000;60:1254-60.

(19) Tlsty TD. Stromal cells can contribute oncogenic signals. Semin Cancer Biol 2001;11:97-104.

(20) Dexter DL, Kowalski HM, Blazar BA, Fligiel Z, Vogel R, Heppner GH. Heterogeneity of tumor cells from a single mouse mammary tumor. Cancer Res 1978;38:3174-81.

(21) Fidler IJ, Kripke ML. Metastasis results from preexisting variant cells within a malignant tumor. Science 1977;197:893-5.

(22) Heppner GH, Miller BE, Miller FR. Tumor subpopulation interactions in neoplasms. Biochim Biophys Acta 1983;695:215-26.

(23) Park SY, Gonen M, Kim HJ, Michor F, Polyak K. Cellular and genetic diversity in the progression of in situ human breast carcinomas to an invasive phenotype. J Clin Invest 2010;120:636-44.

(24) Merlo LM, Pepper JW, Reid BJ, Maley CC. Cancer as an evolutionary and ecological process. Nat Rev Cancer 2006;6:924-35.

(25) Merlo LM, Maley CC. The role of genetic diversity in cancer. J Clin Invest 2010;120:401-3.

(26) Wolman SR. Cytogenetic heterogeneity: its role in tumor evolution. Cancer Genet Cytogenet 1986;19:129-40.

(27) Masters JR. Human cancer cell lines: fact and fantasy. Nat Rev Mol Cell Biol 2000;1:233-6.

(28) Virchow R. Editorial. Virchow Arch Pathol Anat Physhiol Klin Med 1855;3.

(29) Cohnheim J. Ueber entzundung und eiterung. Path Anat Physiol Klin Med 1867;40:1-79.

(30) Cohnheim V. Congenitales, quergestreiftes muskelsarkom der nieren. Virchows Arch Pathol Anat Physiol Klin Med 1875;65:64-9.

(31) SOUTHAM CM, Brunschwig A, Levin AG, Dizon QS. Effect of leukocytes on transplantability of human cancer. Cancer 1966;19:1743-53.

(32) BRUCE WR, VAN DER GAAG. A quantitative assay for the number of murine lymphoma cells capable of proliferation in vivo. Nature 1963;199:79-80.

(33) Fialkow PJ, Gartler SM, Yoshida A. Clonal origin of chronic myelocytic leukemia in man. Proc Natl Acad Sci U S A 1967;58:1468-71.

(34) Fialkow PJ, Singer JW, Adamson JW, Vaidya K, Dow LW, Ochs J, et al. Acute nonlymphocytic leukemia: heterogeneity of stem cell origin. Blood 1981;57:1068-73.

(35) Bonner WA, Hulett HR, Sweet RG, Herzenberg LA. Fluorescence activated cell sorting. Rev Sci Instrum 1972;43:404-9.

(36) Lapidot T, Sirard C, Vormoor J, Murdoch B, Hoang T, Caceres-Cortes J, et al. A cell initiating human acute myeloid leukaemia after transplantation into SCID mice. Nature 1994;367:645-8.

(37) Morrison SJ, Shah NM, Anderson DJ. Regulatory mechanisms in stem cell biology. Cell 1997;88:287-98.

(38) Polyak K, Hahn WC. Roots and stems: stem cells in cancer. Nat Med 2006;12:296-300.

(39) Reya T, Morrison SJ, Clarke MF, Weissman IL. Stem cells, cancer, and cancer stem cells. Nature 2001;414:105-11.

(40) Weissman IL. Translating stem and progenitor cell biology to the clinic: barriers and opportunities. Science 2000;287:1442-6.

(41) Clarke MF, Dick JE, Dirks PB, Eaves CJ, Jamieson CH, Jones DL, et al. Cancer Stem Cells--Perspectives on Current Status and Future Directions: AACR Workshop on Cancer Stem Cells. Cancer Res 2006;66:9339-44.

(42) Bjerkvig R, Tysnes BB, Aboody KS, Najbauer J, Terzis AJ. Opinion: the origin of the cancer stem cell: current controversies and new insights. Nat Rev Cancer 2005;5:899-904.

(43) Clarke MF. Epigenetic regulation of normal and cancer stem cells. Ann N Y Acad Sci 2005;1044:90-3.

(44) Clarke MF, Fuller M. Stem cells and cancer: two faces of eve. Cell 2006;124:1111-5.

(45) Huntly BJ, Gilliland DG. Leukaemia stem cells and the evolution of cancer-stem-cell research. Nat Rev Cancer 2005;5:311-21.

(46) Al-Hajj M, Wicha MS, ito-Hernandez A, Morrison SJ, Clarke MF. Prospective identification of tumorigenic breast cancer cells. Proc Natl Acad Sci U S A 2003;100:3983-8.

(47) Ginestier C, Hur MH, Charafe-Jauffret E, Monville F, Dutcher J, Brown M, et al. ALDH1 is a marker of normal and malignant human mammary stem cells and a predictor of poor clinical outcome. Cell Stem Cell 2007;1:555-67.

(48) Singh SK, Clarke ID, Terasaki M, Bonn VE, Hawkins C, Squire J, et al. Identification of a cancer stem cell in human brain tumors. Cancer Res 2003;63:5821-8.

(49) Singh SK, Hawkins C, Clarke ID, Squire JA, Bayani J, Hide T, et al. Identification of human brain tumour initiating cells. Nature 2004;432:396-401.

(50) Galli R, Binda E, Orfanelli U, Cipelletti B, Gritti A, De VS, et al. Isolation and characterization of tumorigenic, stem-like neural precursors from human glioblastoma. Cancer Res 2004;64:7011-21.

(51) Hemmati HD, Nakano I, Lazareff JA, Masterman-Smith M, Geschwind DH, Bronner-Fraser M, et al. Cancerous stem cells can arise from pediatric brain tumors. Proc Natl Acad Sci U S A 2003;100:15178-83.

(52) Fan X, Eberhart CG. Medulloblastoma stem cells. J Clin Oncol 2008;26:2821-7.

(53) Vescovi AL, Galli R, Reynolds BA. Brain tumour stem cells. Nat Rev Cancer 2006;6:425-36.

(54) Read TA, Fogarty MP, Markant SL, McLendon RE, Wei Z, Ellison DW, et al. Identification of CD15 as a marker for tumor-propagating cells in a mouse model of medulloblastoma. Cancer Cell 2009;15:135-47.

(55) O'Brien CA, Pollett A, Gallinger S, Dick JE. A human colon cancer cell capable of initiating tumour growth in immunodeficient mice. Nature 2007;445:106-10.

(56) Ricci-Vitiani L, Lombardi DG, Pilozzi E, Biffoni M, Todaro M, Peschle C, et al. Identification and expansion of human colon-cancer-initiating cells. Nature 2007;445:111-5.

(57) Shmelkov SV, Butler JM, Hooper AT, Hormigo A, Kushner J, Milde T, et al. CD133 expression is not restricted to stem cells, and both CD133+ and C. J Clin Invest 2008;118:2111-20.

(58) Boiko AD, Razorenova OV, van de Rijn M, Swetter SM, Johnson DL, Ly DP, et al. Human melanoma-initiating cells express neural crest nerve growth factor receptor CD271. Nature 2010;466:133-7.

(59) Frank NY, Margaryan A, Huang Y, Schatton T, Waaga-Gasser AM, Gasser M, et al. ABCB5-mediated doxorubicin transport and chemoresistance in human malignant melanoma. Cancer Res 2005;65:4320-33.

(60) Monzani E, Facchetti F, Galmozzi E, Corsini E, Benetti A, Cavazzin C, et al. Melanoma contains CD133 and ABCG2 positive cells with enhanced tumourigenic potential. Eur J Cancer 2007;43:935-46.

(61) Schatton T, Murphy GF, Frank NY, Yamaura K, Waaga-Gasser AM, Gasser M, et al. Identification of cells initiating human melanomas. Nature 2008;451:345-9.

(62) Baker M. Melanoma in mice casts doubt on scarcity of cancer stem cells. Nature 2008;456:553.

(63) Dirks P. Cancer stem cells: Invitation to a second round. Nature 2010;466:40-1.

(64) Eaves CJ. Cancer stem cells: Here, there, everywhere? Nature 2008;456:581-2.

(65) Heuser M, Humphries RK. Biologic and experimental variation of measured cancer stem cells. Cell Cycle 2010;9:909-12.

(66) Labarge MA, Bissell MJ. Is CD133 a marker of metastatic colon cancer stem cells? J Clin Invest 2008;118:2021-4.

(67) Prestegarden L, Enger PO. Cancer stem cells in the central nervous system--a critical review. Cancer Res 2010;70:8255-8.

(68) Rosen JM, Jordan CT. The increasing complexity of the cancer stem cell paradigm. Science 2009;324:1670-3.

(69) Shipitsin M, Polyak K. The cancer stem cell hypothesis: in search of definitions, markers, and relevance. Lab Invest 2008;88:459-63.

(70) Visvader JE, Lindeman GJ. Cancer stem cells in solid tumours: accumulating evidence and unresolved questions. Nat Rev Cancer 2008;8:755-68.

(71) Gupta PB, Chaffer CL, Weinberg RA. Cancer stem cells: mirage or reality? Nat Med 2009;15:1010-2.

(72) Morrison SJ, Weissman IL. The long-term repopulating subset of hematopoietic stem cells is deterministic and isolatable by phenotype. Immunity 1994;1:661-73.

(73) Reynolds BA, Weiss S. Generation of neurons and astrocytes from isolated cells of the adult mammalian central nervous system. Science 1992;255:1707-10.

(74) Dontu G, Abdallah WM, Foley JM, Jackson KW, Clarke MF, Kawamura MJ, et al. In vitro propagation and transcriptional profiling of human mammary stem/progenitor cells. Genes Dev 2003;17:1253-70.

(75) Beier D, Hau P, Proescholdt M, Lohmeier A, Wischhusen J, Oefner PJ, et al. CD133(+) and CD133(-) glioblastoma-derived cancer stem cells show differential growth characteristics and molecular profiles. Cancer Res 2007;67:4010-5.

(76) Park PC, Selvarajah S, Bayani J, Zielenska M, Squire JA. Stem cell enrichment approaches. Semin Cancer Biol 2007;17:257-64.

(77) Thiery JP. Epithelial-mesenchymal transitions in tumour progression. Nat Rev Cancer 2002;2:442-54.

(78) Thiery JP, Acloque H, Huang RY, Nieto MA. Epithelial-mesenchymal transitions in development and disease. Cell 2009;139:871-90.

(79) Brabletz T, Jung A, Spaderna S, Hlubek F, Kirchner T. Opinion: migrating cancer stem cells - an integrated concept of malignant tumour progression. Nat Rev Cancer 2005;5:744-9.

(80) Hermann PC, Huber SL, Herrler T, Aicher A, Ellwart JW, Guba M, et al. Distinct populations of cancer stem cells determine tumor growth and metastatic activity in human pancreatic cancer. Cell Stem Cell 2007;1:313-23.

(81) Yang ZF, Ho DW, Ng MN, Lau CK, Yu WC, Ngai P, et al. Significance of CD90+ cancer stem cells in human liver cancer. Cancer Cell 2008;13:153-66.

(82) Kucia M, Reca R, Miekus K, Wanzeck J, Wojakowski W, Janowska-Wieczorek A, et al. Trafficking of normal stem cells and metastasis of cancer stem cells involve similar mechanisms: pivotal role of the SDF-1-CXCR4 axis. Stem Cells 2005;23:879-94.

(83) Glavinas H, Krajcsi P, Cserepes J, Sarkadi B. The role of ABC transporters in drug resistance, metabolism and toxicity. Curr Drug Deliv 2004;1:27-42.

(84) Kim M, Turnquist H, Jackson J, Sgagias M, Yan Y, Gong M, et al. The multidrug resistance transporter ABCG2 (breast cancer resistance protein 1) effluxes Hoechst 33342 and is overexpressed in hematopoietic stem cells. Clin Cancer Res 2002;8:22-8.

(85) Scharenberg CW, Harkey MA, Torok-Storb B. The ABCG2 transporter is an efficient Hoechst 33342 efflux pump and is preferentially expressed by immature human hematopoietic progenitors. Blood 2002;99:507-12.

(86) Costello RT, Mallet F, Gaugler B, Sainty D, Arnoulet C, Gastaut JA, et al. Human acute myeloid leukemia CD34+/. Cancer Res 2000;60:4403-11.

(87) de Grouw EP, Raaijmakers MH, Boezeman JB, van der Reijden BA, van de Locht LT, de Witte TJ, et al. Preferential expression of a high number of ATP binding cassette transporters in both normal and leukemic CD34+. Leukemia 2006;20:750-4.

(88) Ishikawa F, Yoshida S, Saito Y, Hijikata A, Kitamura H, Tanaka S, et al. Chemotherapy-resistant human AML stem cells home to and engraft within the bone-marrow endosteal region. Nat Biotechnol 2007;25:1315-21.

(89) Wulf GG, Wang RY, Kuehnle I, Weidner D, Marini F, Brenner MK, et al. A leukemic stem cell with intrinsic drug efflux capacity in acute myeloid leukemia. Blood 2001;98:1166-73.

(90) Eramo A, Ricci-Vitiani L, Zeuner A, Pallini R, Lotti F, Sette G, et al. Chemotherapy resistance of glioblastoma stem cells. Cell Death Differ 2006;13:1238-41.

(91) Li X, Lewis MT, Huang J, Gutierrez C, Osborne CK, Wu MF, et al. Intrinsic resistance of tumorigenic breast cancer cells to chemotherapy. J Natl Cancer Inst 2008;100:672-9.

(92) Dylla SJ, Beviglia L, Park IK, Chartier C, Raval J, Ngan L, et al. Colorectal cancer stem cells are enriched in xenogeneic tumors following chemotherapy. PLoS ONE 2008;3:e2428.

(93) Bao S, Wu Q, McLendon RE, Hao Y, Shi Q, Hjelmeland AB, et al. Glioma stem cells promote radioresistance by preferential activation of the DNA damage response. Nature 2006;444:756-60.

(94) Diehn M, Cho RW, Lobo NA, Kalisky T, Dorie MJ, Kulp AN, et al. Association of reactive oxygen species levels and radioresistance in cancer stem cells. Nature 2009;458:780-3.

(95) Phillips TM, McBride WH, Pajonk F. The response of CD24(-/low)/CD44+ breast cancer-initiating cells to radiation. J Natl Cancer Inst 2006;98:1777-85.

(96) Calabrese C, Poppleton H, Kocak M, Hogg TL, Fuller C, Hamner B, et al. A perivascular niche for brain tumor stem cells. Cancer Cell 2007;11:69-82.

(97) Bao S, Wu Q, Sathornsumetee S, Hao Y, Li Z, Hjelmeland AB, et al. Stem cell-like glioma cells promote tumor angiogenesis through vascular endothelial growth factor. Cancer Res 2006;66:7843-8.

(98) Maniotis AJ, Folberg R, Hess A, Seftor EA, Gardner LM, Pe'er J, et al. Vascular channel formation by human melanoma cells in vivo and in vitro: vasculogenic mimicry. Am J Pathol 1999;155:739-52.

(99) Rothhammer T, Bataille F, Spruss T, Eissner G, Bosserhoff AK. Functional implication of BMP4 expression on angiogenesis in malignant melanoma. Oncogene 2007;26:4158-70.

(100) Piccirillo SG, Reynolds BA, Zanetti N, Lamorte G, Binda E, Broggi G, et al. Bone morphogenetic proteins inhibit the tumorigenic potential of human brain tumour-initiating cells. Nature 2006;444:761-5.

(101) Bartholomew A, Sturgeon C, Siatskas M, Ferrer K, McIntosh K, Patil S, et al. Mesenchymal stem cells suppress lymphocyte proliferation in vitro and prolong skin graft survival in vivo. Exp Hematol 2002;30:42-8.

(102) le BK, Tammik L, Sundberg B, Haynesworth SE, Ringden O. Mesenchymal stem cells inhibit and stimulate mixed lymphocyte cultures and mitogenic responses independently of the major histocompatibility complex. Scand J Immunol 2003;57:11-20.

(103) le BK, Ringden O. Immunomodulation by mesenchymal stem cells and clinical experience. J Intern Med 2007;262:509-25.

(104) Tse WT, Pendleton JD, Beyer WM, Egalka MC, Guinan EC. Suppression of allogeneic T-cell proliferation by human marrow stromal cells: implications in transplantation. Transplantation 2003;75:389-97.

(105) Kawasaki BT, Mistree T, Hurt EM, Kalathur M, Farrar WL. Co-expression of the toleragenic glycoprotein, CD200, with markers for cancer stem cells. Biochem Biophys Res Commun 2007;364:778-82.

(106) Wei J, Barr J, Kong LY, Wang Y, Wu A, Sharma AK, et al. Glioma-associated cancer-initiating cells induce immunosuppression. Clin Cancer Res 2010;16:461-73.

(107) Wei J, Barr J, Kong LY, Wang Y, Wu A, Sharma AK, et al. Glioblastoma cancer-initiating cells inhibit T-cell proliferation and effector responses by the signal transducers and activators of transcription 3 pathway. Mol Cancer Ther 2010;9:67-78.

(108) Schatton T, Schutte U, Frank NY, Zhan Q, Hoerning A, Robles SC, et al. Modulation of T-cell activation by malignant melanoma initiating cells. Cancer Res 2010;70:697-708.

(109) Fuchs E, Tumbar T, Guasch G. Socializing with the neighbors: stem cells and their niche. Cell 2004;116:769-78.

(110) Moore KA, Lemischka IR. Stem cells and their niches. Science 2006;311:1880-5.

(111) Louissaint A, Jr., Rao S, Leventhal C, Goldman SA. Coordinated interaction of neurogenesis and angiogenesis in the adult songbird brain. Neuron 2002;34:945-60.

(112) Palmer TD, Willhoite AR, Gage FH. Vascular niche for adult hippocampal neurogenesis. J Comp Neurol 2000;425:479-94.

(113) Ramirez-Castillejo C, Sanchez-Sanchez F, Andreu-Agullo C, Ferron SR, Aroca-Aguilar JD, Sanchez P, et al. Pigment epithelium-derived factor is a niche signal for neural stem cell renewal. Nat Neurosci 2006;9:331-9.

(114) Shen Q, Goderie SK, Jin L, Karanth N, Sun Y, Abramova N, et al. Endothelial cells stimulate self-renewal and expand neurogenesis of neural stem cells. Science 2004;304:1338-40.

(115) Wodarz A, Gonzalez C. Connecting cancer to the asymmetric division of stem cells. Cell 2006;124:1121-3.

(116) Wurdak H, Zhu S, Romero A, Lorger M, Watson J, Chiang CY, et al. An RNAi screen identifies TRRAP as a regulator of brain tumor-initiating cell differentiation. Cell Stem Cell 2010;6:37-47.

(117) Gupta PB, Onder TT, Jiang G, Tao K, Kuperwasser C, Weinberg RA, et al. Identification of selective inhibitors of cancer stem cells by high-throughput screening. Cell 2009;138:645-59.

(118) Parkin DM, Kramarova E, Draper D, Masuyer E, Michaelis J, Neglia J, et al. International Incidence of Childhood Cancer. IARC scientific publications 1998;2.

(119) Maris JM, Hogarty MD, Bagatell R, Cohn SL. Neuroblastoma. Lancet 2007;369:2106-20.

(120) Scotting PJ, Walker DA, Perilongo G. Childhood solid tumours: a developmental disorder. Nat Rev Cancer 2005;5:481-8.

(121) Ciccarone V, Spengler BA, Meyers MB, Biedler JL, Ross RA. Phenotypic diversification in human neuroblastoma cells: expression of distinct neural crest lineages. Cancer Res 1989;49:219-25.

(122) Dyer MA. Mouse models of childhood cancer of the nervous system. J Clin Pathol 2004;57:561-76.

(123) Mora J, Gerald WL. Origin of neuroblastic tumors: clues for future therapeutics. Expert Rev Mol Diagn 2004;4:293-302.

(124) Nakagawara A, Ohira M. Comprehensive genomics linking between neural development and cancer: neuroblastoma as a model. Cancer Lett 2004;204:213-24.

(125) Brodeur G, Maris J. Neuroblastoma. Principles and practice of Pediatric Oncology 2006;933-70.

(126) Brodeur GM. Neuroblastoma: biological insights into a clinical enigma. Nat Rev Cancer 2003;3:203-16.

(127) Matthay KK. Neuroblastoma: biology and therapy. Oncology (Williston Park) 1997;11:1857-66.

(128) Hero B, Simon T, Horz S, Berthold F. Metastatic neuroblastoma in infancy: what does the pattern of metastases contribute to prognosis? Med Pediatr Oncol 2000;35:683-7.

(129) Shimada H, Ambros IM, Dehner LP, Hata J, Joshi VV, Roald B. Terminology and morphologic criteria of neuroblastic tumors: recommendations by the International Neuroblastoma Pathology Committee. Cancer 1999;86:349-63.

(130) Lastowska M, Cullinane C, Variend S, Cotterill S, Bown N, O'Neill S, et al. Comprehensive genetic and histopathologic study reveals three types of neuroblastoma tumors. J Clin Oncol 2001;19:3080-90.

(131) Mosse YP, Greshock J, Margolin A, Naylor T, Cole K, Khazi D, et al. High-resolution detection and mapping of genomic DNA alterations in neuroblastoma. Genes Chromosomes Cancer 2005;43:390-403.

(132) Schleiermacher G, Raynal V, Janoueix-Lerosey I, Combaret V, Aurias A, Delattre O. Variety and complexity of chromosome 17 translocations in neuroblastoma. Genes Chromosomes Cancer 2004;39:143-50.

(133) Vandesompele J, Van RN, Van GM, Laureys G, Ambros P, Heimann P, et al. Genetic heterogeneity of neuroblastoma studied by comparative genomic hybridization. Genes Chromosomes Cancer 1998;23:141-52.

(134) Attiyeh EF, London WB, Mosse YP, Wang Q, Winter C, Khazi D, et al. Chromosome 1p and 11q deletions and outcome in neuroblastoma. N Engl J Med 2005;353:2243-53.

(135) Fong CT, White PS, Peterson K, Sapienza C, Cavenee WK, Kern SE, et al. Loss of heterozygosity for chromosomes 1 or 14 defines subsets of advanced neuroblastomas. Cancer Res 1992;52:1780-5.

(136) White PS, Thompson PM, Gotoh T, Okawa ER, Igarashi J, Kok M, et al. Definition and characterization of a region of 1p36.3 consistently deleted in neuroblastoma. Oncogene 2005;24:2684-94.

(137) Ejeskar K, Aburatani H, Abrahamsson J, Kogner P, Martinsson T. Loss of heterozygosity of 3p markers in neuroblastoma tumours implicate a tumour-suppressor locus distal to the FHIT gene. Br J Cancer 1998;77:1787-91.

(138) Guo C, White PS, Weiss MJ, Hogarty MD, Thompson PM, Stram DO, et al. Allelic deletion at 11q23 is common in MYCN single copy neuroblastomas. Oncogene 1999;18:4948-57.

(139) Srivatsan ES, Ying KL, Seeger RC. Deletion of chromosome 11 and of 14q sequences in neuroblastoma. Genes Chromosomes Cancer 1993;7:32-7.

(140) Diskin SJ, Hou C, Glessner JT, Attiyeh EF, Laudenslager M, Bosse K, et al. Copy number variation at 1q21.1 associated with neuroblastoma. Nature 2009;459:987-91.

(141) Islam A, Kageyama H, Takada N, Kawamoto T, Takayasu H, Isogai E, et al. High expression of Survivin, mapped to 17q25, is significantly associated with poor prognostic factors and promotes cell survival in human neuroblastoma. Oncogene 2000;19:617-23.

(142) Janoueix-Lerosey I, Novikov E, Monteiro M, Gruel N, Schleiermacher G, Loriod B, et al. Gene expression profiling of 1p35-36 genes in neuroblastoma. Oncogene 2004;23:5912-22.

(143) Lastowska M, Viprey V, Santibanez-Koref M, Wappler I, Peters H, Cullinane C, et al. Identification of candidate genes involved in neuroblastoma progression by combining genomic and expression microarrays with survival data. Oncogene 2007.

(144) Kaneko Y, Kanda N, Maseki N, Sakurai M, Tsuchida Y, Takeda T, et al. Different karyotypic patterns in early and advanced stage neuroblastomas. Cancer Res 1987;47:311-8.

(145) Kaneko Y, Knudson AG. Mechanism and relevance of ploidy in neuroblastoma. Genes Chromosomes Cancer 2000;29:89-95.

(146) Look AT, Hayes FA, Shuster JJ, Douglass EC, Castleberry RP, Bowman LC, et al. Clinical relevance of tumor cell ploidy and N-myc gene amplification in childhood neuroblastoma: a Pediatric Oncology Group study. J Clin Oncol 1991;9:581-91.

(147) Brodeur GM, Minturn JE, Ho R, Simpson AM, Iyer R, Varela CR, et al. Trk receptor expression and inhibition in neuroblastomas. Clin Cancer Res 2009;15:3244-50.

(148) Nakagawara A, Arima-Nakagawara M, Scavarda NJ, Azar CG, Cantor AB, Brodeur GM. Association between high levels of expression of the TRK gene and favorable outcome in human neuroblastoma. N Engl J Med 1993;328:847-54.

(149) Ho R, Eggert A, Hishiki T, Minturn JE, Ikegaki N, Foster P, et al. Resistance to chemotherapy mediated by TrkB in neuroblastomas. Cancer Res 2002;62:6462-6.

(150) Nakagawara A, Azar CG, Scavarda NJ, Brodeur GM. Expression and function of TRK-B and BDNF in human neuroblastomas. Mol Cell Biol 1994;14:759-67.

(151) Nakagawara A, Arima-Nakagawara M, Azar CG, Scavarda NJ, Brodeur GM. Clinical significance of expression of neurotrophic factors and their receptors in neuroblastoma. Prog Clin Biol Res 1994;385:155-61.

(152) Nakagawara A. The NGF story and neuroblastoma. Med Pediatr Oncol 1998;31:113-5.

(153) Chan HS, Haddad G, Thorner PS, DeBoer G, Lin YP, Ondrusek N, et al. P-glycoprotein expression as a predictor of the outcome of therapy for neuroblastoma. N Engl J Med 1991;325:1608-14.

(154) Combaret V, Gross N, Lasset C, Frappaz D, Peruisseau G, Philip T, et al. Clinical relevance of CD44 cell-surface expression and N-myc gene amplification in a multicentric analysis of 121 pediatric neuroblastomas. J Clin Oncol 1996;14:25-34.

(155) Goldstein LJ, Fojo AT, Ueda K, Crist W, Green A, Brodeur G, et al. Expression of the multidrug resistance, MDR1, gene in neuroblastomas. J Clin Oncol 1990;8:128-36.

(156) Gross N, Balmas K, Brognara CB. Absence of functional CD44 hyaluronan receptor on human NMYC-amplified neuroblastoma cells. Cancer Res 1997;57:1387-93.

(157) Haber M, Smith J, Bordow SB, Flemming C, Cohn SL, London WB, et al. Association of high-level MRP1 expression with poor clinical outcome in a large prospective study of primary neuroblastoma. J Clin Oncol 2006;24:1546-53.

(158) Caren H, Abel F, Kogner P, Martinsson T. High incidence of DNA mutations and gene amplifications of the ALK gene in advanced sporadic neuroblastoma tumours. Biochem J 2008;416:153-9.

(159) Chen Y, Takita J, Choi YL, Kato M, Ohira M, Sanada M, et al. Oncogenic mutations of ALK kinase in neuroblastoma. Nature 2008;455:971-4.

(160) George RE, Sanda T, Hanna M, Frohling S, Luther W, Zhang J, et al. Activating mutations in ALK provide a therapeutic target in neuroblastoma. Nature 2008;455:975-8.

(161) Janoueix-Lerosey I, Lequin D, Brugieres L, Ribeiro A, de PL, Combaret V, et al. Somatic and germline activating mutations of the ALK kinase receptor in neuroblastoma. Nature 2008;455:967-70.

(162) Mosse YP, Laudenslager M, Longo L, Cole KA, Wood A, Attiyeh EF, et al. Identification of ALK as a major familial neuroblastoma predisposition gene. Nature 2008;455:930-5.

(163) Scott F. Developmental Biology. Gilbert 6th edition Sinauer 2010.

(164) Sauka-Spengler T, Bronner-Fraser M. A gene regulatory network orchestrates neural crest formation. Nat Rev Mol Cell Biol 2008;9:557-68.

(165) Schneider C, Wicht H, Enderich J, Wegner M, Rohrer H. Bone morphogenetic proteins are required in vivo for the generation of sympathetic neurons. Neuron 1999;24:861-70.

(166) Shah NM, Groves AK, Anderson DJ. Alternative neural crest cell fates are instructively promoted by TGFbeta superfamily members. Cell 1996;85:331-43.

(167) Shah NM, Anderson DJ. Integration of multiple instructive cues by neural crest stem cells reveals cell-intrinsic biases in relative growth factor responsiveness. Proc Natl Acad Sci U S A 1997;94:11369-74.

(168) Morrison SJ, Perez SE, Qiao Z, Verdi JM, Hicks C, Weinmaster G, et al. Transient Notch activation initiates an irreversible switch from neurogenesis to gliogenesis by neural crest stem cells. Cell 2000;101:499-510.

(169) Shah NM, Marchionni MA, Isaacs I, Stroobant P, Anderson DJ. Glial growth factor restricts mammalian neural crest stem cells to a glial fate. Cell 1994;77:349-60.

(170) Wakamatsu Y, Maynard TM, Weston JA. Fate determination of neural crest cells by NOTCH-mediated lateral inhibition and asymmetrical cell division during gangliogenesis. Development 2000;127:2811-21.

(171) Lahav R, Ziller C, Dupin E, Le Douarin NM. Endothelin 3 promotes neural crest cell proliferation and mediates a vast increase in melanocyte number in culture. Proc Natl Acad Sci U S A 1996;93:3892-7.

(172) Lahav R, Dupin E, Lecoin L, Glavieux C, Champeval D, Ziller C, et al. Endothelin 3 selectively promotes survival and proliferation of neural crest-derived glial and melanocytic precursors in vitro. Proc Natl Acad Sci U S A 1998;95:14214-9.

(173) Stone JG, Spirling LI, Richardson MK. The neural crest population responding to endothelin-3 in vitro includes multipotent cells. J Cell Sci 1997;110 (Pt 14):1673-82.

(174) Kasemeier-Kulesa JC, Kulesa PM, Lefcort F. Imaging neural crest cell dynamics during formation of dorsal root ganglia and sympathetic ganglia. Development 2005;132:235-45.

(175) Kulesa PM, Fraser SE. In ovo time-lapse analysis of chick hindbrain neural crest cell migration shows cell interactions during migration to the branchial arches. Development 2000;127:1161-72.

(176) Teddy JM, Kulesa PM. In vivo evidence for short- and long-range cell communication in cranial neural crest cells. Development 2004;131:6141-51.

(177) Santiago A, Erickson CA. Ephrin-B ligands play a dual role in the control of neural crest cell migration. Development 2002;129:3621-32.

(178) Smith A, Robinson V, Patel K, Wilkinson DG. The EphA4 and EphB1 receptor tyrosine kinases and ephrin-B2 ligand regulate targeted migration of branchial neural crest cells. Curr Biol 1997;7:561-70.

(179) Wang HU, Anderson DJ. Eph family transmembrane ligands can mediate repulsive guidance of trunk neural crest migration and motor axon outgrowth. Neuron 1997;18:383-96.

(180) Gammill LS, Gonzalez C, Bronner-Fraser M. Neuropilin 2/semaphorin 3F signaling is essential for cranial neural crest migration and trigeminal ganglion condensation. Dev Neurobiol 2007;67:47-56.

(181) Osborne NJ, Begbie J, Chilton JK, Schmidt H, Eickholt BJ. Semaphorin/neuropilin signaling influences the positioning of migratory neural crest cells within the hindbrain region of the chick. Dev Dyn 2005;232:939-49.

(182) Jia L, Cheng L, Raper J. Slit/Robo signaling is necessary to confine early neural crest cells to the ventral migratory pathway in the trunk. Dev Biol 2005;282:411-21.

(183) Young HM, Hearn CJ, Farlie PG, Canty AJ, Thomas PQ, Newgreen DF. GDNF is a chemoattractant for enteric neural cells. Dev Biol 2001;229:503-16.

(184) Baroffio A, Dupin E, Le Douarin NM. Common precursors for neural and mesectodermal derivatives in the cephalic neural crest. Development 1991;112:301-5.

(185) Morrison SJ, White PM, Zock C, Anderson DJ. Prospective identification, isolation by flow cytometry, and in vivo self-renewal of multipotent mammalian neural crest stem cells. Cell 1999;96:737-49.

(186) Stemple DL, Anderson DJ. Isolation of a stem cell for neurons and glia from the mammalian neural crest. Cell 1992;71:973-85.

(187) Trentin A, Glavieux-Pardanaud C, Le Douarin NM, Dupin E. Self-renewal capacity is a widespread property of various types of neural crest precursor cells. Proc Natl Acad Sci U S A 2004;101:4495-500.

(188) Biedler JL, Helson L, Spengler BA. Morphology and growth, tumorigenicity, and cytogenetics of human neuroblastoma cells in continuous culture. Cancer Res 1973;33:2643-52.

(189) Seeger RC, Rayner SA, Banerjee A, Chung H, Laug WE, Neustein HB, et al. Morphology, growth, chromosomal pattern and fibrinolytic activity of two new human neuroblastoma cell lines. Cancer Res 1977;37:1364-71.

(190) Tumilowicz JJ, Nichols WW, Cholon JJ, Greene AE. Definition of a continuous human cell line derived from neuroblastoma. Cancer Res 1970;30:2110-8.

(191) Ross RA, Spengler BA, Domenech C, Porubcin M, Rettig WJ, Biedler JL. Human neuroblastoma I-type cells are malignant neural crest stem cells. Cell Growth Differ 1995;6:449-56.

(192) Ross RA, Biedler JL, Spengler BA. A role for distinct cell types in determining malignancy in human neuroblastoma cell lines and tumors. Cancer Lett 2003;197:35-9.

(193) Walton JD, Kattan DR, Thomas SK, Spengler BA, Guo HF, Biedler JL, et al. Characteristics of stem cells from human neuroblastoma cell lines and in tumors. Neoplasia 2004;6:838-45.

(194) Ross RA, Spengler BA. Human neuroblastoma stem cells. Semin Cancer Biol 2006.

(195) Cui H, Ma J, Ding J, Li T, Alam G, Ding HF. Bmi-1 regulates the differentiation and clonogenic self-renewal of I-type neuroblastoma cells in a concentration-dependent manner. J Biol Chem 2006;281:34696-704.

(196) Hirschmann-Jax C, Foster AE, Wulf GG, Nuchtern JG, Jax TW, Gobel U, et al. A distinct "side population" of cells with high drug efflux capacity in human tumor cells. Proc Natl Acad Sci U S A 2004;101:14228-33.

(197) Hansford LM, McKee AE, Zhang L, George RE, Gerstle JT, Thorner PS, et al. Neuroblastoma cells isolated from bone marrow metastases contain a naturally enriched tumor-initiating cell. Cancer Res 2007;67:11234-43.

(198) Smith KM, Datti A, Fujitani M, Grinshtein N, Zhang L, Morozova O, et al. Selective targeting of neuroblastoma tumour-initiating cells by compounds identified in stem cell-based small molecule screens. EMBO Mol Med 2010;2:371-84.

(199) Biernaskie J, Paris M, Morozova O, Fagan BM, Marra M, Pevny L, et al. SKPs derive from hair follicle precursors and exhibit properties of adult dermal stem cells. Cell Stem Cell 2009;5:610-23.

(200) Fernandes KJ, McKenzie IA, Mill P, Smith KM, Akhavan M, Barnabe-Heider F, et al. A dermal niche for multipotent adult skin-derived precursor cells. Nat Cell Biol 2004;6:1082-93.

(201) Toma JG, Akhavan M, Fernandes KJ, Barnabe-Heider F, Sadikot A, Kaplan DR, et al. Isolation of multipotent adult stem cells from the dermis of mammalian skin. Nat Cell Biol 2001;3:778-84.

(202) Yilmaz OH, Valdez R, Theisen BK, Guo W, Ferguson DO, Wu H, et al. Pten dependence distinguishes haematopoietic stem cells from leukaemia-initiating cells. Nature 2006;441:475-82.

(203) Morozova O, Vojvodic M, Grinshtein N, Hansford LM, Blakely KM, Maslova A, et al. System-level analysis of neuroblastoma tumor-initiating cells implicates AURKB as a novel drug target for neuroblastoma. Clin Cancer Res 2010;16:4572-82.

(204) Fix A, Peter M, Pierron G, Aurias A, Delattre O, Janoueix-Lerosey I. High-resolution mapping of amplicons of the short arm of chromosome 1 in two neuroblastoma tumors by microarray-based comparative genomic hybridization. Genes Chromosomes Cancer 2004;40:266-70.

(205) Ross AH, Grob P, Bothwell M, Elder DE, Ernst CS, Marano N, et al. Characterization of nerve growth factor receptor in neural crest tumors using monoclonal antibodies. Proc Natl Acad Sci U S A 1984;81:6681-5.

(206) Fuchs S, Herzog D, Sumara G, Buchmann-Moller S, Civenni G, Wu X, et al. Stage-specific control of neural crest stem cell proliferation by the small rho GTPases Cdc42 and Rac1. Cell Stem Cell 2009;4:236-47.

(207) Eberl LP, Valdenaire O, Saintgiorgio V, Jeannin JF, Juillerat-Jeanneret L. Endothelin receptor blockade potentiates FasL-induced apoptosis in rat colon carcinoma cells. Int J Cancer 2000;86:182-7.

(208) Psarros M, Heber S, Sick M, Thoppae G, Harshman K, Sick B. RACE: Remote Analysis Computation for gene Expression data. Nucleic Acids Res 2005;33:W638-W643.

(209) Joseph JM, Gross N, Lassau N, Rouffiac V, Opolon P, Laudani L, et al. In vivo echographic evidence of tumoral vascularization and microenvironment interactions in metastatic orthotopic human neuroblastoma xenografts. Int J Cancer 2005;113:881-90.

(210) Lee J, Kotliarova S, Kotliarov Y, Li A, Su Q, Donin NM, et al. Tumor stem cells derived from glioblastomas cultured in bFGF and EGF more closely mirror the phenotype and genotype of primary tumors than do serum-cultured cell lines. Cancer Cell 2006;9:391-403.

(211) Janoueix-Lerosey I, Schleiermacher G, Michels E, Mosseri V, Ribeiro A, Lequin D, et al. Overall genomic pattern is a predictor of outcome in neuroblastoma. J Clin Oncol 2009;27:1026-33.

(212) McConville CM, Forsyth J. Neuroblastoma - a developmental perspective. Cancer Lett 2003;197:3-9.

(213) Sidell N. Retinoic acid-induced growth inhibition and morphologic differentiation of human neuroblastoma cells in vitro. J Natl Cancer Inst 1982;68:589-96.

(214) Gaetano C, Matsumoto K, Thiele CJ. In vitro activation of distinct molecular and cellular phenotypes after induction of differentiation in a human neuroblastoma cell line. Cancer Res 1992;52:4402-7.

(215) Tsokos M, Scarpa S, Ross RA, Triche TJ. Differentiation of human neuroblastoma recapitulates neural crest development. Study of morphology, neurotransmitter enzymes, and extracellular matrix proteins. Am J Pathol 1987;128:484-96.

(216) Zorina Y, Iyengar R, Bromberg KD. Cannabinoid 1 receptor and interleukin-6 receptor together induce integration of protein kinase and transcription factor signaling to trigger neurite outgrowth. J Biol Chem 2010;285:1358-70.

(217) Flahaut M, Muhlethaler-Mottet A, Martinet D, Fattet S, Bourloud KB, Auderset K, et al. Molecular cytogenetic characterization of doxorubicin-resistant neuroblastoma cell lines: evidence that acquired multidrug resistance results from a unique large amplification of the 7q21 region. Genes Chromosomes Cancer 2006;45:495-508.

(218) Buchstaller J, Sommer L, Bodmer M, Hoffmann R, Suter U, Mantei N. Efficient isolation and gene expression profiling of small numbers of neural crest stem cells and developing Schwann cells. J Neurosci 2004;24:2357-65.

(219) Ramalho-Santos M, Yoon S, Matsuzaki Y, Mulligan RC, Melton DA. "Stemness": transcriptional profiling of embryonic and adult stem cells. Science 2002;298:597-600.

(220) Takahashi K, Tanabe K, Ohnuki M, Narita M, Ichisaka T, Tomoda K, et al. Induction of pluripotent stem cells from adult human fibroblasts by defined factors. Cell 2007;131:861-72.

(221) Mizrak D, Brittan M, Alison MR. CD133: molecule of the moment. J Pathol 2008;214:3-9.

(222) Dalerba P, Dylla SJ, Park IK, Liu R, Wang X, Cho RW, et al. Phenotypic characterization of human colorectal cancer stem cells. Proc Natl Acad Sci U S A 2007;104:10158-63.

(223) Banziger C, Soldini D, Schutt C, Zipperlen P, Hausmann G, Basler K. Wntless, a conserved membrane protein dedicated to the secretion of Wnt proteins from signaling cells. Cell 2006;125:509-22.

(224) Dang L, Yoon K, Wang M, Gaiano N. Notch3 signaling promotes radial glial/progenitor character in the mammalian telencephalon. Dev Neurosci 2006;28:58-69.

(225) Sansone P, Storci G, Giovannini C, Pandolfi S, Pianetti S, Taffurelli M, et al. p66Shc/Notch-3 interplay controls self-renewal and hypoxia survival in human stem/progenitor cells of the mammary gland expanded in vitro as mammospheres. Stem Cells 2007;25:807-15.

(226) Yamaguchi N, Oyama T, Ito E, Satoh H, Azuma S, Hayashi M, et al. NOTCH3 signaling pathway plays crucial roles in the proliferation of ErbB2-negative human breast cancer cells. Cancer Res 2008;68:1881-8.

(227) Shin MK, Levorse JM, Ingram RS, Tilghman SM. The temporal requirement for endothelin receptor-B signalling during neural crest development. Nature 1999;402:496-501.

(228) Stanchina L, Baral V, Robert F, Pingault V, Lemort N, Pachnis V, et al. Interactions between Sox10, Edn3 and Ednrb during enteric nervous system and melanocyte development. Dev Biol 2006;295:232-49.

(229) Yoshida H, Kunisada T, Kusakabe M, Nishikawa S, Nishikawa SI. Distinct stages of melanocyte differentiation revealed by anlaysis of nonuniform pigmentation patterns. Development 1996;122:1207-14.

(230) Adachi M, Hashido K, Trzeciak A, Watanabe T, Furuichi Y, Miyamoto C. Functional domains of human endothelin receptor. J Cardiovasc Pharmacol 1993;22 Suppl 8:S121-S124.

(231) Levin ER. Endothelins. N Engl J Med 1995;333:356-63.

(232) Bagnato A, Salani D, Di C, V, Wu-Wong JR, Tecce R, Nicotra MR, et al. Expression of endothelin 1 and endothelin A receptor in ovarian carcinoma: evidence for an autocrine role in tumor growth. Cancer Res 1999;59:720-7.

(233) Battistini B, Chailler P, D'Orleans-Juste P, Briere N, Sirois P. Growth regulatory properties of endothelins. Peptides 1993;14:385-99.

(234) Stiles JD, Ostrow PT, Balos LL, Greenberg SJ, Plunkett R, Grand W, et al. Correlation of endothelin-1 and transforming growth factor beta 1 with malignancy and vascularity in human gliomas. J Neuropathol Exp Neurol 1997;56:435-9.

(235) Bagnato A, Spinella F, Rosano L. The endothelin axis in cancer: the promise and the challenges of molecularly targeted therapy. Can J Physiol Pharmacol 2008;86:473-84.

(236) Lahav R, Heffner G, Patterson PH. An endothelin receptor B antagonist inhibits growth and induces cell death in human melanoma cells in vitro and in vivo. Proc Natl Acad Sci U S A 1999;96:11496-500.

(237) Rosano L, Di C, V, Spinella F, Tortora G, Nicotra MR, Natali PG, et al. Combined targeting of endothelin A receptor and epidermal growth factor receptor in ovarian cancer shows enhanced antitumor activity. Cancer Res 2007;67:6351-9.

(238) Dawe CJ. Phylogeny and oncogeny. Natl Cancer Inst Monogr 1969;31:1-40.

(239) de GJ, de NC, Cantu JM, Bilski-Pasquier G, Bousser J. Models for clonal evolutions: a study of chronic myelogenous leukemia. Am J Hum Genet 1966;18:485-503.

(240) FORD CE, CLARKE CM. CYTOGENETIC EVIDENCE OF CLONAL PROLIFERATION IN PRIMARY RETICULAR NEOPLASMS. Proc Can Cancer Conf 1963;5:129-46.

(241) Maley CC, Galipeau PC, Finley JC, Wongsurawat VJ, Li X, Sanchez CA, et al. Genetic clonal diversity predicts progression to esophageal adenocarcinoma. Nat Genet 2006;38:468-73.

(242) Siegmund KD, Marjoram P, Woo YJ, Tavare S, Shibata D. Inferring clonal expansion and cancer stem cell dynamics from DNA methylation patterns in colorectal cancers. Proc Natl Acad Sci U S A 2009;106:4828-33.

(243) Tsao JL, Tavare S, Salovaara R, Jass JR, Aaltonen LA, Shibata D. Colorectal adenoma and cancer divergence. Evidence of multilineage progression. Am J Pathol 1999;154:1815-24.

(244) Alison MR, Guppy NJ, Lim SM, Nicholson LJ. Finding cancer stem cells: are aldehyde dehydrogenases fit for purpose? J Pathol 2010;222:335-44.

(245) Todaro M, Iovino F, Eterno V, Cammareri P, Gambara G, Espina V, et al. Tumorigenic and metastatic activity of human thyroid cancer stem cells. Cancer Res 2010;70:8874-85.

(246) Collins AT, Berry PA, Hyde C, Stower MJ, Maitland NJ. Prospective identification of tumorigenic prostate cancer stem cells. Cancer Res 2005;65:10946-51.

(247) Chaudhary PM, Roninson IB. Expression and activity of P-glycoprotein, a multidrug efflux pump, in human hematopoietic stem cells. Cell 1991;66:85-94.

(248) Rentala S, Sagar Balla MM, Khurana S, Mukhopadhyay A. MDR1 gene expression enhances long-term engraftibility of cultured bone marrow cells. Biochem Biophys Res Commun 2005;335:957-64.

(249) Yamamoto A, Shofuda T, Islam MO, Nakamura Y, Yamasaki M, Okano H, et al. ABCB1 is predominantly expressed in human fetal neural stem/progenitor cells at an early development stage. J Neurosci Res 2009;87:2615-23.

(250) Gottesman MM, Fojo T, Bates SE. Multidrug resistance in cancer: role of ATP-dependent transporters. Nat Rev Cancer 2002;2:48-58.

(251) Huang Y, Anderle P, Bussey KJ, Barbacioru C, Shankavaram U, Dai Z, et al. Membrane transporters and channels: role of the transportome in cancer chemosensitivity and chemoresistance. Cancer Res 2004;64:4294-301.

(252) Sharma SV, Lee DY, Li B, Quinlan MP, Takahashi F, Maheswaran S, et al. A chromatin-mediated reversible drug-tolerant state in cancer cell subpopulations. Cell 2010;141:69-80.

(253) Voulgari A, Pintzas A. Epithelial-mesenchymal transition in cancer metastasis: mechanisms, markers and strategies to overcome drug resistance in the clinic. Biochim Biophys Acta 2009;1796:75-90.

(254) Keshet GI, Goldstein I, Itzhaki O, Cesarkas K, Shenhav L, Yakirevitch A, et al. MDR1 expression identifies human melanoma stem cells. Biochem Biophys Res Commun 2008;368:930-6.

(255) Oue T, Yoneda A, Uehara S, Yamanaka H, Fukuzawa M. Increased expression of multidrug resistance-associated genes after chemotherapy in pediatric solid malignancies. J Pediatr Surg 2009;44:377-80.

(256) Qiu YY, Mirkin BL, Dwivedi RS. MDR1 hypermethylation contributes to the progression of neuroblastoma. Mol Cell Biochem 2007;301:131-5.

(257) de CP, Jourdan-Da-Silva N, Couturier J, Tran-Perennou C, Schleiermacher G, Fehlbaum P, et al. Role of chemotherapy resistance genes in outcome of neuroblastoma. Pediatr Blood Cancer 2007;48:311-7.

(258) Louvi A, Artavanis-Tsakonas S. Notch signalling in vertebrate neural development. Nat Rev Neurosci 2006;7:93-102.

(259) Gaiano N, Fishell G. The role of notch in promoting glial and neural stem cell fates. Annu Rev Neurosci 2002;25:471-90.

(260) Sestan N, Artavanis-Tsakonas S, Rakic P. Contact-dependent inhibition of cortical neurite growth mediated by notch signaling. Science 1999;286:741-6.

(261) Solecki DJ, Liu XL, Tomoda T, Fang Y, Hatten ME. Activated Notch2 signaling inhibits differentiation of cerebellar granule neuron precursors by maintaining proliferation. Neuron 2001;31:557-68.

(262) Bray SJ. Notch signalling: a simple pathway becomes complex. Nat Rev Mol Cell Biol 2006;7:678-89.

(263) Allenspach EJ, Maillard I, Aster JC, Pear WS. Notch signaling in cancer. Cancer Biol Ther 2002;1:466-76.

(264) Houde C, Li Y, Song L, Barton K, Zhang Q, Godwin J, et al. Overexpression of the NOTCH ligand JAG2 in malignant plasma cells from multiple myeloma patients and cell lines. Blood 2004;104:3697-704.

(265) Leong KG, Karsan A. Recent insights into the role of Notch signaling in tumorigenesis. Blood 2006;107:2223-33.

(266) Pinnix CC, Lee JT, Liu ZJ, McDaid R, Balint K, Beverly LJ, et al. Active Notch1 confers a transformed phenotype to primary human melanocytes. Cancer Res 2009;69:5312-20.

(267) Rehman AO, Wang CY. Notch signaling in the regulation of tumor angiogenesis. Trends Cell Biol 2006;16:293-300.

(268) Sahlgren C, Gustafsson MV, Jin S, Poellinger L, Lendahl U. Notch signaling mediates hypoxia-induced tumor cell migration and invasion. Proc Natl Acad Sci U S A 2008;105:6392-7.

(269) Westhoff B, Colaluca IN, D'Ario G, Donzelli M, Tosoni D, Volorio S, et al. Alterations of the Notch pathway in lung cancer. Proc Natl Acad Sci U S A 2009;106:22293-8.

(270) Harrison H, Farnie G, Brennan KR, Clarke RB. Breast Cancer Stem Cells: Something Out of Notching? Cancer Res 2010.

(271) Harrison H, Farnie G, Howell SJ, Rock RE, Stylianou S, Brennan KR, et al. Regulation of breast cancer stem cell activity by signaling through the Notch4 receptor. Cancer Res 2010;70:709-18.

(272) Fan X, Matsui W, Khaki L, Stearns D, Chun J, Li YM, et al. Notch pathway inhibition depletes stem-like cells and blocks engraftment in embryonal brain tumors. Cancer Res 2006;66:7445-52.

(273) Fan X, Khaki L, Zhu TS, Soules ME, Talsma CE, Gul N, et al. NOTCH pathway blockade depletes CD133-positive glioblastoma cells and inhibits growth of tumor neurospheres and xenografts. Stem Cells 2010;28:5-16.

(274) Grynfeld A, Pahlman S, Axelson H. Induced neuroblastoma cell differentiation, associated with transient HES-1 activity and reduced HASH-1 expression, is inhibited by Notch1. Int J Cancer 2000;88:401-10.

(275) Kim Y, Lin Q, Zelterman D, Yun Z. Hypoxia-regulated delta-like 1 homologue enhances cancer cell stemness and tumorigenicity. Cancer Res 2009;69:9271-80.

(276) Pahlman S, Stockhausen MT, Fredlund E, Axelson H. Notch signaling in neuroblastoma. Semin Cancer Biol 2004;14:365-73.

(277) Pannuti A, Foreman K, Rizzo P, Osipo C, Golde T, Osborne B, et al. Targeting Notch to target cancer stem cells. Clin Cancer Res 2010;16:3141-52.

(278) Chien AJ, Moon RT. WNTS and WNT receptors as therapeutic tools and targets in human disease processes. Front Biosci 2007;12:448-57.

(279) Gregorieff A, Pinto D, Begthel H, Destree O, Kielman M, Clevers H. Expression pattern of Wnt signaling components in the adult intestine. Gastroenterology 2005;129:626-38.

(280) Mikels AJ, Nusse R. Wnts as ligands: processing, secretion and reception. Oncogene 2006;25:7461-8.

(281) Lustig B, Behrens J. The Wnt signaling pathway and its role in tumor development. J Cancer Res Clin Oncol 2003;129:199-221.

(282) Merle P, Kim M, Herrmann M, Gupte A, Lefrancois L, Califano S, et al. Oncogenic role of the frizzled-7/beta-catenin pathway in hepatocellular carcinoma. J Hepatol 2005;43:854-62.

(283) Milovanovic T, Planutis K, Nguyen A, Marsh JL, Lin F, Hope C, et al. Expression of Wnt genes and frizzled 1 and 2 receptors in normal breast epithelium and infiltrating breast carcinoma. Int J Oncol 2004;25:1337-42.

(284) Ueno K, Hiura M, Suehiro Y, Hazama S, Hirata H, Oka M, et al. Frizzled-7 as a potential therapeutic target in colorectal cancer. Neoplasia 2008;10:697-705.

(285) Liu X, Mazanek P, Dam V, Wang Q, Zhao H, Guo R, et al. Deregulated Wnt/beta-catenin program in high-risk neuroblastomas without MYCN amplification. Oncogene 2008;27:1478-88.

(286) Katoh M, Katoh M. Transcriptional mechanisms of WNT5A based on NF-kappaB, Hedgehog, TGFbeta, and Notch signaling cascades. Int J Mol Med 2009;23:763-9.

(287) Iozzo RV, Eichstetter I, Danielson KG. Aberrant expression of the growth factor Wnt-5A in human malignancy. Cancer Res 1995;55:3495-9.

(288) Garcia-Castro MI, Marcelle C, Bronner-Fraser M. Ectodermal Wnt function as a neural crest inducer. Science 2002;297:848-51.

(289) Witze ES, Litman ES, Argast GM, Moon RT, Ahn NG. Wnt5a control of cell polarity and directional movement by polarized redistribution of adhesion receptors. Science 2008;320:365-9.

(290) Katoh M, Katoh M. STAT3-induced WNT5A signaling loop in embryonic stem cells, adult normal tissues, chronic persistent inflammation, rheumatoid arthritis and cancer (Review). Int J Mol Med 2007;19:273-8.

(291) Dissanayake SK, Wade M, Johnson CE, O'Connell MP, Leotlela PD, French AD, et al. The Wnt5A/protein kinase C pathway mediates motility in melanoma cells via the inhibition of metastasis suppressors and initiation of an epithelial to mesenchymal transition. J Biol Chem 2007;282:17259-71.

(292) Weeraratna AT, Jiang Y, Hostetter G, Rosenblatt K, Duray P, Bittner M, et al. Wnt5a signaling directly affects cell motility and invasion of metastatic melanoma. Cancer Cell 2002;1:279-88.

(293) Blanc E, Roux GL, Benard J, Raguenez G. Low expression of Wnt-5a gene is associated with high-risk neuroblastoma. Oncogene 2005;24:1277-83.

(294) Olson DJ, Gibo DM, Saggers G, Debinski W, Kumar R. Reversion of uroepithelial cell tumorigenesis by the ectopic expression of human wnt-5a. Cell Growth Differ 1997;8:417-23.

(295) Moustakas A, Heldin CH. Signaling networks guiding epithelial-mesenchymal transitions during embryogenesis and cancer progression. Cancer Sci 2007;98:1512-20.

(296) Thiery JP, Sleeman JP. Complex networks orchestrate epithelial-mesenchymal transitions. Nat Rev Mol Cell Biol 2006;7:131-42.

(297) Mani SA, Guo W, Liao MJ, Eaton EN, Ayyanan A, Zhou AY, et al. The epithelial-mesenchymal transition generates cells with properties of stem cells. Cell 2008;133:704-15.

(298) Polyak K, Weinberg RA. Transitions between epithelial and mesenchymal states: acquisition of malignant and stem cell traits. Nat Rev Cancer 2009;9:265-73.

(299) Guo Y, Zi X, Koontz Z, Kim A, Xie J, Gorlick R, et al. Blocking Wnt/LRP5 signaling by a soluble receptor modulates the epithelial to mesenchymal transition and suppresses met and metalloproteinases in osteosarcoma Saos-2 cells. J Orthop Res 2007;25:964-71.

(300) Ullmann U, Gilles C, De RM, Van d, V, Sermon K, Liebaers I. GSK-3-specific inhibitor-supplemented hESC medium prevents the epithelial-mesenchymal transition process and the up-regulation of matrix metalloproteinases in hESCs cultured in feeder-free conditions. Mol Hum Reprod 2008;14:169-79.

(301) Yook JI, Li XY, Ota I, Hu C, Kim HS, Kim NH, et al. A Wnt-Axin2-GSK3beta cascade regulates Snail1 activity in breast cancer cells. Nat Cell Biol 2006;8:1398-406.

(302) Cho HJ, Yoo J. Rho activation is required for transforming growth factor-beta-induced epithelial-mesenchymal transition in lens epithelial cells. Cell Biol Int 2007;31:1225-30.

(303) Xie L, Law BK, Chytil AM, Brown KA, Aakre ME, Moses HL. Activation of the Erk pathway is required for TGF-beta1-induced EMT in vitro. Neoplasia 2004;6:603-10.

(304) Zavadil J, Bottinger EP. TGF-beta and epithelial-to-mesenchymal transitions. Oncogene 2005;24:5764-74.

(305) Rosano L, Spinella F, Di C, V, Dedhar S, Nicotra MR, Natali PG, et al. Integrin-linked kinase functions as a downstream mediator of endothelin-1 to promote invasive behavior in ovarian carcinoma. Mol Cancer Ther 2006;5:833-42.

(306) Bindels S, Mestdagt M, Vandewalle C, Jacobs N, Volders L, Noel A, et al. Regulation of vimentin by SIP1 in human epithelial breast tumor cells. Oncogene 2006;25:4975-85.

(307) Alves CC, Carneiro F, Hoefler H, Becker KF. Role of the epithelial-mesenchymal transition regulator Slug in primary human cancers. Front Biosci 2009;14:3035-50.

(308) Cano A, Perez-Moreno MA, Rodrigo I, Locascio A, Blanco MJ, del Barrio MG, et al. The transcription factor snail controls epithelial-mesenchymal transitions by repressing E-cadherin expression. Nat Cell Biol 2000;2:76-83.

(309) Kurrey NK, Jalgaonkar SP, Joglekar AV, Ghanate AD, Chaskar PD, Doiphode RY, et al. Snail and slug mediate radioresistance and chemoresistance by antagonizing p53-mediated apoptosis and acquiring a stem-like phenotype in ovarian cancer cells. Stem Cells 2009;27:2059-68.

(310) Leong KG, Niessen K, Kulic I, Raouf A, Eaves C, Pollet I, et al. Jagged1-mediated Notch activation induces epithelial-to-mesenchymal transition through Slug-induced repression of E-cadherin. J Exp Med 2007;204:2935-48.

(311) Timmerman LA, Grego-Bessa J, Raya A, Bertran E, Perez-Pomares JM, Diez J, et al. Notch promotes epithelial-mesenchymal transition during cardiac development and oncogenic transformation. Genes Dev 2004;18:99-115.

(312) Fischer A, Steidl C, Wagner TU, Lang E, Jakob PM, Friedl P, et al. Combined loss of Hey1 and HeyL causes congenital heart defects because of impaired epithelial to mesenchymal transition. Circ Res 2007;100:856-63.

(313) Bailey KM, Liu J. Caveolin-1 up-regulation during epithelial to mesenchymal transition is mediated by focal adhesion kinase. J Biol Chem 2008;283:13714-24.

(314) Katoh M. WNT signaling in stem cell biology and regenerative medicine. Curr Drug Targets 2008;9:565-70.

(315) Vermeulen L, De Sousa E Melo, van der Heijden M, Cameron K, de Jong JH, Borovski T, et al. Wnt activity defines colon cancer stem cells and is regulated by the microenvironment. Nat Cell Biol 2010;12:468-76.

(316) Held MA, Curley DP, Dankort D, McMahon M, Muthusamy V, Bosenberg MW. Characterization of melanoma cells capable of propagating tumors from a single cell. Cancer Res 2010;70:388-97.

(317) Roesch A, Fukunaga-Kalabis M, Schmidt EC, Zabierowski SE, Brafford PA, Vultur A, et al. A temporarily distinct subpopulation of slow-cycling melanoma cells is required for continuous tumor growth. Cell 2010;141:583-94.

(318) Chen R, Nishimura MC, Bumbaca SM, Kharbanda S, Forrest WF, Kasman IM, et al. A hierarchy of self-renewing tumor-initiating cell types in glioblastoma. Cancer Cell 2010;17:362-75.

(319) Wu Y, Wu PY. CD133 as a marker for cancer stem cells: progresses and concerns. Stem Cells Dev 2009;18:1127-34.

(320) Ogden AT, Waziri AE, Lochhead RA, Fusco D, Lopez K, Ellis JA, et al. Identification of A2B5+C. Neurosurgery 2008;62:505-14.

(321) Joo KM, Kim SY, Jin X, Song SY, Kong DS, Lee JI, et al. Clinical and biological implications of CD133-positive and CD133-negative cells in glioblastomas. Lab Invest 2008;88:808-15.

(322) Gunther HS, Schmidt NO, Phillips HS, Kemming D, Kharbanda S, Soriano R, et al. Glioblastoma-derived stem cell-enriched cultures form distinct subgroups according to molecular and phenotypic criteria. Oncogene 2008;27:2897-909.

(323) Maeda S, Shinchi H, Kurahara H, Mataki Y, Maemura K, Sato M, et al. CD133 expression is correlated with lymph node metastasis and vascular endothelial growth factor-C expression in pancreatic cancer. Br J Cancer 2008;98:1389-97.

(324) Al DR, Sartelet H, Powell J, Kokta V. Expression of CD133+ cancer stem cells in childhood malignant melanoma and its correlation with metastasis. Mod Pathol 2010;23:376-80.

(325) Rappa G, Fodstad O, Lorico A. The stem cell-associated antigen CD133 (Prominin-1) is a molecular therapeutic target for metastatic melanoma. Stem Cells 2008;26:3008-17.

(326) Kim M, Koh YJ, Kim KE, Koh BI, Nam DH, Alitalo K, et al. CXCR4 signaling regulates metastasis of chemoresistant melanoma cells by a lymphatic metastatic niche. Cancer Res 2010.

(327) Quintana E, Shackleton M, Sabel MS, Fullen DR, Johnson TM, Morrison SJ. Efficient tumour formation by single human melanoma cells. Nature 2008;456:593-8.

(328) Kawasaki BT, Farrar WL. Cancer stem cells, CD200 and immunoevasion. Trends Immunol 2008;29:464-8.

(329) Schatton T, Frank MH. Antitumor immunity and cancer stem cells. Ann N Y Acad Sci 2009;1176:154-69.

APPENDIX 1

Appendix 1-1: Genomic map of the 4q gain measured by arrayCGH in the NB1 tumor genome
Refseq genes located in the gained portion of the chr4 long arm in NB1 tumor are listed in blue.

Appendix 1-2: Genomic map of the 8q gain measured by arrayCGH in the NB1 tumor genome
Refseq genes located in the gained portion of the chr8 long arm in NB1 tumor are listed in blue.

APPENDIX 2

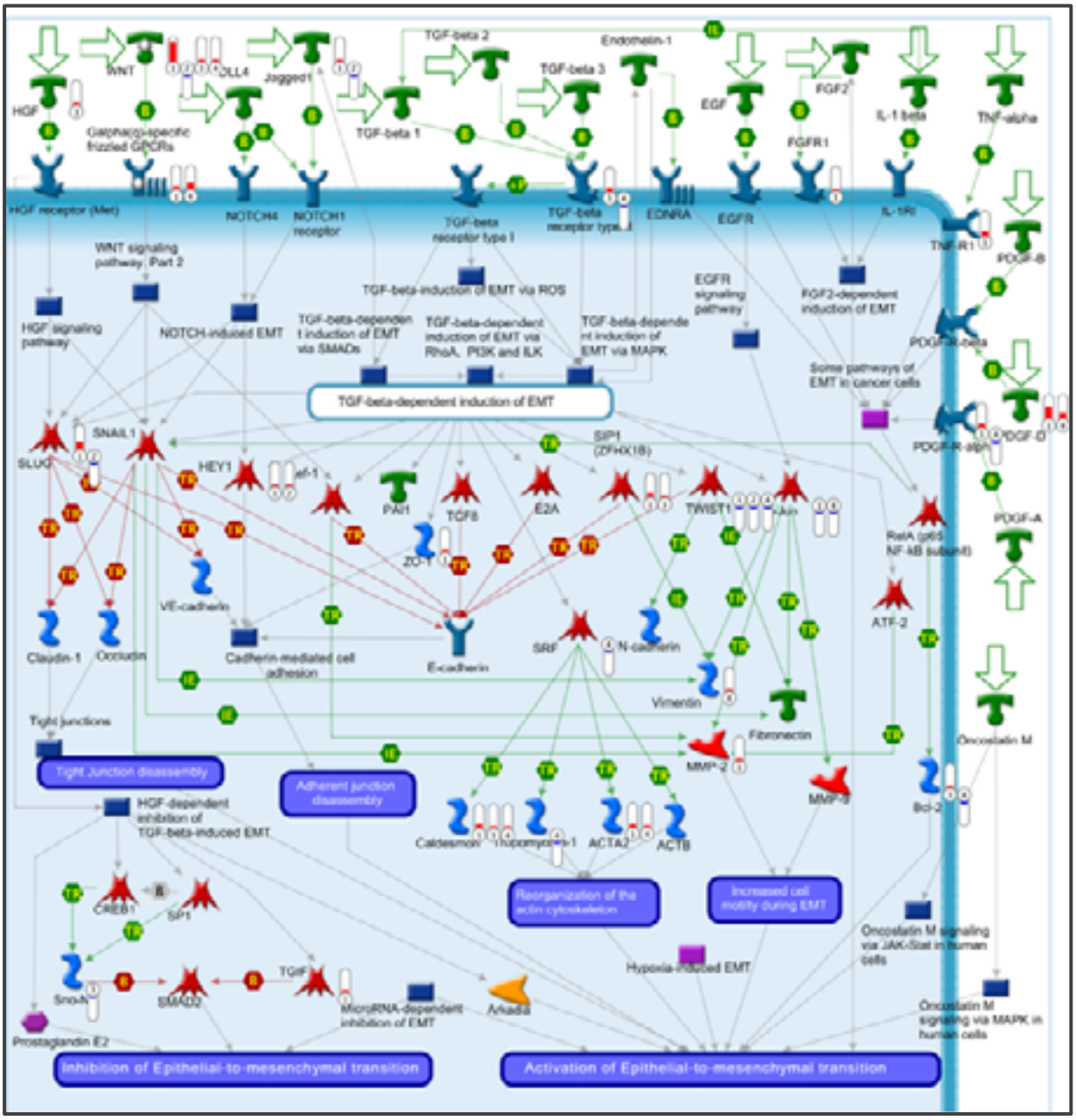

<u>Appendix 2-1</u>: Canonical map of epithelial to mesenchymal transition (EMT) signaling in human cells (from GeneGo, map 1)

Thermometers at the right of each molecule indicate the level of deregulation for genes that were differentially expressed in NB1-T (1), NB1-NBM (2), NB2-T (3) and NB4-T (4) spheres. Upregulated genes appear in red and downregulated in blue.

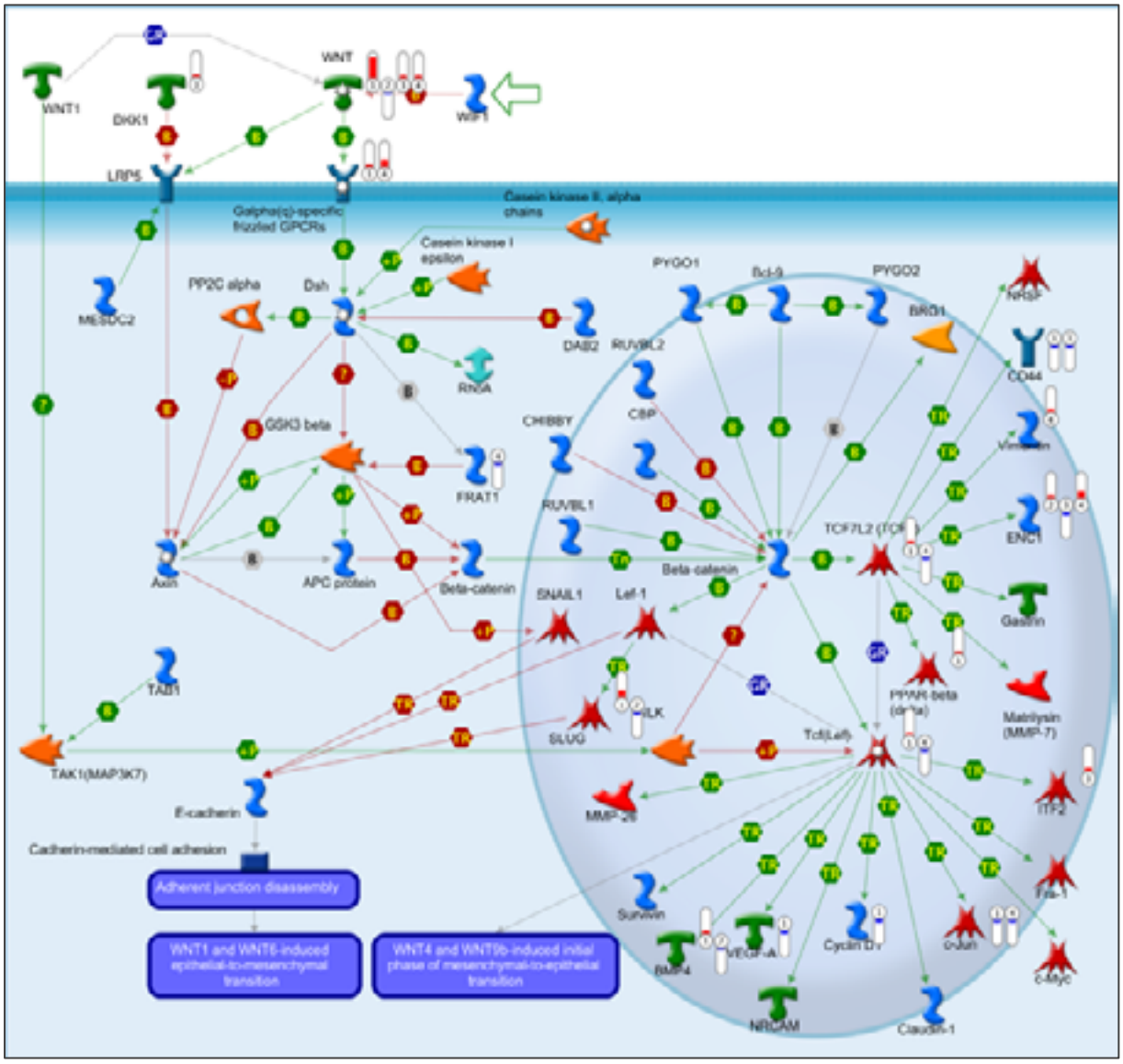

<u>Appendix 2-2</u>: Canonical map of WNT signaling pathway in human cells (from GeneGo, map 8)
Thermometers at the right of each molecule indicate the level of deregulation for genes that were differentially expressed in NB1-T (1), NB1-NBM (2), NB2-T (3) and NB4-T (4) spheres. Upregulated genes appear in red and downregulated in blue.

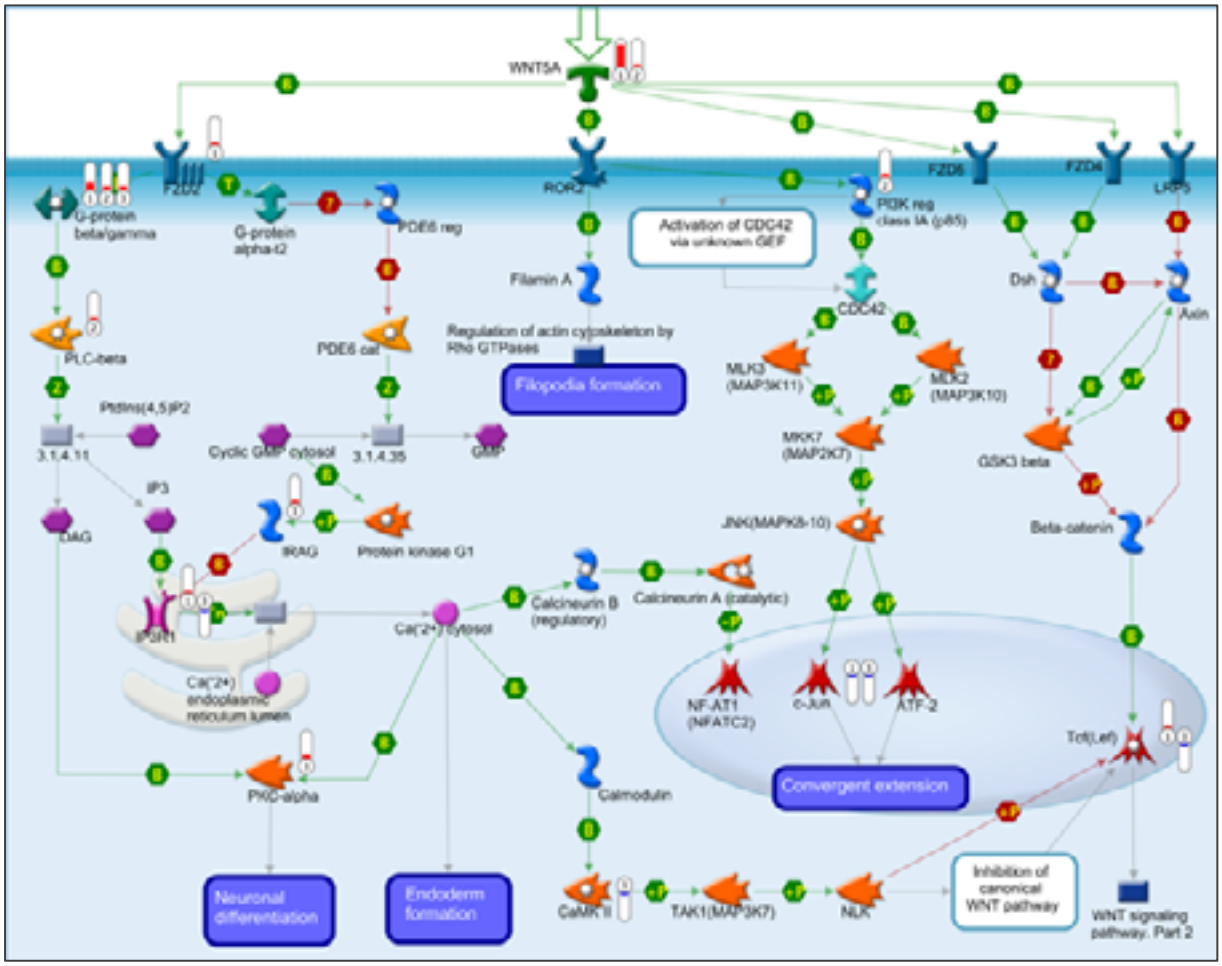

<u>Appendix 2-3</u>: Canonical map of WNT5A signaling pathway in human cells (from GeneGo)

Thermometers at the right of each molecule indicate the level of deregulation for genes that were differentially expressed in NB1-T (1), NB1-NBM (2), NB2-T (3) and NB4-T (4) spheres. Upregulated genes appear in red and downregulated in blue.

APPENDIX 3

Gene Symbol	Foldchange NB1-T4	Other lists	Protein name	Chromosome	Function
CD133	[illegible]	NCSC	prominin 1	chr4p15.32	[illegible]
LAMA1	[illegible]	NCSC	laminin, alpha 1	chr18p11.31-p11.23	[illegible]
VEGFC	[illegible]	NCSC	vascular endothelial growth factor C	chr4q34.1-q34.3	[illegible]
TPD52L1	[illegible]	NCSC	tumor protein D52-like 1	chr6q22-q23	[illegible]
PTGIS	[illegible]	NCSC	prostaglandin I2 (prostacyclin) synthase	chr20q13.13	[illegible]
ARID3A	[illegible]	NCSC	AT rich interactive domain 3A (BRIGHT-like)	chr19p13.3	[illegible]
FGFR2	[illegible]	NCSC	fibroblast growth factor receptor 2	chr10q26	[illegible]
IGDCC3	[illegible]	NCSC	immunoglobulin superfamily, DCC subclass, member 3	chr15q22.31-q23	[illegible]
TPBG	[illegible]	NCSC	trophoblast glycoprotein	chr6q14-q15	[illegible]
HOXB5	[illegible]	NCSC	homeobox B5	chr17q21.3	[illegible]
ACVR2B	[illegible]	NCSC	activin A receptor, type IIB	chr3p22	[illegible]
U2AF1	[illegible]	NCSC	U2 small nuclear RNA auxiliary factor 1	chr21q22.3	[illegible]
HOXC4	[illegible]	NCSC	homeobox C4	chr12q13.3	[illegible]
SENP3	[illegible]	NCSC	SUMO1/sentrin/SMT3 specific peptidase 3	chr17p13	[illegible]

<u>Appendix 3-1</u>: Table of the genes that are both deregulated in NB1-T4 cells and expressed in neural crest stem cells (NCSC) (218)

Foldchange of up-regulated (red) or down-regulated (blue) genes as measured by the microarray analyses are shown for the NB1-T experiments.

APPENDIX 3

Gene Symbol	Foldchange NB1-T4	Other lists	Protein name	Chromosome	*Function*
HMGA2	262.11	**NCDC**	high mobility group AT-hook 2	chr12q15	*This protein contains structural DNA-binding domains and may act as a transcriptional regulating factor. Identification of the deletion, amplification, and rearrangement of this gene that are associated with myxoid liposarcoma suggests a role in adipogenesis and mesenchymal differentiation.*
GJA1	36.59	**NCDC**	gap junction protein, alpha 1, 43kDa	chr6q21-q23.2	*One gap junction consists of a cluster of closely packed pairs of transmembrane channels, the connexons, through which materials of low MW diffuse from one cell to a neighboring cell. May play a critical role in the physiology of hearing by participating in the recycling of potassium to the cochlear endolymph.*
TGIF1	3.03	**NCDC**	TGFB-induced factor homeobox 1	chr18p11.3	*Binds to a retinoid X receptor (RXR) responsive element from the cellular retinol-binding protein II promoter (CRBPII-RXRE). Inhibits the 9-cis-retinoic acid-dependent RXR alpha transcription activation of the retinoic acid responsive element. Active transcriptional corepressor of SMAD2. Links the nodal signaling pathway to the bifurcation of the forebrain and the establishment of ventral midline structures. May participate in the transmission of nuclear signals during development and in the adult, as illustrated by the down-modulation of the RXR alpha activities.*
GLCE	2.42	**NCDC**	glucuronic acid epimerase	chr15q23	*Converts D-glucuronic acid residues adjacent to N-sulfate sugar residues to L-iduronic acids.*
CNN2	2.17	**NCDC**	calponin 2	chr19p13.3	*Thin filament-associated protein that is implicated in the regulation and modulation of smooth muscle contraction. It is capable of binding to actin, calmodulin, troponin C and tropomyosin. The interaction of calponin with actin inhibits the actomyosin Mg-ATPase activity.*
PEPD	2.09	**NCDC**	peptidase D	chr19q12-q13.2	*Splits dipeptides with a prolyl or hydroxyprolyl residue in the C-terminal position. Plays an important role in collagen metabolism because the high level of iminoacids in collagen.*
TP53BP1	-2.12	**NCDC**	tumor protein p53 binding protein 1	chr15q15-q21	*May have a role in checkpoint signaling during mitosis (By similarity). Enhances TP53-mediated transcriptional activation. Plays a role in the response to DNA damage.*

Appendix 3-2: Table of the genes that are both deregulated in NB1-T4 cells and expressed in neural crest derived cells (NCDC) (218)

Foldchange of up-regulated (red) or down-regulated (blue) genes as measured by the microarray analyses are shown for the NB1-T experiments.

Gene Symbol	Protein name	Foldchange NB1-T4	Other lists	Chromosome
SH3BGRL	SH3 domain binding glutamic acid-rich protein like	39.51	NSC	chrXq13.3
COL5A2	collagen, type V, alpha 2	38.38	NSC	chr2q14-q32
EDNRB	endothelin receptor type B	33.34	NSC	chr13q22
WWTR1	WW domain containing transcription regulator 1	27.78	NSC	chr3q23-q24
CSDA	cold shock domain protein A	21.87	NSC	chr12p13.1
MGST1	microsomal glutathione S-transferase 1	17.37	NSC	chr12p12.3-p12.1
ABCA1	ATP-binding cassette, sub-family A (ABC1), member 1	16.59	NSC	chr9q31.1
TANC1	tetratricopeptide repeat, ankyrin repeat and coiled-coil containing 1	15.14	NSC	chr2q24.2
STK3	serine/threonine kinase 3 (STE20 homolog, yeast)	13.14	NSC	chr8q22.2
NSBP1	high-mobility group nucleosome binding domain 5	8.93	NSC	chrXq13.3
SERPINH1	serpin peptidase inhibitor, clade H (heat shock protein 47), member 1, (collagen binding protein 1)	7.39	NSC	chr11q13.5
FBN1	fibrillin 1	7.25	NSC	chr15q21.1
CD302	CD302 molecule	7.00	NSC	chr2q24.2
SNAP23	synaptosomal-associated protein, 23kDa	6.75	NSC	chr15q15.1-q15.2
MYO6	myosin VI	6.13	NSC	chr6q13
CTSC	cathepsin C	6.01	NSC	chr11q14.1-q14.3
RRBP1	ribosome binding protein 1 homolog 180kDa (dog)	6.01	NSC	chr20p12
GNG12	guanine nucleotide binding protein (G protein), gamma 12	4.92	NSC	chr1p31.3
CASP6	caspase 6, apoptosis-related cysteine peptidase	4.78	NSC	chr4q25
NPL	N-acetylneuraminate pyruvate lyase (dihydrodipicolinate synthase)	4.50	NSC	chr1q25
BAG2	BCL2-associated athanogene 2	3.92	NSC	chr6p12.1-p11.2
ATP6V0E	ATPase, H+ transporting, lysosomal 9kDa, V0 subunit e1	3.74	NSC	chr5q35.1
AKAP7	A kinase (PRKA) anchor protein 7	3.71	NSC	chr6q23
ROD1	ROD1 regulator of differentiation 1 (S. pombe)	3.58	NSC	chr9q32

<u>Appendix 3-3 (Part 1)</u>: Table of the genes that are both deregulated in NB1-T4 cells and expressed in neural stem cells (NSC) (219)

Foldchange of up-regulated (red) or down-regulated (blue) genes as measured by the microarray analyses are shown for the NB1-T experiments.

Gene Symbol	Protein name	Foldchange NB1-T4	Other lists	Chromosome
IFIT2	interferon-induced protein with tetratricopeptide repeats 2	3.56	NSC	chr10q23-q25
NEDD4	neural precursor cell expressed, developmentally down-regulated 4	3.53	NSC	chr15q
TJP1	tight junction protein 1 (zona occludens 1)	3.52	SC	chr15q13
AKAP2 /// PALM2-AKAP2	A-kinase (PRKA) anchor protein 2 /// PALM2-AKAP2 readthrough	3.51	NSC	chr9q31-q33
FCGR2A	Fc fragment of IgG, low affinity IIa, receptor (CD32)	3.49	NSC	chr1q23
PCDH7	protocadherin 7	3.18	NSC	chr4p15
LRRN1	leucine rich repeat neuronal 1	2.91	NSC	chr3p26.2
SYPL1	synaptophysin-like 1	2.82	NSC	chr7q22.3
COL18A1	collagen, type XVIII, alpha 1	2.82	NSC	chr21q22.3
FGFR1	fibroblast growth factor receptor 1	2.70	NSC	chr8p11.2-p11.1
HSDL2	hydroxysteroid dehydrogenase like 2	2.65	NSC	chr9q32
BAX	BCL2-associated X protein	2.62	NSC	chr19q13.3-q13.4
LOC158563	chloride channel 5	2.57	NSC	chrXp11.23-p11.22
CASP7	caspase 7, apoptosis-related cysteine peptidase	2.55	NSC	chr10q25
CD164	CD164 molecule, sialomucin	2.48	NSC	chr6q21
SOAT1	sterol O-acyltransferase 1	2.41	NSC	chr1q25
MAGED2	Melanoma Antigen Family D, 2	2.36	NSC	chrXp11.2
PPA2	pyrophosphatase (inorganic) 2	2.34	NSC	chr4q25
NMI	N-myc (and STAT) interactor	2.32	NSC	chr2q23
IDE	insulin-degrading enzyme	2.23	NSC	chr10q23-q25
TPMT	thiopurine S-methyltransferase	2.22	NSC	chr6p22.3
FKSG44	FERM domain containing 8	2.19	NSC	chr11q13
KIAA0247	KIAA0247	2.17	NSC	chr14q24.1
PPA2 /// RNF36	pyrophosphatase (inorganic) 2	2.14	NSC	chr4q25
DFNA5	deafness, autosomal dominant 5	2.14	NSC	chr7p15
KIAA0103	tetratricopeptide repeat domain 35	2.10	NSC	chr8q23.1
DNAJC13	DnaJ (Hsp40) homolog, subfamily C, member 13	2.08	NSC	chr3q22.1
HIST1H2BD	histone cluster 1, H2bd	2.07	NSC	chr6p21.3
PECI	peroxisomal D3,D2-enoyl-CoA isomerase	2.06	NSC	chr6p24.3

<u>Appendix 3-3 (Part 2)</u>: Table of the genes that are both deregulated in NB1-T4 cells and expressed in neural stem cells (NSC) (219)

Foldchange of up-regulated (red) or down-regulated (blue) genes as measured by the microarray analyses are shown for the NB1-T experiments.

Gene Symbol	Protein name	Foldchange NB1-T4	Other lists	Chromosome
SF3B1	splicing factor 3b, subunit 1, 155kDa	-2.06	NSC	chr2q33.1
ATP5C1	ATP synthase, H+ transporting, mitochondrial F1 complex, gamma polypeptide 1	-2.06	NSC	chr10p15.1
FADS1	fatty acid desaturase 1	-2.07	NSC	chr11q12.2-q13.1
HTATIP2	HIV-1 Tat interactive protein 2, 30kDa	-2.08	NSC	chr11p15.1
RGS7	regulator of G-protein signaling 7	-2.16	NSC	chr1q43|1q23.1
SIPA1L2	signal-induced proliferation-associated 1 like 2	-2.21	NSC	chr1q42.2
KRTCAP2	keratinocyte associated protein 2	-2.22	NSC	chr1q22
RBPSUH /// LOC652675	recombination signal binding protein for immunoglobulin kappa J region	-2.22	NSC	chr4p15.2
NBR1	Neighbor of BRCA1 gene 1	-2.24	NSC	chr17q21.31
SFRS7	splicing factor, arginine/serine-rich 7, 35kDa	-2.27	NSC	chr2p22.1
SQLE	squalene epoxidase	-2.30	NSC	chr8q24.1
TMEM56	transmembrane protein 56	-2.37	NSC	chr1p21.3
USP22	ubiquitin specific peptidase 22	-2.49	NSC	chr17p11.2
STT3B	STT3, subunit of the oligosaccharyltransferase complex, homolog B (S. cerevisiae)	-2.57	NSC	chr3p23
ATG7	ATG7 autophagy related 7 homolog (S. cerevisiae)	-2.72	NSC	chr3p25.3
STX12	syntaxin 12	-2.86	NSC	chr1p35-p34.1
GPR56	G protein-coupled receptor 56	-3.17	NSC	chr16q12.2-q21
TNFAIP6	tumor necrosis factor, alpha-induced protein 6	-3.21	NSC	chr2q23.3
GABRG1	gamma-aminobutyric acid (GABA) A receptor, gamma 1	-3.34	NSC	chr4p12
SMC3	structural maintenance of chromosomes 3	-3.62	NSC	chr10q25
SUZ12	Suppressor of zeste 12 homolog (Drosophila)	-3.95	NSC	chr17q11.2
GPX7	glutathione peroxidase 7	-4.01	NSC	chr1p32
KIF23	Kinesin family member 23	-4.47	NSC	chr15q23
ARHGAP21	Rho GTPase activating protein 21	-4.87	NSC	chr10p12.1|10p12.3

<u>Appendix 3-3 (Part 3)</u>: Table of the genes that are both deregulated in NB1-T4 cells and expressed in neural stem cells (NSC) (219)

Foldchange of up-regulated (red) or down-regulated (blue) genes as measured by the microarray analyses are shown for the NB1-T experiments.

APPENDIX 3

Gene Symbol	Foldchange NB1-T4	Other lists	Protein name	Chromosome	Function
YAP1	113.17	NSC//SC	Yes-associated protein 1	chr11q13	*Transcriptional regulator which can act both as a coactivator and a corepressor and is the critical downstream regulatory target in the Hippo signaling pathway that plays a pivotal role in organ size control and tumor suppression by restricting proliferation and promoting apoptosis. The core of this pathway is composed of a kinase cascade wherein MST1/MST2, in complex with its regulatory protein SAV1, phosphorylates and activates LATS1/2 in complex with its regulatory protein MOB1, which in tum phosphorylates and inactivates YAP1 oncoprotein. YAP1 plays a key role to control cell proliferation in response to cell contact. Phosphorylation by LATS1/2 inhibits its translocation into the nucleus to regulate cellular genes important for cell proliferation, cell death, and cell migration. Isoform 2 and isoform 3 can activate the C-terminal fragment (CTF) of ERBB4 (isoform 3).*
PPIC	32.11	NSC//SC	peptidylprolyl isomerase C (cyclophilin C)	chr5q23.2	*PPIases accelerate the folding of proteins. It catalyzes the cis-trans isomerization of proline imidic peptide bonds in oligopeptides.*
PLS3	13.02	NCDC//NSC	plastin 3	chrXq23	*Role in the response of DNA damage*
SUCLG2	10.94	NSC//SC	succinate-CoA ligase, GDP-forming, beta subunit	chr3p14.1	*This gene encodes a GTP-specific beta subunit of succinyl-CoA synthetase. Succinyl-CoA synthetase catalyzes the reversible reaction involving the formation of succinyl-CoA and succinate.*
GPR177 (WLS)	10.20	NCDC//NSC	Wntless homolog	chr1p31.3	*Regulates Wnt proteins sorting and secretion in a feedback reglatory mechanism. This reciprocical interaction plays a key role in the regulation of expression, subcellular location, binding and organelle-specific association of Wnt proteins. Plays also an important role in establishment of the anterior-posterior body axis formation during development.*
GAS2	7.92	NSC//SC	growth arrest-specific 2	chr11p14.3-p15.2	*May play a role in apoptosis by acting as a cell death substrate for caspases. Is cleaved during apoptosis and the cleaved form induces dramatic rearrangements of the actin cytoskeleton and potent changes in the shape of the affected cells. May be involved in the membrane ruffling process.*
NOTCH3	6.78	NCDC//NSC	Notch homolog 3 (Drosophila)	chr19p13.2-p13.1	*Functions as a receptor for membrane-bound ligands Jagged1, Jagged2 and Delta1 to regulate cell-fate determination. Upon ligand activation through the released notch intracellular domain (NICD) it forms a transcriptional activator complex with RBP-J kappa and activates genes of the enhancer of split locus. Affects the implementation of differentiation, proliferation and apoptotic programs.*
ROBO1	5.70	NCSC//NSC	roundabout, axon guidance receptor, homolog 1 (Drosophila)	chr3p12	*Receptor for SLIT1 and SLIT2 which are thought to act as molecular guidance cue in cellular migration, including axonal navigation at the ventral midline of the neural tube and projection of axons to different regions during neuronal development. In axon growth cones, the silencing of the attractive effect of NTN1 by SLIT2 may require the formation of a ROBO1-DCC complex. May be required for lung development.*
TEAD2	5.07	NSC//SC	TEA domain family member 2	chr19q13.3	*Putative transcription factor that binds to the SPH and GT-IIC "enhansons" (5'-GTGGAATGT-3'). May be involved in the gene regulation of neural development. Binds to the M-CAT motif.*
ETS1	3.52	NCSC//NC	v-ets erythroblastosis virus E26 oncogene homolog 1 (avian)	chr11q23.3	*ETS transcriptions factors, such as ETS1, regulate numerous genes and are involved in stem cell development, cell senescence and death, and tumorigenesis. The conserved ETS domain within these proteins is a winged helix-turn-helix DNA-binding domain that recognizes the core consensus DNA sequence GGAA/T of target genes.*
MEIS1	3.28	NCSC//NSC	Meis homeobox 1	chr2p14	*Acts as a transcriptional regulator of PAX6. Acts as a transcriptional activator of PF4 in complex with PBX1 or PBX2. Required for hematopoiesis, megakaryocyte lineage development and vascular patterning. May function as a cofactor for HOXA7 and HOXA9 in the induction of myeloid leukemias.*
YES1	2.85	NSC//SC	v-yes-1 Yamaguchi sarcoma viral oncogene homolog 1	chr18p11.31-p11.21	*Promotes infectivity of Neisseria gonorrhoeae in epithelial cells by phosphorylating MCP/CD46.*
SH3D19	2.42	NSC//SC	SH3 domain containing 19	chr4q31.3	*May play a role in regulating A disintegrin and metalloproteases (ADAMs) in the signaling of EGFR-ligand shedding. May be involved in suppression of Ras-induced cellular transformation and Ras-mediated activation of ELK1.*
TSPAN6	2.22	NCDC//NSC	tetraspanin 6	chrXq22	*The protein encoded by this gene is a member of the transmembrane 4 superfamily, also known as the tetraspanin family. Most of these members are cell-surface proteins that are characterized by the presence of four hydrophobic domains. The proteins mediate signal transduction events that play a role in the regulation of cell development, activation, growth and motility. This encoded protein is a cell surface glycoprotein and is highly similar in sequence to the transmembrane 4 superfamily member 2. The use of alternate polyadenylation sites has been found for this gene.*
KRAS	-2.04	NSC//SC	v-Ki-ras2 Kirsten rat sarcoma viral oncogene homolog	chr12p12.1	*This gene, a Kirsten ras oncogene homolog from the mammalian ras gene family, encodes a protein that is a member of the small GTPase superfamily. A single amino acid substitution is responsible for an activating mutation. The transforming protein that results is implicated in various malignancies, including lung adenocarcinoma, mucinous adenoma, ductal carcinoma of the pancreas and colorectal carcinoma. Alternative splicing leads to variants encoding two isoforms that differ in the C-terminal region.*
BLZF1	-2.04	NSC//SC	basic leucine zipper nuclear factor 1	chr1q24	*Required for normal Golgi structure and for protein transport from the endoplasmic reticulum (ER) through the Golgi apparatus to the cell surface.*
ELP2	-2.17	NCSC//NSC//S	Elongation protein 2 homolog (S. cerevisiae)	chr18q12.2	*Regulates the ligand-dependent activation of STAT3. Acts as subunit of the RNA polymerase II elongator complex, which is a histone acetyltransferase component of the RNA polymerase II (Pol II) holoenzyme and is involved in transcriptional elongation. Elongator may play a role in chromatin remodeling and is involved in acetylation of histones H3 and probably H4.*
TXNL1	-2.19	NSC//SC	Thioredoxin-like 1	chr18q21.31	*Cytoplasmic.*
GART	-3.24	NCSC//NSC	phosphoribosylglycinamide formyltransferase, phosphoribosylglycinamide synthetase, phosphoribosylaminoimidazole synthetase	chr21q22.11	*The protein encoded by this gene is a trifunctional polypeptide. It has phosphoribosylglycinamide formyltransferase, phosphoribosylglycinamide synthetase, phosphoribosylaminoimidazole synthetase activity which is required for de novo purine biosynthesis.*
SNRPA1	-3.30	NCSC//NSC	Small nuclear ribonucleoprotein polypeptide A'	chr15q26.3	*This protein is associated with sn-RNP U2. It helps the A' protein to bind stem loop IV of U2 snRNA.*
CCND1	-4.16	NSC//SC	cyclin D1	chr11q13	*Essential for the control of the cell cycle at the G1/S (start) transition. This cyclin forms a complex with and functions as a regulatory subunit of CDK4 or CDK6, whose activity is required for cell cycle G1/S transition. This protein has been shown to interact with tumor suppressor protein Rb and the expression of this gene is regulated positively by Rb. Mutations, amplification and overexpression of this gene, which alters cell cycle progression, are observed frequently in a variety of tumors and may contribute to tumorigenesis.*

<u>Appendix 3-4</u>: Table of the genes that are both deregulated in NB1-T4 cells and found at least in one of the published lists (NSC, NCDC, NSC or SC) (218, 219)

Foldchange of up-regulated (red) or down-regulated (blue) genes as measured by the microarray analyses are shown for the NB1-T experiments.

Gene Symbol	Foldchange NB1-T4	Other lists	Protein name	Chromosome	Function
PTN	6.86	**LR**	pleiotrophin	chr7q33-q34	*Heparin binding mitogenic protein. Has neurite extension activity.*
NHLH2	-2.01	**HR**	nescient helix loop helix 2	chr1p12-p11	*May serve as DNA-binding protein and may be involved in the control of cell-type determination, possibly within the developing nervous system.*
ARHGEF7	-2.41	**LR**	Rho guanine nucleotide exchange factor (GEF) 7	chr13q34	*Acts as a RAC1 guanine nucleotide exchange factor (GEF) and can induce membrane ruffling. May function as a positive regulator of apoptosis. May function in cell migration.*
DDC	-2.69	**LR**	dopa decarboxylase (aromatic L-amino acid decarboxylase)	chr7p12.2	*Catalyzes the decarboxylation of L-3,4-dihydroxyphenylalanine (DOPA) to dopamine, L-5-hydroxytryptophan to serotonin and L-tryptophan to tryptamine.*
FYN	-3.23	**LR**	FYN oncogene related to SRC, FGR, YES	chr6q21	*Implicated in the control of cell growth. Plays a role in the regulation of intracellular calcium levels, with isoform 2 showing the greater ability to mobilize cytoplasmic calcium in comparison to isoform 1. Required in brain development and mature brain function with important roles in the regulation of axon growth, axon guidance, and neurite extension. Blocks axon outgrowth and attraction induced by NTN1 by phosphorylating its receptor DDC.*
MTSS1	-4.77	**LR**	metastasis suppressor 1	chr8p22	*May be related to cancer progression or tumor metastasis in a variety of organ sites, most likely through an interaction with the actin cytoskeleton.*
EPHA5	-5.10	**LR**	EPH receptor A5	chr4q13.1	*EPH-related receptors have been implicated in mediating developmental events, particularly in the nervous system. Binds to ephrin-A1, -A2, -A3, -A4 and -A5.*

Appendix 3-5: Table of the genes that are both deregulated in NB1-T4 cells and expressed in the low risk/high risk (LR/HR) (203)

Foldchange of up-regulated (red) or down-regulated (blue) genes as measured by the microarray analyses are shown for the NB1-T experiments.

CURRICULUM VITAE

Aurélie COULON

Rue du Village 8

1052 Le-Mont-sur Lausanne, Switzerland

Tel: 00 41 (0)21 544 626 08/ 00 41 (0)76 206 64 54

E-mail: aurelie.coulon@gmail.com

EDUCATION

09.2006-02.2011 ***PhD project entitled « Molecular and functional characterization of neuroblastoma-tumor initiating cells ».*** Group of Dr Nicole Gross, Pediatric Oncology Research Unit, University Hospital of Lausanne (CH)

09.2005-09.2006 ***M.Sc. in Oncology "Biology and genetics of cancer" (2nd year).*** Biochemistry and Bio-engineering Department in the Ecole Normale Supérieure and Medical School of the University Paris XI (Cachan and Orsay, F)

09.2004-09.2005 ***M.Sc in Biology "Cellular Signalization and Neuroscience" (1st year).*** Ecole Normale Supérieure and University Paris XI in (Cachan and Orsay, F)

.

09.2003-09.2004 ***B.Sc in Cellular Biology and Physiology.*** Ecole Normale Supérieure and University Paris XI (Cachan and Orsay, F)

09.2001-09.2003 Post High School advanced biology, mathematics, physics and chemistry classes in preparation of the competitive entrance exams to the French engineering schools. ***Lycée Henri IV (Paris, F)***

06.2001 ***French Baccalauréat in sciences (G.C.E. "A" levels), with honor***. Lycée Henri IV (Paris, F)

INTERNSHIPS

11.2005-06.2006 ***M.Sc professional training (2nd year).*** Group « Molecular Pathology of Cancers » of Dr. O. Delattre, Research Center of the Curie Institute (Paris, F)

07/08.2005 M.Sc professional training (1st year). ***Group « Genetic Neuropsychiatry » of Prof. A. Malafosse, Psychiatric Hospital of Geneva (CH)***

07/08.2004 ***B.Sc professional training***. Group "Cellular and molecular Physiopathology of Mitochondrial Diseases" of Dr. A. Lombes, University Hospital of Pitié-Salpêtrière (Paris, F)

SCIENTIFIC SKILLS

Transcriptom analysis: Array-based Comparative Genomic Hybridization (array-CGH), analysis of genechips based on Affymetrix technology and pathway enrichment study (GeneGo© program), gene clustering analysis (Cluster© and Treeview© software)

Molecular biology: Protein, RNA and DNA extractions, DNA cloning, Polymerase Chain reaction (PCR), gene expression analysis by real-time PCR (TaqMan© technology) and SDS2.2© software, DNA migration and observation with AlphaImager©, DNA purification, primer design with SECentral©, Western Blot

Cell biology: Primary cell and cell line cultures, immuno-fluorescence staining on living cells and fixed cells, flow cytometry and cell sorting (WinMDI2.8© software), drug resistance assay, soft agar assay

In vivo experimentation: Sub-cutaneous implantation of cancer cells in mice, sub-cutaneous and orthotopic tumor resection, preparation of paraffin embedded sections, tumor dissociation

Microscopic analysis: Confocal microscopy using Leica© SP5 microscope, Leica© DM2000 microscope for natural and fluorescence conditions, camera imaging and analysis with LAS 6000 AF software

GRANTS

09.2009-02.2011 ***Research grant from the National Found for Research (FNS)*** (CH)

09.2006-08.2009 ***PhD Fellowship in Life Science from the University of Lausanne*** (CH)

PUBLICATIONS

2009 **The Wnt receptor FZD1 mediates chemoresistance in neuroblastoma through activation of the Wnt/beta-catenin pathway.** *Flahaut M, Meier R, **Coulon A**, Nardou KA, Niggli FK, Martinet D, Beckmann JS, Joseph JM, Mühlethaler-Mottet A, Gross N.Oncogene. 2009 May 4.*

2007 **The chemokine receptor CXCR4 strongly promotes neuroblastoma primary tumour and metastatic growth, but not invasion.** *Meier R, Mühlethaler-Mottet A, Flahaut M, **Coulon A**, Fusco C, Louache F, Auderset K, Bourloud KB, Daudigeos E, Ruegg C, Vassal G, Gross N, Joseph JM. PLoS ONE, 2007 Oct 10; 2(10):e1016.*

CONGRESS PARTICIPATIONS

Abstracts selected for oral presentations:

2010 **7th Swiss Stem Cell Network annual meeting (SSCN), Lausanne, Switzerland.** *"Heterogeneity and plasticity of neuroblastoma tumour-initiating cells"* **A. Coulon**, M. Flahaut, A. Mülhethaler-Mottet, J.Liberman, K. Bourloud-Balmas, K. Nardou, J.-M. Joseph, L. Sommer and N. Gross

2010 **International Congress of Advances in Neuroblastoma Research (ANR), Stockholm, Sweden.** *"Identification and molecular characterization of human Neuroblastoma tumor-initiating cells"* **A. Coulon**, M. Flahaut, A. Mülhethaler-Mottet, J.Liberman, G. Kiowski, L. Sommer and N. Gross

2010 **Annual Research day of Pediatrics Young Scientists, Montana, Switzerland.** *"Molecular and Functional Characterization of Neuroblastoma Initiating Cells: Methods and Issues"* A. Coulon, M. Flahaut, A. Mülhethaler-Mottet, **J.Liberman**, G. Kiowski, L. Sommer and N. Gross

2009 **Swiss Pediatric Oncology group (SPOG) Scientific Meeting, Lugano, Suisse.** *"Identification of neuroblastoma tumor-initiating cells by micro-array time-course analysis of neurospheres"* **A.Coulon**

2009 **PhD Research Day, University of Lausanne, Switzerland.** *"Identification of neuroblastoma tumour-initiating cells by micro-array time-course analysis of neurospheres"* **A. Coulon**, M. Flahaut, A. Mülhethaler-Mottet, J.Liberman, S. Fuchs, G. Kiowski, L. Sommer and N. Gross

2008 **International Congress of Advances in Neuroblastoma Research (ANR), Chiba, Japan.** *"Identification of neuroblastoma specific stem cell markers by micro-array time-course analysis of neurospheres"* A. Coulon, M. Flahaut, G. Kiowski, A. Mülhethaler-Mottet, R. Meier, S. Fuchs, J.-M. Joseph, L. Sommer and **N. Gross**

2008 **8th International Congress of the Integrative Biology Research Unit of Paris VI University: « The Biology of Stem Cells », Paris, France.** *"Identification of neuroblastoma specific stem cell markers by micro-array time-course analysis of neurospheres"* **A. Coulon**, M. Flahaut, G. Kiowski, A. Mülhethaler-Mottet, R. Meier, S. Fuchs, J.-M. Joseph, L. Sommer and N. Gross

2007 **Annual research day of the Pediatric Department, University Hospital of Lausanne, Switzerland.** *"Identification of neuroblastoma progenitor gene expression profile by micro-array time-course analysis of neurospheres"* A. Coulon, A. Mülhethaler-Mottet, R. Meier, S. Fuchs, L. Sommer and **N. Gross**

Invited oral presentation:

2009 **Annual scientific meeting of the Research Foundation for the Pediatric Cancers (FORCE Foundation), University Hospital of Lausanne, Switzerland.** *"The cancer stem cells: myth or reality for an efficient targeted treatment in cancers"* **A. Coulon**

LANGUAGES AND SKILLS

French Native

English Fluent ***(read, written and spoken), TOEIC (may 2005): 880 points***

German Baccalaureate level ***(read, written)***

Italian Beginner level

Computer skills Microsoft Office ***(Word, Excel, Power-Point),*** Adobe Photoshop, Adobe Illustrator, GraphPad Prism

TEACHING

01.2007-2.2011 ***160 hours of scientific mediation*** for children (8-12 years old), teenagers and adults (curricular and extra-curricular audience). Public laboratory "Eprouvette" of the Science-Society Interface, University of Lausanne (http://www.unil.ch/interface/page14152.html) and Musée de la Main, Claude Verdan Foundation, Lausanne (CH)

11.2010 ***"Genetics and Pathogenesis" course*** for 2nd year student nurses, Clinique de la Source, Lausanne (CH)

09.2008-2010 ***"Cell life and death" course*** for 4th year medical students, pediatric program of the University Hospital of Lausanne (CH)

11/12.2003 Professional training of teaching ***for 3rd year students. Department of Bio-Engineering, University Institute of Technology, Créteil (F)***